A Theoretical and Experimental Investigation of the BTA Deep Hole Tool Support in the Machining Zone

Sinisa Kojic

A Thesis

in

The Department

of

Mechanical Engineering

Presented in Partial Fulfilment of the Requirements
for the Degree of Master of Applied Science at
Concordia University
Montreal, Quebec, Canada

March 1997

Abstract

A Theoretical and Experimental Investigation of

the BTA Deep Hole Tool Support in the Machining Zone

Self-piloting tools feature the unique use of two support pads and the surrounding hole as a guide bushing to steer itself along the hole being machined. The piloting hole, in conjunction with the two support pads, provides for the tool balance in the hole transverse cross-section. However, in the axial section plane, the tool alignment with the piloting hole depends on the boring bar to which the tool appears as a solid extension. This study shows that the alterations in the output quality and the support pads' wear pattern can be explained by in-process encountered boring bar bending. This is because even minor inclinations near the tool tip appear significant when considered in the small front-end area of the support pads where burnishing occurs. The study is to explain the inherent feature of the conventional self-piloting tool design to deflect the boring bar in 3D enough to make a difference between the effective area involved in burnishing and the area as designed.

Acknowledgements

The author expresses his sincere gratitude to the three of his co-supervisors, Prof. V.N. Latinovic, Prof. M.O.M. Osman and Prof. V. Astakhov, each of whom has made his own impact on this work.

The thanks are extended to Mr.G.Seeger for his invaluable assistance with the experimental part of the work.

Table of Contents

List of Figures

List of Tables

Nomenclature

b	Support Pad's Width
D_k	Piloting Hole Diameter
D_{1max}	Max. Diameter of the Rear Mating Sleeve
D_{2max}	Max. Diameter of the Front Mating Sleeve
d_{1max}	Max. Diameter of the Rear Mating Shoulder
d_{2max}	Max. Diameter of the Front Mating Shoulder
EI	Boring Bar Flexural Rigidity
F_C	Cutting Component
F_T	Thrust Component
F_{tcr}	Critical Thrust to Cause Buckling
F_R	Radial Component
$\underline{F}$	Stress Vector
GI_0	Boring Bar Torsional Rigidity
h	Support Pads' Lag Length
$\underline{i\,j\,k}$	Unit Vectors in Oxyz Coord. System
l,L	Boring Bar Length
l_1	Span between the Intermediate Support and the Cutting Tip
l_0	Mating Shoulders' Distance
$\underline{M}$	External Forces Moment
M_f	Flexural Moment
M_R	Burnishing Torque (Reibmoment [9])

M_{R0}	Steady Component of Burnishing Torque
P	Cutting Tip Lateral Force
$\underline{r}$	Center Line Point Position Vector
R_n	Support Pads' Radius
s	Curvilinear Coord. along the Deflection Curve
T	Drilling Torque
$\underline{T}$	Internal Forces Moment
T_{cr}	Critical Torque to Cause Buckling
$\underline{t}$	Vector Tangential to the Deflection Curve
u	Center Line Point Movement in X-direction
v	Center Line Point Movement in Y-Direction
w	Center Line Point Movement in Z-Direction
α_k	Contact Angle in Transverse Plane
δ_1	Max. Clearance above the Rear Shoulder
δ_2	Max. Clearance above the Front Shoulder
δ_n	Nominal Primary Flank Angle
δ_v	Tool Inclination Projection
$\theta_{A\text{-}C}$	Angle between the Tangents to the Points A and C of an Elastic Curve
θ_{eff}	Effective Tool Backtaper
θ_1	Tool Tip Inclination due to the Drilling Forces
θ_2	Tool Tip Inclination due to the Centrifugal Force
θ_3	Tool Tip Inclination due to the Manufacturing Tolerances

θ_4	Tool Tip Inclination due to the Misalignment
θ_Σ	Total Tool Tip Inclination
ν	Support Pads' Angular Span
ν_1	Angle between the Cornering Points of Contact with Respect to the Tool Axis
ν_2	Angle between the Cornering Points of Contact with Respect to the Hole Axis
σ_{max1}	Max. Contact Stress on Pad 1
σ_{max2}	Max. Contact Stress on Pad 2
Ω_z	Elastic Rod Torsion

Chapter 1

Deep Hole Machining

1.1. Introduction

Since this work deals with a metal cutting tool that is rather special, it behooves the author at this point to tell the basics of the related family of tools just as to set up the frame for the following discussion. The standard method of precision hole producing requires as many as four or five operations: drilling, boring, rough and finish reaming, and finally honing. The sequence starts with the drilling employing the conventional tool known as the twist drill. Though the tool has proven successful in the great majority of every-day applications, the problem still remains with the production of deep holes. For high length to diameter ratios, where hole depth exceeds flute length, the twist drill has to be repeatedly withdrawn from the bore for lubrication and chip removal. This results in production losses and poor surface finish. Moreover, being weak in cross-section, for higher lengths the drill becomes more susceptible to any imbalance of forces acting on the drill tip. Practice has shown that the occurrence of unbalanced forces is inevitable, because of small resharpening errors and different wear rate of two cutting lips. Thus, a new concept which would bring some form of control near the point of cutting had to be developed. The origin of gun-type tools can be found in "D"-bit and the spade drill, introducing the idea of supporting the cutter head and using a high-pressure cutting fluid flow to flush the swarf back and out of the hole. Soon after the tungsten carbide was developed, around 1935, a German engineer Beisner came to the idea to fully enclose the old type D-bit in a tube and to incorporate rubbing pads, made of carbide, on the outside of the tube. The first change in the design increased the rigidity

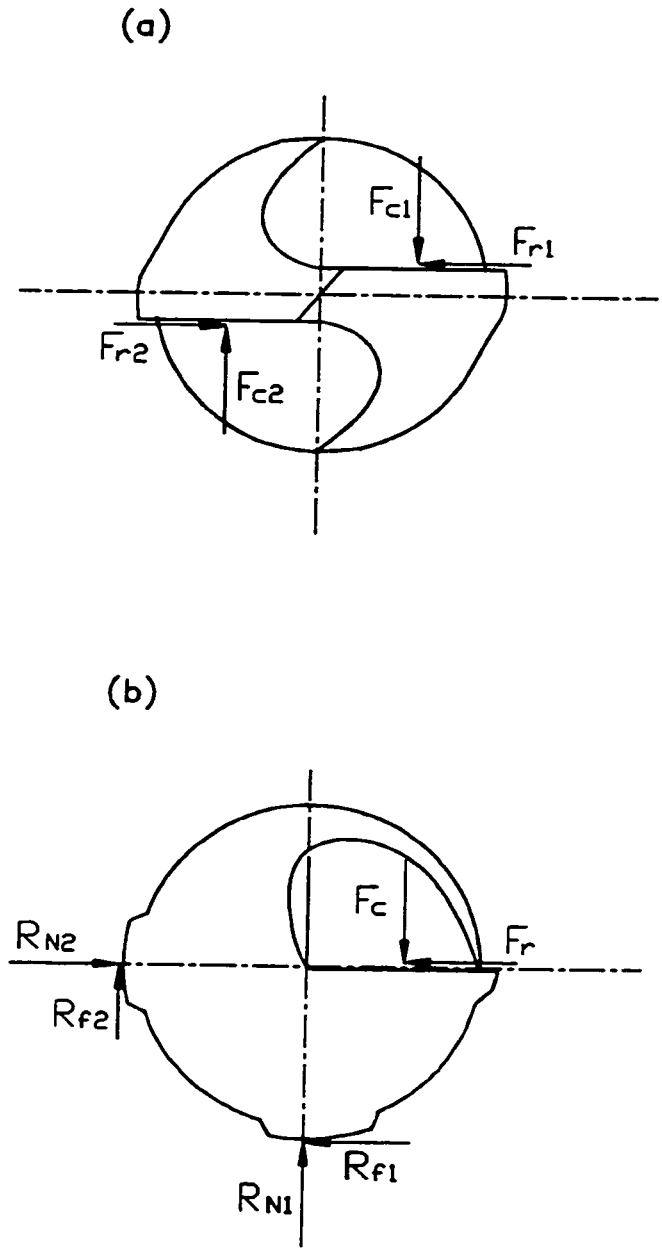

Fig.1.1. (a) Twist Drill and (b) Self-Piloting Drill

and the strength, thus allowing 5-6 times greater cutting speeds in order to make an efficient use of the new carbide material. The second change ingeniously ensured balancing of the cutter while simultaneously providing for a unique additional machining operation today known as burnishing. The fact that the pads bear against the bore wall right behind the cutting edge effectively means that the cutting head machines its own bushing. Fig.1.1 shows the principal difference between the balance of a gun-type tool and that of a twist drill. The concept of self-guidance (or self-piloting), meaning the tool guiding or steering itself along the bore, has been recognized as the main underlying principle of the design. The terms "gun-type tools" and "deep hole tools" have been used occasionally for historical reasons, though they do not convey the idea of the concept. Therefore, the term "self-piloting tools" has been found more appropriate [14] and, in this work, it will be insisted upon.

Not only does the self-piloting design make it possible to machine deep holes but it provides rather stable conditions at the tool tip. Moreover, owing to the high cutting speed, even the use of light feeds assures very high penetration rates thus bringing about an increase in productivity. This is especially true for the tools used in short to medium depth applications since the short tools can be run at extremely high speeds. For 20 years after the invention, the tool was ahead of machine tool designs thus being difficult to implement. Machine tool manufacturers had to provide enough power as well as smooth feed drives. The reason for this lies in the carbide tool failure when exposed to even small jerky movements in the feed direction. Once special machine tools had been designed, the self-piloting tools proved capable of maintaining close size control and producing good surface finish that met the input requirements of honing. The elimination of the whole sequence of standard operations makes

the use of self-piloting tools appealing even for machining shallow holes. Thus, the use of self-piloting tools is considered whenever one or more of the following conditions exist:

- the precision requirements - size, finish, and straightness - are difficult to attain by more conventional methods,
- the location of the hole must be held accurately with respect to other holes or surfaces,
- the material allows for a self-piloting tool to produce the degree of precision required in a single operation,
- the configuration of the part makes it difficult to index from one station to another, etc.

However, several factors contributed to the slow expansion of deep hole drilling from its first application in the armament industry into other industries such as automotive, aircraft, etc. First, there was not enough knowledge of the process available for manufacturing engineers to justify the initial capital investment. Second, the use of special cutting oil in self-piloting tools made it difficult to incorporate the operation into transfer lines. Introducing additional washing operations meant interrupting the production cycle and assigning more operators. Moreover, problems with excessive noise have been reported necessitating the full enclosure of the work station within the machine shop. On the other hand, once properly set the machines proved to be very reliable offering the advantage of better engineering control and less dependency on the skill and judgement of the operator.

1.2. Deep Hole Machining Processes

There are several hole machining processes employing self-piloting (SP) tools:

(1) SP Drilling - implies a manufacture of a hole from the solid by cutting across the whole diameter of the tool where all the material removed is converted into swarf (Fig. 1.2.a).

(2) Trepanning - means a manufacture of a hole from the solid by cutting only along the outer segment of the tool diameter, thus producing an annular groove and leaving a turned core of solid material known as the slug (Fig.1.2.b). The operation extends the application of self-piloting tools to greater diameters i.e. above 2 *ins*. The core-/or pin-cutting tools, of less then 2 *ins* in diameter, are usually considered as falling in the drilling rather than in the trepanning category.

(3) SP Boring - means boring out the existing holes with the aim of enlarging and possibly correcting them. The operation produces a hole considerably larger than the pre-drilled hole (Fig.1.2.c). Special gunbores that cut to the center may be used to form a specific shape in the bottom of the hole or between two holes.

(4) SP Reaming - employs self-piloting tools for sizing the existing holes to a close tolerance while producing high surface finish.

It is beyond the scope of this work to elaborate on each of these hole-making operations and the related tools; the work will rather deal with a particular kind of self-piloting tool i.e. a drill. However, the other tools will be cross-referenced whenever a finding implies differences in its application to those classes.

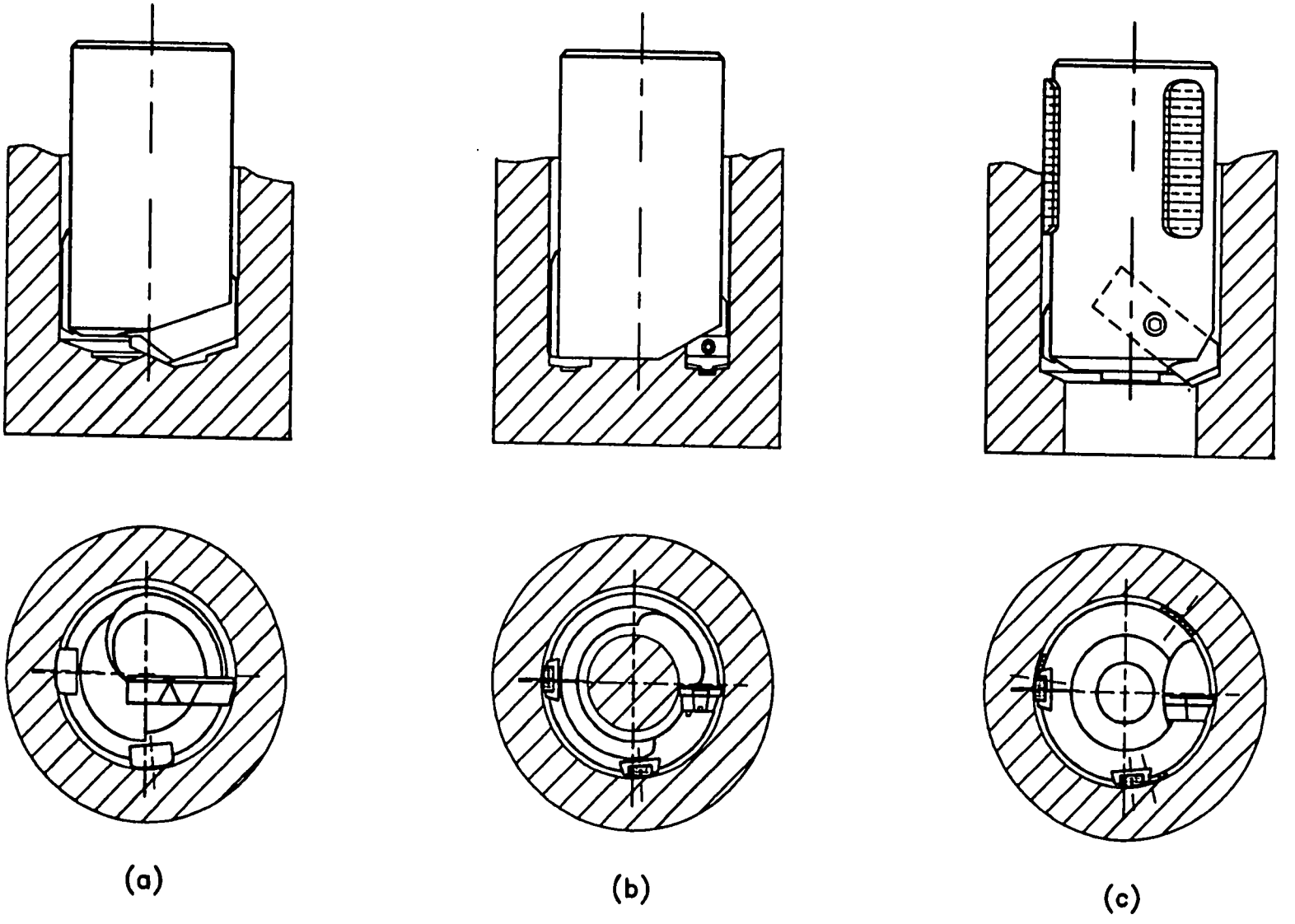

Fig. 1.3. The principle of (a) Gundrilling, (b) BTA Drilling and (c) Ejector Drilling

1.3. Self-Piloting Drill Classification

Up to date, a whole variety of self-piloting tools have been developed, each of them to suite a particular application. The place of each tool among the related designs can be recognized based on the similarities it shares with some of them and the ways it differs from others. However, no simple classification can be established. Here, only a rough and the most often used classification of self-piloting drills will be presented, together with a short discussion of the problems associated with each of the distinguished types.

Self-piloting tools are designed to produce holes of any reasonable depth in one continuous pass. This means that the chips have to be removed as fast as they are cut. To achieve this, a high-pressure type, light viscosity oil is to be introduced into the machining zone and taken out mixed with swarf at a sufficiently high speed. The way a particular design addresses the fluid circulation problem can be used to distinguish three basic types of self-piloting drills:

1. Gundrill - the fluid is pumped in through a single, kidney-shaped and V-fluted shank and forced out down the flute in the external chip removal system (Fig.1.3.a),

2. B.T.A.[1] Drill - the fluid is forced in passed the outside of a single, tubular shank and pumped out down the inside of the tube in the internal chip removal system employing a single tube (Fig.1.3.b),

3. Ejector Drill - the fluid is pumped in through the annular opening in between two concentric tubular shanks and sucked out down the interior of the inner tube in the internal chip removal system employing a double-wall tube (Fig.1.3.c).

---

[1] B.T.A. = Boring and Trepanning Association

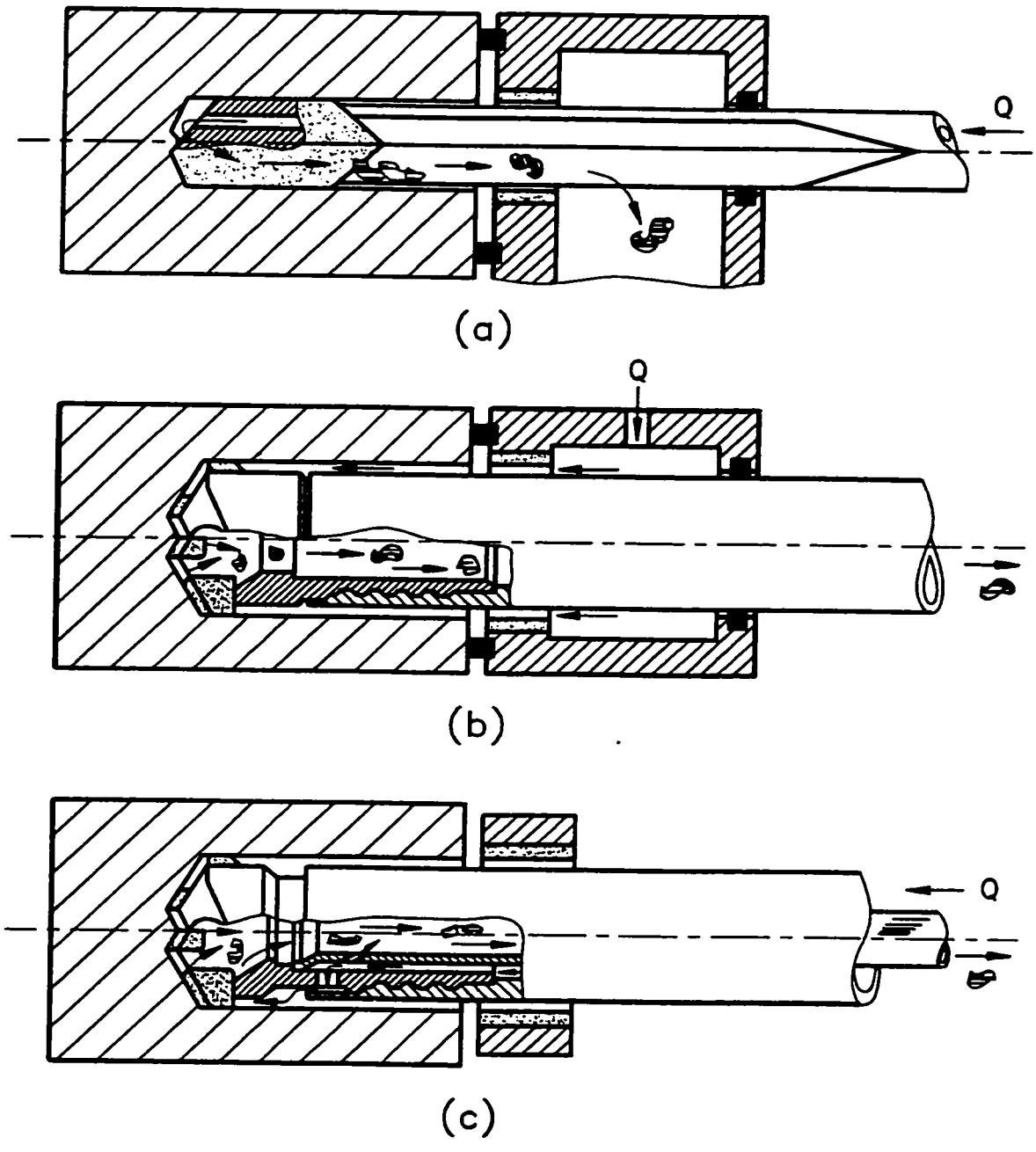

Fig. 1.3. The principle of (a) Gundrilling, (b) BTA Drilling and (c) Ejector Drilling

Gundrills offer the advantage of relatively simple oil sealing at the workpiece/drill bushing interface, since the oil at this point is not much above atmospheric pressure. Indeed, a knife edge seal integral with the drill bushing has proven successful, especially where a large number of holes are to be drilled under numerical control. BTA machining creates much more severe problems in oil sealing. Oil must first be introduced into a pressure head which contains a drill bushing and a chamfered reception plate facing the workpiece. Here, sealing at the workpiece/drill bushing interface is critical, since the seal is subjected to the full pump pressure. Moreover, the unfavorable annular section of the inlet channel presents a high hydraulic resistance thus necessitating pump pressures higher than those usually employed for gundrilling.

Ejector drills, introduced in the '60s by Sandvik Coromant Co., have eliminated the need for both the pressure head and the seal between the drill bushing and the workpiece. In this system, about one-third of the inlet flow bypasses the machining zone through the annular nozzle right into the outlet channel, moving at a sufficient velocity to set up a partial vacuum within the two chip mouths. The remaining fluid passes through a number of holes around the tool head to provide cooling and lubrication for the cutting elements and to pick up the swarf. The system relies on the sucking effect of the chip mouths to draw the fluid back into the inner tube and carry the chips away. In case of a chip jam, the oil will take the alternate way out through the gap between the workpiece and the outer tube thus causing a leak. The system allows the retrofitting of standard machines for deep hole machining operations. Recommended fluid pressures for gundrills and ejector drills vary with the length of the shank to be used, but do not depend on the hole depth. Contrary to the ejector drills, the BTA-type

tools need a considerable increase in fluid pressure as the hole depth increases. In case the chips get the outlet channel plugged, BTA systems will react favorably by raising the pressure on the obstruction thus increasing the chances of its removal.

The drill designs somewhat differ in the way they address the problem of chip control. Gundrills, owing to the ample room provided by the V-flute, favor flexible, curly chips that can be easily flushed out. The fluted shank cross-section is weak and can stand only a limited torque what imposes the upper limit on diameter and depth of holes to be gundrilled. With BTA and ejector systems, to enter the boring bar interior, chips have to pass through a comparably narrow chip mouth in the tool head which can handle only small-size or powder chips. Thus, chip size must be closely controlled to permit free evacuation from the cutting area. However, the round boring bar has less torque windup and can resist heavier feeds. This allows for an increase in feed per revolution to make the chips more rigid and the chip-brakers associated with this type of tool effective.

The carbide tips in gundrills can be easily resharpened as long as there is enough left for support i.e. almost back to the shank. Since resharpening BTA heads is much more complicated, when they have brazed cutting elements, these are considered to be of disposable type. Therefore, for small diameters resharpening costs and service life favor external chip removal drills. However, internal chip removal drills can cut 3-4 times faster thus requiring fewer machine spindles. As the applicable ranges for different tools somewhat overlap, for some diameters and hole depths the tools can be meaningfully compared.

1.4. BTA-Type Drill

Internal chip removal drill of BTA type consists of a hollow steel body with a single carbide cutting edge and two carbide support pads (Fig.1.4). These can be either brazed to the body or detachable, the former ones being used in disposable drills and the latter ones in indexable drills. The cutting element may be one-piece or partitioned. The tool is designed to balance the resultant cutting force by the counter-acting reactions on the two support pads. These have been located so as to meet two following conditions: (1) to ensure leaning against the bore at both support pads in order to achieve stability and self-guidance, and (2) to provide an optimal ratio of forces on two support pads that will lead to a high-quality surface after burnishing.

A number of studies only confirmed that the initial design by Heller (Bremen) has been right on the point. The design has the pads located at 178 and 276 degrees measured from the cutting edge as shown in Fig.1.4.b. The pads are usually termed the leading/or supporting pad and the trailing/or measuring pad respectively. While the leading pad provides the main support for the tool head by counteracting the major part of the resultant cutting force, the main function of the trailing pad is to control the hole diameter. The ratio of the two normal reactions averages 3 in favor of the leading pad [9,33]. The edges of the pads are relieved to specific angles to form the ramps and the leading chamfer both of which play the major role in burnishing. The pads are usually made of carbide of a different grade than that used for the cutting element. The drills with partitioned cutting edge offer the advantage of using different carbide grades at various radial distances. The tool point is slightly offset from the axis of the tool head to avoid zero velocity and to ease extrusion conditions on the inner cutting element.

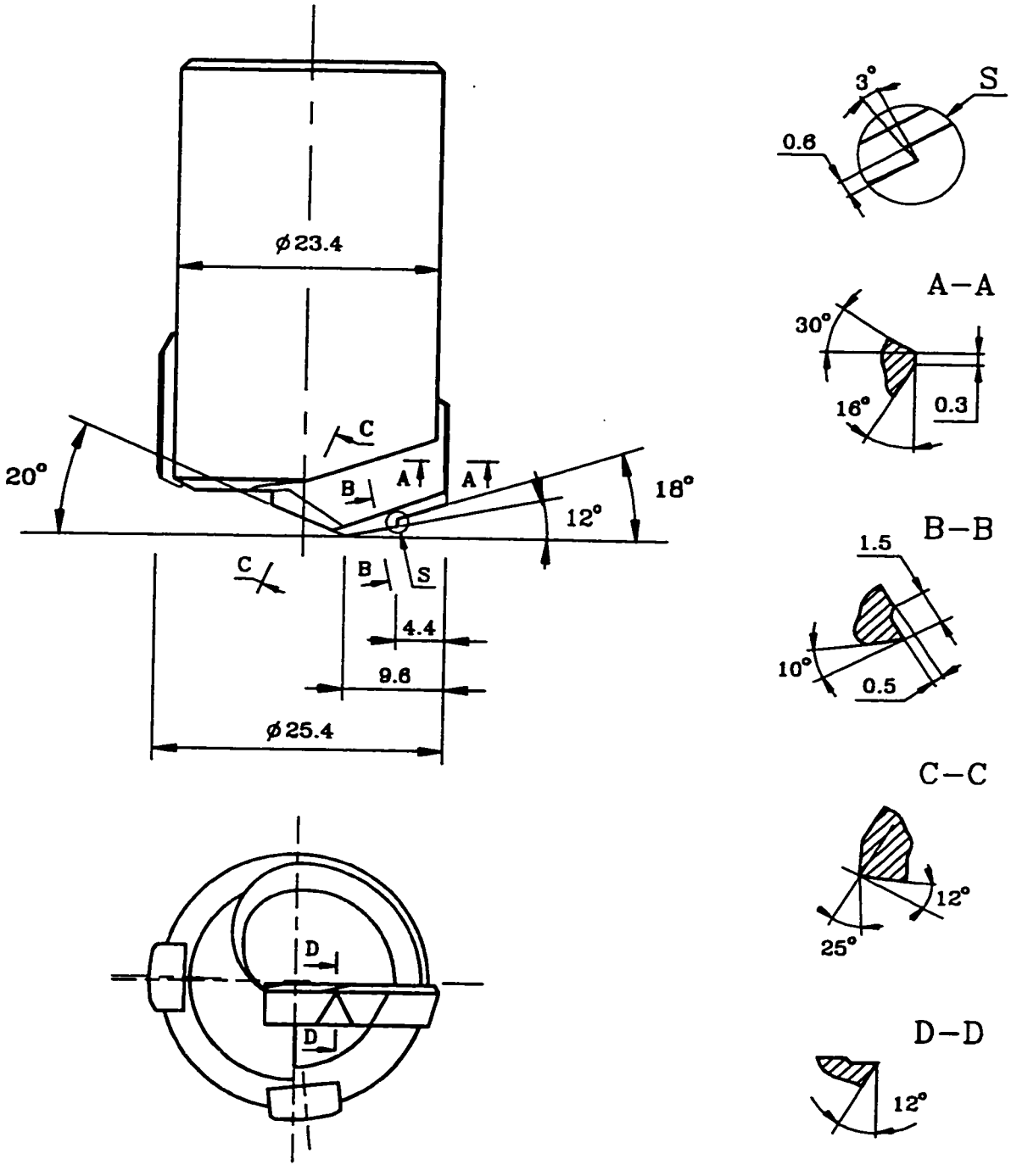

Fig. 1.4.a. BTA-Type Drill of Heller Design (Cutting Geometry)

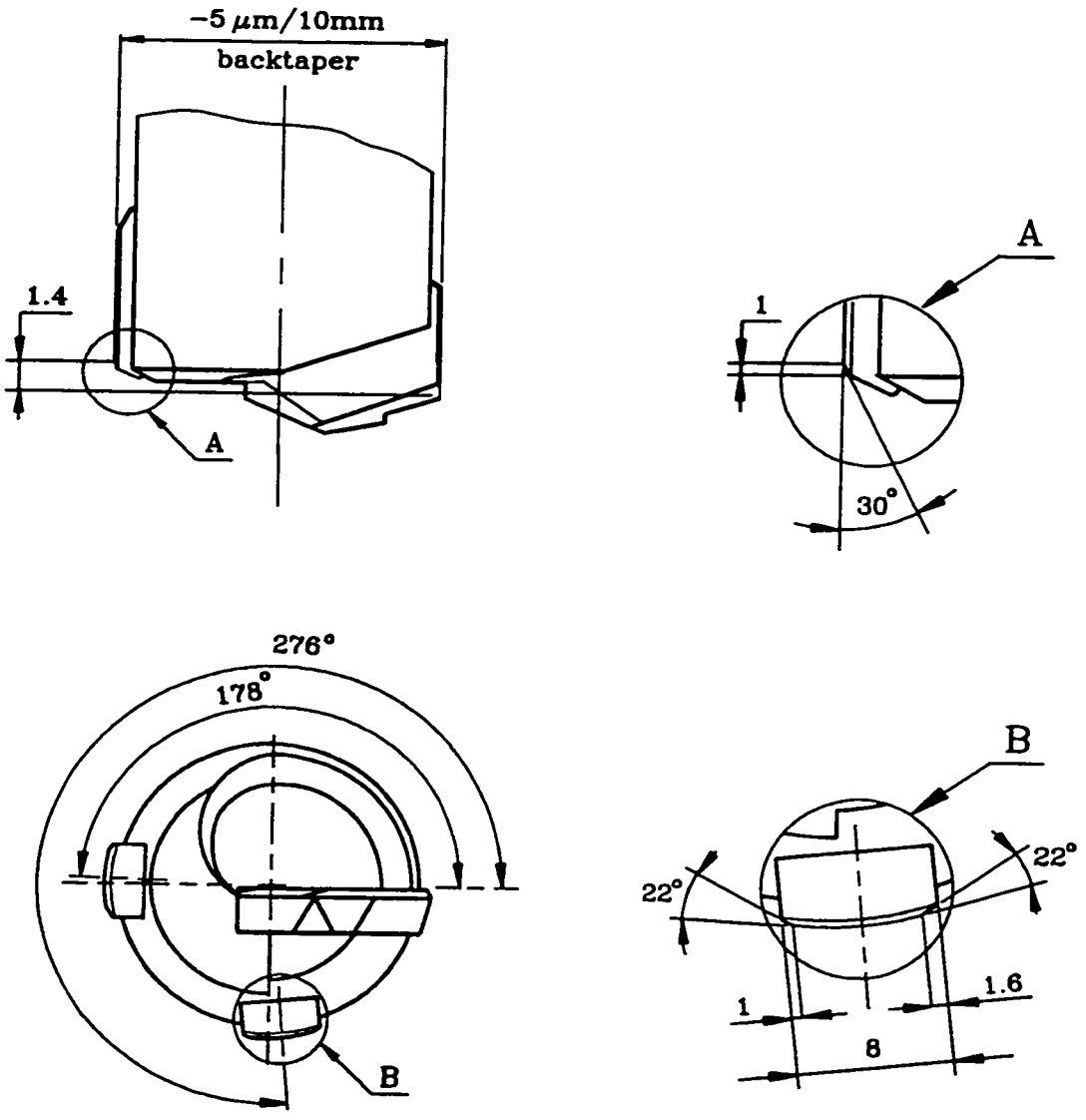

Fig. 1.4.b. BTA-Type Drill of Heller Design (Burnishing Geometry)

Nevertheless, to prevent its failure, the inner edge has to be strengthened by introducing a negative rake angle. To obtain chips of a manageable size, chip separators are employed dividing a one-piece cutting edge into steps. The number of steps is two or three depending on the tool diameter. To facilitate forming of favorable C-shape chips, chip breakers have to be used together with a sufficiently high feed per revolution. The smaller the tool, the more significant the tool geometry becomes, because of the diminished space available for chip ejection.

The inner and the outer cutting angle intersect at the nose tip which is located about 1/4 of the drill diameter away from the margin. At the nose tip, the chips sheared by the two angles impinge on each other to help themselves break. The compression produced as the two chips meet results in a heavy backbone especially if the included angle is not large enough.

The flank side is relieved twice to form a small primary clearance followed by a larger secondary clearance. The primary clearance serves to strengthen the cutting edge. The secondary clearance provides the access for the cutting fluid to lubricate and cool the cutting edge. High-pressures exerted on the flanks make the use of a cutting fluid with excellent lubricating properties imperative for drilling a ductile material. The flank geometry plays the major role in preventing heeling as a cause of premature tool wear and failure. For optimal tool performance, the angles and lengths have to be varied depending upon the material to be drilled.

The tool connects to the boring bar by means of a flat internal thread and two shoulders. The shoulders serve to assure centering of the tool with respect to the shank. The face of the

smaller shoulder transmits the thrust force while the thread is to transmit the torque only. Once the drilling forces start acting on the tool, the connection becomes very rigid and the tool behaves as a solid extension to the boring bar.

1.5. Deep Hole Drilling Machine of BTA Type

Though this section is mainly to describe a particular machine tool that was used for this work, it will also outline the features of the machine tools for deep hole machining operations in general.

The machines show a clear descent from the center lathe, though they have to meet some special requirements. In view of the high penetration rates associated with the self-piloting tools, the machines have to provide ample power and to be sturdier in construction, especially if work-hardening materials are to be drilled. They require an extended bed at least twice as long as the maximum length of the workpiece to be drilled. To maintain optimum machining rates and to get the best out of a relatively expensive machining operation, the machines have to provide a close control of cutting conditions. This usually means a smooth and infinitely variable feed drive and speed control. This applies to both drive units if the machine is to provide both the work rotating and the tool rotating method. The machine used for this work (Fig.1.5) has been equipped with three AC inverters to fully meet that condition. The spindle designs have to feature high-precision bearings to operate at the highest anticipated speed with an absolute minimum of end play. Because of the small feeds employed, the absence of

any spindle end play is imperative to prevent the tools from cutting a variable thickness from one to the next revolution.

All aligning elements, including the drill bushing liner and the reception plate, have to be integral with the machine, not part of fixturing, in order to attain a near-perfect alignment. Another special feature of these machine tools is a cutting fluid recirculation system incorporating both filtration and cooling facilities. The system used here has been equipped with the whole line of filters, including mesh-type, baffle-type, magnetic-type and eventually cartridge-type filters capable of separating particles down to 5 micron size. Pumps have to be capable of delivering pressures as high as 7-8 MPa for small diameter tools and longer holes, as well as flow rates as high as 200 l/min when drilling bigger diameters. In view of these requirements, especially for a research facility accommodating a range of diameters and different tools, pumps with variable flow rate are preferred over those with constant flow rate. The pump unit is separate from the machine and connected to the pressure head assembly by a flexible line to prevent the transfer of vibrations to the drill itself. The system handles 3,000_l of special chlorine-free oil: Castrol Almacut 534.

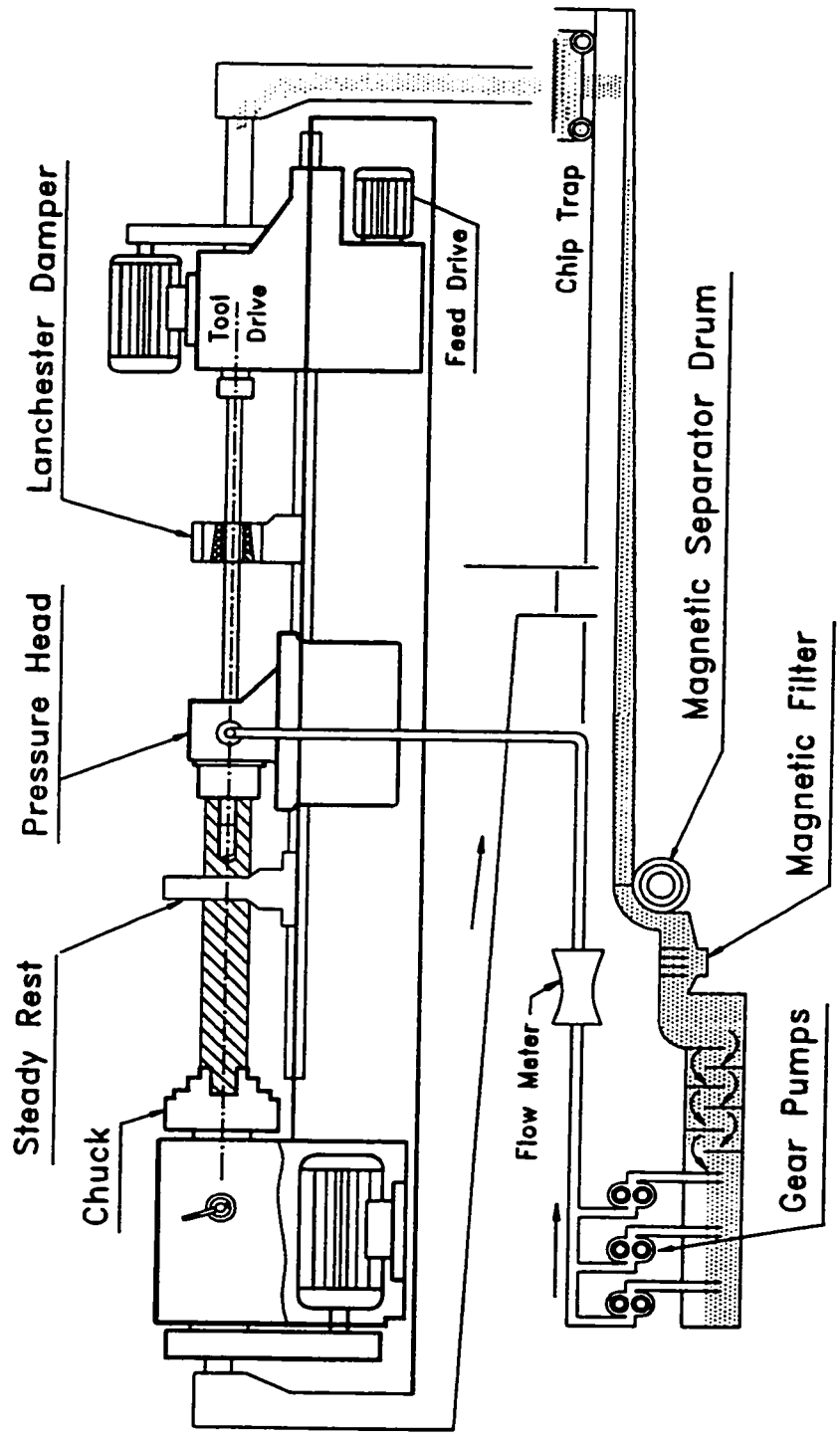

Fig. 1.5. Machine Tool for BTA-Type Deep Hole Machining

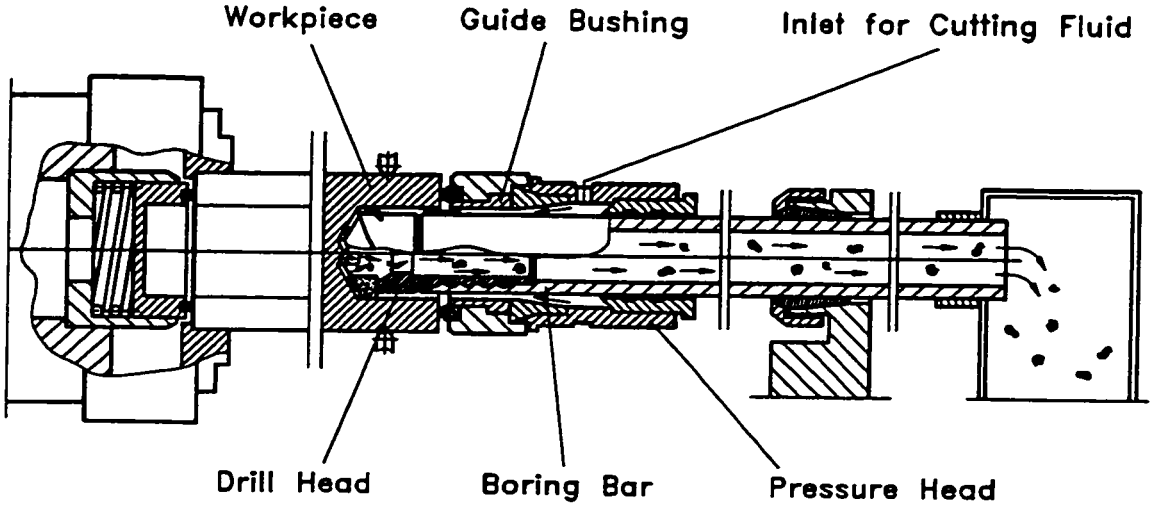

Fig. 1.6. Setup for BTA Drilling Process

1.6. Working Methods

In principle, the machining of deep holes can be realized in the following systems:

1. Tool Rotating System - the tool rotates while being fed into a stationary workpiece,

2. Workpiece Rotating System - the workpiece rotates while a non-rotating tool is fed in,

3. Counter-Rotating System - both the tool and the workpiece rotate in opposite sense while the tool headstock traverses along the bed.

Occasionally, if the machine available has a traversing table, the workpiece is fed in. The workpiece rotating scheme is applicable for small, symmetrical pieces that can be held in the chuck. Since the workpiece is heavier than the tool, rotating workpiece requires a considerably heavier and more expensive spindle. This is because the spindle has to provide more power while featuring a negligible end play. In addition to that, when the workpiece rotates, the spindle has to be stopped for loading and unloading. Thus, if the drilling time is short compared to floor-to-floor time, the workpiece rotating setup is not economical. On the other hand, this method is known for small runouts of deep holes. The tool rotating method not only requires a less expensive spindle but is also the only possible for the large workpieces of complex shape that cannot be held in the chuck. The counter-rotating scheme is sometimes used for drilling small diameters with two spindles, each of which is not capable of high-enough speed to be used alone. Little data are available regarding this method, though the comments attributing the best results to the method are not uncommon.

Chapter 2

Previous Work

2.1. Literature Review

About 35 years ago, deep-hole tools designed empirically were already known for giving a superior performance provided the right process parameters could be chosen. The costly method of trial-and-error was used to relate the process parameters to the output quality in each particular application. Since the results varied from one occasion to another, people recognized the need for systematic research of the principles governing the performance of the deep-hole tools. Soon, it was acknowledged that the special design of the tools featured the unique self-guiding action as well as the unique combination of cutting and burnishing. The following work has covered numerous aspects of the tools, but as the review of the related previous research will reveal, the most of it has been descriptive, merely explaining the empirically designed tools.

The work of Greuner [11] was the first breakthrough in deep-hole machining force measurements. The author measured cutting forces using a dynamometer integrated in the machine tool setup between the drill bushing and the workpiece. Thus, the forces were recorded over the entry period while building up from zero to their steady state values. He pointed out the mutual action of the cutting edge land face and two pads as being responsible for the "bell mouth"creation. He made no attempt to separate the individual contributions of these. He emphasized the study of the clearance in the drill bushing implying that the entry period was the most critical and would affect the tool performance down the hole. He quoted

the force ratios as being 2:2:1 (F_C:F_T:F_R) and, because the thrust (F_T) was so much higher than expected, he suggested that a reassessment was necessary of the layout and rigidity of the deep hole drilling tools, machines, jigs and fixtures.

Soon after Greuner's work, the attention diverted towards the conditions encountered down the hole. Many researchers [33,34] applied strain gages to the compliant shank to measure the thrust and the torque when the drill is deep in the workpiece. The work of Weber [37] revealed the separate contributions of the cutting edge and the pads to the measured torque as being ca. 65% and 35% respectively. The author even attempted to separate the contribution of burnishing from that of friction by measuring torque when redrilling a hole plugged with the bar of the same material. Weber's work stands out as a major attempt to measure forces at the point of cutting rather than at a remote point, since he integrated small load cells in a BTA drill head right beneath the cutting edge. He, as well as Stockert [33], acknowledged the difficulties inherent to the pad forces measurement and suggested to resort to their theoretical modeling. Revealing significant energy consumption by the pads, Weber aroused other researchers' interest in the pads and the burnishing process.

It was Griffiths [17] who distinguished between the effects of each of the burnishing pads and the cutting edge land face. To prevent the drill from changing the machined surface while being disengaged, the author designed a quick stop device to retract the drill almost instantaneously. He provided a number of micro-photographs showing the changes the hole surface underwent at each of the elements involved in burnishing. Griffiths showed that the plateau-valley surface form obtained in deep hole burnishing was unique when compared with

surfaces burnished by conventional tools employing balls or rollers. When studying the effect of speed and feed on various surface integrity measures, he found that, except for the hardness, all other properties featured so much scatter that "trends could not be suggested with confidence". Thus, Griffiths has indirectly showed that the conventional BTA tool design does not feature stable burnishing conditions.

The following work seems to have taken a new direction considering mainly the out-of-roundness error. In 1971, Troicky *et al.* [36] described the effect that was going to be termed later as "spiraling". The authors recognized the mechanism of multi-lobe formation that led to the creation of multi-start grooves in the walls of deep holes machined by self-guided tools. According to them, the grooves tended to form when using tools with improperly located pads at low cutting speeds. Owing to an optical effect, the grooves sometimes could be easily seen by the naked eye. The authors observed spiral patterns with a skew varying from the left to the right for the same direction of tool rotation. In rare cases when straight, meaning along the hole axis, the grooves appeared to be even more pronounced. The authors even managed to produce a spiral with a changing skew by gradually increasing the length of the boring bar from 1 to 2m while machining. As the authors noted, once the tool started grooving in a spiral manner the phenomena tended to keep up till the end of the hole, thus indicating a self-reproducing mechanism. The authors even tried to bring the out-of-balance tools to stability by incorporating the third pad in different angular positions, even a pad on an elastic support, which proved to be ineffective. They did not report any change in the number of lobes along the holes. They also did not comment on the repeatability of the phenomena. They claimed successful suppression of spiraling by using an additional row of support pads to carry an

elastic support for the boring bar. Though they found the phenomena interesting, the authors did not claim it to be a significant problem. Even if the grooves were produced, in most cases they could be removed by honing. Moreover, when machining 1.5m-deep holes in a variety of materials at higher speeds (up to 200m/min), with properly balanced tools (including two- and three-lip tools), the authors could not induce the multi-lobe formation mechanism.

Pfleghar [22,23] initiated a series of papers which tried to establish the design criteria for ensuring the static stability of the self-guided tools. He presented a comprehensive analysis of the forces acting on the tool, first on a gundrill, then on a multi-insert BTA tool. He clarified the role of the support pads in balancing the cutting forces. He emphasized the need for meaningful location of the support pads to ensure stability in the presence of the dynamic component of the resultant cutting force. Pfleghar was the first to consider the tilting of the tool around the leading pad as instability, thus relating instability directly to the change in hole diameter. Performing experiments with gundrills, the author showed that the location of the support pads was related to the tendency of the tool to oversize or undersize the holes. Applying statics, he introduced a quantitative measure of tool stability as the ratio of the moment trying to keep the trailing pad pressed against the bore versus the moment tending to lift it up. The author calculated that the tool design with the maximum degree of stability would lead to the forces at the leading pad twice as high as those at the trailing pad. To obtain the first estimate of stability, the author measured cutting forces using simple strain-gage based transducers. The work has been broadly recognized as the first attempt to ensure stability at the tool design stage.

The work of Stockert and Weber [32] is the same Pfleghar's analysis applied to the BTA tools. They backed up his conclusion that supporting the tool with two pads should be enough to ensure stability. Interesting enough, they found the application of the third pad to be unable to balance a tool with the other two pads improperly located, thus confirming the experience of Troicky [36]. When justifying the need for their work, the authors named shiny spiral traces ("Drallerscheinungen") and hole runout as undesirable effects of machining deep holes with tools which do not meet the stability requirement set by Pfleghar [23]. From their experience, they assumed 10% change in the cutting force when analyzing the safety margin of the tools' stability.

Stockert [33] conducted the first vibration measurements to show the main contribution of the self-excited torsional vibrations of the boring bar to the increasing dynamic load on a deep hole machine tool. According to his work, in a broad range of cutting conditions no natural frequency characterizing the boring bar bending could be excited. Thus, the lateral vibrations of the boring bar were forced by the cutting process conveying energy from the self-excited torsion to bending. The conclusion was backed up with a figure showing coinciding peaks in two spectra taken from the transducers measuring torsional and bending vibrations simultaneously. Interesting enough, the same idea of the cutting process providing for the transfer of energy from one type of vibrations to another can be found in the work on the workpiece chatter in turning [7]. Furthermore, Stockert claimed additional support of longer boring bars to be effective enough in suppressing excessive bending vibrations.

Streicher [34] tried to account for the self-excited torsional vibrations of gundrills by introducing the idea of a decreasing Drill Torque-Cutting Speed relationship. Based only on the measurement of the cutting torque *after* the onset of self-excited torsional vibrations, he assumed a great variation in cut, which would mean that the lower limiting values of the relative cutting speed take negative values. Obviously, this would introduce "negative damping" into the system. However, when trying to account for the vibrations of BTA tools by the same cause, Weber [38] could measure only increasing Torque-Cutting Speed characteristics thus denying Streicher's conclusion. Weber also found that, when the self-excited torsional vibrations build-up, a significant dynamic component is superimposed over the static cutting torque, while on the other hand, the cutting forces show comparatively small variation. Thus, Weber concluded, that at least in the case of BTA type tools, the cut is more stable than one might infer based on Streicher's research. To improve stability at higher feeds, a Lanchester damper was applied to the b.bar which gave an off-set to the onset of chatter.

Further, Stockert [33] introduced the idea of spiraling ("Drallbildung") as being a dynamic problem in machining deep holes. He also recognized the formation of hole profiles that more-or-less resembled multi-corner shapes as phenomena behind it. Both effects were encountered while machining steel. The author emphasized the crucial role of the self-guiding principle and tool geometry as opposed to the other approach neglecting this and emphasizing the self-excited vibrations of the boring bar. In that context, he drew the attention towards the bending rigidity of the boring bar, which the authors of some later works seem to have misunderstood. Stockert was the first to try measuring the forces on the support pads, which led to the explanation of spiraling as the result of the tool tilting around the leading pad and the trailing pad losing contact with the machined surface.

Sakuma *et al.* [28] tried to explain the formation of lobed holes in BTA drilling by exploiting the idea of boring bars being naturally weak at very low frequencies (50-150 Hz). They pointed out the problem of modeling the stuffing box as a support, as well as that of accounting for variable overhang of the boring bar while machining. Even if the rigidity of the setup was assumed to be as low as presented, the hypothesis could not account for the same effect when using boring bars of other diameters, let alone those of other lengths. To account for the fact that different number of lobes can be produced with the same boring bar (as shown by Stockert), the authors took the stuffing box to play a significant support thus emphasizing the variable overhang and its effect on the changing natural frequency in bending. Continuous increase in overhang should lead to continuous change in natural frequency, thus making the number of lobes change along the depth of the hole. No later study reported such a pattern. Moreover, Sakuma *et al.* claimed possible the formation of only odd number of lobes. In addition to that, they determined the frequency of the setup out of cutting thus denying any support at the cutting tip. Finally, the authors avoided to include the discussion into their conclusion, although they based the whole article on it. Moreover, despite finding the low natural frequencies in bending to be responsible for multi-lobe formation, they documented their occurrence by showing the matching peaks in the spectra of torsional vibration. They claimed the pronounced multi-lobe formation occured only at greater depths but conducted tests with shallow holes. To help formation of multi-lobe holes they changed the geometry of the tool by narrowing the width of the pads. In addition to that, the authors used pre-drilled holes to support the tool at the entrance. For no reason, they resorted to machining duraluminum at very low feeds . The only result of the work might be that the

formation of multi-lobe hole profiles can be observed by changes in the spectra of torsional vibrations. That might be understood as being in favor of a more extensive use of frequency domain functions when investigating the dynamics related problems in deep hole machining.

In their following work [29], Sakuma *et al.* investigated runout in deep holes drilled under different (mis)alignment conditions. The runout was measured on holes drilled with (a) a misaligned guide bushing, (b) a misaligned additional bar support, (c) an off-set prebored hole, (d) the inclined workpiece face, and with (e) a one-side-thin workpiece. As the authors kept changing between gundrills and BTA drills when running experiments with different setups, the work has no clear reference to a particular type of tool or tool geometry. They re-confirmed the well-known superiority of the work-rotating over the tool-rotating method in terms of reducing the hole runout. As they showed, in both cases (a) and (b), once the tool took the inclined direction it tended to keep it at least over a 200mm -depth which they chose to drill. Sakuma *et al.* found the low bending rigidity of the boring bar to be the major cause of the tool sensitivity to misalignment. On the other hand, they did not provide any information on the rigidity of the boring bar they used in the experiments.

In their subsequent work on BTA-type tools [30], Sakuma *et al.* moved the emphasis completely from the boring bar towards the support pads and burnishing. The authors recognized the inherent difficulty of distinguishing between the cutting and the burnishing process occurring together in real machining. They tried first to keep the methodology simple and to deal only with the burnishing process. They made a model tool with only one pad which was used to burnish carefully prebored holes while measuring the burnishing forces.

The authors confirmed Griffiths conclusion [17] that final feed marks on a burnished surface are made by the pads. Moreover, they found that heavier loads on a burnishing pad would cause the burnished surface to become more wavy thus affecting the hole diametral accuracy. The authors failed to show how well the results obtained by using the single-pad model tool could be related to the burnishing on the real tool pads occurring simultaneously with the cutting on the tool margin. The reason is that they again changed from burnishing steel by means of a BTA tool to burnishing duraluminum using the model-tool. They did so for the excuse of getting "good machinability and less tool wear". Afterwards, they used a formula proposed by Tabor in cold working to calculate the depth of burnishing. They made an attempt to calculate the hole oversize based only on the geometrical considerations of the sinking of the burnishing pads. Here, they emphasized the role of the leading pad as providing for the major counterbalance to the cutting force as opposed to the trailing pad that carried only minor load. Finally, they ended up concluding that "experimental value is smaller than theoretical value" and suspected not enough knowledge of the contact conditions to be the reason. They neither explained how they measured nor how significant the difference was. However, this paper confirmed the general feeling about the burnishing process as being extremely sensitive to the small changes in tool geometry.

Chandrashekhar [4] took a theoretical approach towards the dynamics of a deep hole machine tool. He calculated the drill torque without accounting for the burnishing process and with no reference to a particular tool geometry. When contemplating over the dynamic model of the machine tool, the author started with numerous springs and dashpots only to end up with the boring bar and vague boundary conditions. With a view of the machine tool as a stochastic

system, he presented a stream of analytical expressions with often missing nomenclature thus making it impossible for a reader to follow. A little measurement that was attempted resulted in frequency spectra with wrong dimensions etc. When attempting the analytical modeling of the tool tip motion, the author overlooked the major fact that the underlying theory could not solve much simpler problems. The work did not offer any conclusion which could by any means be related to the deep hole machining practice.

The work of Gessesse [10] addressed the problem of multi-lobe formation and spiraling. As the author admitted, to produce the grooves that resembled the "spirals", he had to resort to the usage of either defective tools or reground tools with an excessive margin. Thus, the author has implicitly showed that commercial BTA drill designs, as far as out-of-roundness error when machining steel is concerned, give a stable performance. This conforms to the fact that, after Stockert, many researchers did not name spiraling to be a common problem. The author overlooked the fact that ensuring trouble-free machining with defective tools could not be a goal. He repeated the explanation of Stockert [33], as well as that of Sakuma *et al.* [30]. The latter hypothesis does not hold for the reasons already named. The work suffers from the same problem of not providing the dimensions of boring bars whose dynamic properties were cited. The presented power spectral densities have wrong dimensions which implies the problems with the measurement methodology etc.

Jin-Hua and Li-Wei, in their work [18], demonstrated the elemental capabilities of the modern facilities for modal analysis. They performed experimental modal analysis on a "boring bar" hanged on two strings (free-free boundary conditions). By applying Euler beam theory they

calculated the natural frequencies in order to verify the theory. They overlooked the fact that same examples verifying the theory for simple cases of beams could be found in almost any textbook. Since the same mode shapes and natural frequencies would have been obtained if they had used any steel pipe of the same dimensions, the setup could by no means be related to a boring bar and a deep hole machine tool.

A. Katsuki *et. al.* [19] offered another proof of the current trend of moving the emphasis back from the shank towards the tool geometry. They presented an original idea of using a convex-shape cutting edge in a gundrill design when greater values of the outer angle were necessary. The idea was to balance radial forces this way, which could easily be realized by modern technology. Though there might be other problems such as chip breaking etc. to be solved in order to develop the design, the authors have showed the direction and pointed out that there is still great potential in changing the tool geometry. As far as the hole accuracy is concerned, the work has re-confirmed that the hole profiles with even number of lobes are just as possible as those with odd number of lobes. In addition to this, the authors seem to have achieved a stabilizing and lowering effect on hole oversize. However, the authors did not pay any attention to the shank rigidity.

Though the need for a systematic study of the cutting regime, tool wear and quality in deep-hole machining was recognized (Fink [8]), there have been few works covering this problem. Fink considered a tool life criterion based on flank wear or cutting edge chipping, whichever occurred earlier, to arrive at the optimum cutting conditions. Griffiths [15] related drill life to the mean flank wear of the cutting edge, assuming the critical value of 0.5mm. He pointed

out that the choice of cutting data should not account for the minimum wear only, but for the chip formation, the required dimensional accuracy and surface integrity, as well. In an attempt to evaluate different tool materials, Sakuma *et al.* [27] considered the flank wear growth at each cutting edge together with the changes in cutting torque, thrust and surface finish. Osman *et al.* [21] compared the wear occurring at the cutting edge, the pads and the circular land to formulate a relative performance index which would be useful in evaluating different cutting fluids. Grieve and Griffiths [12] brought out the significance of the support pad wear and incorporated it, together with the cutting edge wear, into a cost model to carry out the economic analysis. Rao and Shunmugam [25] studied the effect of speed and feed on the rake-, flank- and pad wear. The same authors [24] investigated the effect of speed and feed on different measures of dimensional accuracy and surface finish. The study also considered the quality variations along the hole. The work of Lukic [20] tackled the influence of speed and feed on the roughness and the hardness of BTA drilled holes. The work also included the study of the effect of pad geometry and pad material on the bore quality. Fuss [9] covered in a very thorough manner the effect of various burnishing process variables on the hole quality and the pad wear. In addition to the changes of the pad radius and the pad ramps, which were covered by Lukic too, the work of Fuss encompassed the leading chamfer geometry and the pad coating as well.

2.2. Summary of Achievements and Problems in Deep Hole Machining Research

At this stage it might be appropriate to give a short summary of previous research in the area of deep hole machining. The review in Sec.2 has not covered all the work in detail, but the intention is to include fully only the work that can be, or has been declared to be, related by any means to the dynamics of self-guided tools and burnishing. The review could, of course, encompass only the results available in the open literature, thus leaving room for speculation on what has been achieved so far by research done for industry, especially that involving military programs. The very existence of that independent line of research might in part explain why academic research frequently appears to be lagging behind the practice. As the research deals with metal cutting tools developed empirically, it often merely explains different aspects of a tool that, in general, performs very well. The most probable reason why the problem does not suit the academic environment is the high cost of research. The cost can be readily explained by (a) a great number of parameters in the system, most of them influencing one another, (b) the unique combination of cutting and burnishing action, (c) the difficult access to the tool tip causing measurement problems, (d) the high cost of machining (high penetration rate, expensive tools, accessories, oil etc.).

The systematic research began in the late 60's to result in a number of good works, most of them done by German authors and Griffiths (UK). These works presented first dynamometry considerations in deep hole machining. Reasonably good estimates of forces and torques encountered in deep drilling have been obtained. The measurements have covered both the

tool entry phase and steady machining deep in the hole. The role of tool geometry in assuring the unique self-guiding action has been recognized and reasonably well explained in 2D. Significant energy consumption by the burnishing process has been revealed. The first attempts have been made towards understanding of the burnishing process and its effects on the bore surface integrity. The individual roles of each of the support pads and the circular land have been explained. The plateau-valley surface form produced by deep hole tools has been compared with the conventionally burnished surfaces. The difficulties inherent to the pad forces measurement have been pointed out and their theoretical modeling has been suggested. A great scatter in different measures of surface integrity has been observed, making it difficult to evaluate pads' performance for different speeds and feeds. Hence, to investigate burnishing, researchers have resorted to the use of special setups for burnishing carefully prebored holes. The results obtained have brought out the awareness of the high sensitivity of the burnishing process. The difficulties to relate the results to the real tool performance have been attributed to the obscure knowledge of the real tool contact conditions.

Self-excited torsional vibrations have been identified as the main cause of the increasing dynamic load on a deep hole machine tool. To ease the problem, researchers simply applied a Lanchester damper to the boring bar setup to dissipate the energy through friction. No details have ever been provided on optimal dimensioning, tuning and positioning the damper. Even less is known about another type of damper that industry adopted to use between the boring bar and the driver. Relating excessive vibrations to the tool geometry and the cutting regime has never been attempted.

The original objective of the research appeared to be trouble-free drilling at higher feeds with longer boring bars. The attention diverted from the maximum penetration rate when research introduced the problem of multi-lobe formation and spiraling. Both phenomena were recognized first as occurring when using the tools with the inadequate location of the support pads, to be later misunderstood for a common problem with no reference to the tool geometry. Moreover, some researchers started attributing the problem to the machine tool setup. No work has provided a clear reference to the conditions bringing "spiraling" into effect nor has reported whether the phenomenon could be repeatedly reproduced under those conditions. It appears that the research started taking off the firm ground. Rare became the works on the cutting regime, tool wear and hole quality considerations. Little has been done to show what difference in dynamics has been brought by the prevailing use of tools with partitioned cutting edge or multi-edge tools employing different balance principle.

Thus, over the last 25 years, the research has brought little new to the deep hole machining practice. The credit goes to Beisner who's initial idea of the tool design has proved to be a perfect application of carbides, which after accommodating only minor changes has been able to meet practical requirements over many years.

2.3. Main Conclusion Drawn Based on Literature Review

As shown in Sec.2, there has been a lot of confusion in the research area addressing what is usually referred to as "the dynamics of deep-hole tools". Despite the lack of systematicity, the research has undoubtedly shown that, in terms of dynamics, the deep-hole machining tools introduced a new dimension when compared to the tools in turning, milling, conventional boring etc. The problem of ensuring stability in machining deep holes comprises the problem of stability encountered in general machining and more. That "more" refers to the specific conditions that make the deep hole machining processes special.

First, the tool is specially designed to allow for what is known as "the self-guiding action" (or "the self-piloting action"). Second, while guiding itself against the bore being machined the tool is mounted on a comparatively weak boring bar. These two features have been recognized as the main landmarks as far as the dynamics of the self-piloting tools is concerned.

The striking feature of the research addressing the dynamics of deep-hole machining tools is constant moving of the scope from the tool geometry to the boring bar, and back. All papers took sides claiming either tool geometry or the rigidity of the setup to be a decisive factor governing the performance of the tools. This is because, in reality, the tool, with the cutting tip balanced in 2D to the best of the available knowledge, enforces a motion on the weak boring bar thus making the boring bar take a role in guiding the tool. So far, it has not been explicitly acknowledged that:

- The unique self-guiding action of the tools is the result of the interaction between the tool geometry and the boring bar rigidity. Thus, to ensure stable tool performance, all analytical models should consider the tool, the bar and the piloting hole *together*.

2.4. Scope of the Work

This work is to provide a SP tool designer with practical guidelines for ensuring steady burnishing action and high output quality at the tool design stage. To outline the shortcomings of the conventional design, for the first time, the tool balance considerations will be extended beyond the transverse plane to include the tool effective inclination in 3D. The study should provide an explanation of the support pads' wear pattern and offer a comprehensive model of the tool head support in the machining zone. The model is to emphasize a new approach considering the tool head geometry and the force system together with the boring bar setup arrangement. The focus will be on the factors determining the effective tool mating with the piloting hole and the effective contact area involved in burnishing. In that context, the significance of changing various tool design parameters at the tool design stage will be estimated and compared with the contribution of in-process encountered effects which are beyond the tool designer's control.

The work will also include an attempt to explain one aspect of the fundamental difference between the working methods as these appear in the deep hole machining practice. The conclusion will, in principle, point towards a new layout of self-piloting tools which should make the tools perform virtually the same in out-of-ideal machine shop conditions regardless of the method used.

Chapter 3

Self-Piloting Tool Support Model

3.1. Burnishing

Burnishing is a unique machining operation typical of deep-hole machining tools. As already explained in Sec.1.4, owing to the suitable location of two support pads with respect to the cutting edge, the resultant cutting force will cause the tool head of BTA type to lean against the bore wall thus balancing the tool (Fig.1.1). Furthermore, this will result in heavy rubbing of the support pads against the hole being machined which is referred to as "burnishing". Since cutting takes place ahead of burnishing, its only role is (1) to brake the volume of material ahead of the tool into chips of favorable shape which can be easily evacuated down the flute, and (2) to provide the force input to the following burnishing action. Therefore, being performed the last, it is the burnishing action that has decisive effect on the final hole quality. It should be noted, however, that the cutting margin plays some role as well, by cutting very fine chips, which is referred to as "shaving". Actually, as the past work has shown [17,30], shaving is nothing but truncating the crest formed in front of the pads as part of the burnishing process. Thus, the output quality is produced by the joint action of two support pads and the cutting margin. This is best emphasized by extensive wear studies which found that the trailing pad can even take over the role of a worn-out cutting margin, performing shaving under difficult conditions, to allow just enough time for the tool to finish a hole before being changed [9].

Over the last 20 years, because of its undeniable importance, burnishing has been subject to

an extensive research by Sakuma et al.[30], Griffiths [17], and a number of German authors [9,39]. The research covered various aspects of the input to the burnishing process such as pad material, pad coating, pad geometry and pad forces. Burnishing was performed both with real tools equipped with transducers and with special measuring setups designed for "pure" burnishing on carefully prepared surfaces. The study has shown that the burnishing action takes place at the step-like transition from the leading chamfer towards the rounded surface of the pads. Therefore, the deformation occurs only along the 2-3mm-long front end of the pad thus involving extremely high pressures, which is also revealed by the pad wear marks (Fig.3.1). The results surfaced out the fact that burnishing output, especially hardness and some measures of surface integrity, feature high sensitivity to minor changes in input to the process, for example pad coating or pad geometry. This is easy to understand, since a minor change will appear significant in the small forefront working area of the pad affecting heat generation, "sticking" occurrence, and other phenomena [17]. Moreover, the sensitivity is so high that researchers have found it difficult to fully reproduce results obtained with a special setup or a real tool using another tool or another machine tool. Therefore two conclusions may be drawn:

- Since the quality requirements for holes produced by self-piloting tools are defined in terms of micrometers, the geometry considerations should account for the changes with the same order of magnitude, and

- Inaccuracies encountered in deep-hole machining practice make a difference between the "effective" tool geometry involved in the burnishing process and the ideal tool geometry as designed.

This work cannot afford elaborating on the numerous studies on burnishing, so it will rather refer only to particular results which relate to what will be presented later. Here, to support the conclusion about high sensitivity of the burnishing process with respect to the tool geometry, a closing remark from the work of Fuss [9] is quoted as follows: "The first condition to be met in order to achieve quality deep holes is the exact manufacture of the ideal tool geometry i.e. the assembly joining the tool body with the cutting elements and the support pads" (the author's translation of the original text being:" Erste Voraussetzung fuer the Guete von Tiefbohrungen ist die exakte Einhaltung der idealen Werkzeuggeometrie bei der Herstellung bzw. bei der Bestueckung des Werkzeugs mit Schneidelementen und Fuehrungsleisten").

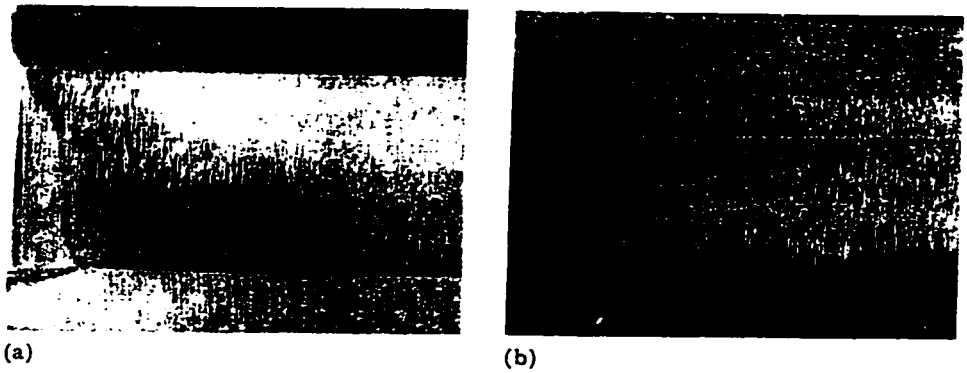

Fig.3.1. Wear Marks at (a) Leading Pad and (b) Trailing Pad [25]

3.2. The Accuracy of Self-Piloting Tool Location within the Piloting Hole

3.2.1. Objective

As explained earlier (Sec.1.1), self-piloting tools feature the unique use of the surrounding hole as a guide bushing; the hole being either a real guide bushing for initializing the drilling or a previously cut hole. Thus, it is only logical that the first conclusion made in Sec.3.1 implies the geometric consideration of the self-piloting (SP) tool together with the piloting hole. The real location of a SP tool within the piloting hole defines the effective geometry involved in the burnishing process thus affecting the output quality. So far, there has been no published reference addressing this problem.

- This section is to provide a comprehensive analysis of the influence of the various tool design parameters and machine tool setup parameters on the effective geometry involved in burnishing.

This is aimed at starting a line of research which may hopefully lead to practical guidelines regarding SP tool design, SP tool manufacture tolerances, wear tolerances in the guide bushing, alignment requirements, etc.

3.2.2. Transverse Section Plane

The length l and the width b of a support pad define its nominal contact area to be involved in burnishing. The contact area assumes its nominal value only if: (1) the radius of the pads is the same as that of the piloting hole, and (2) the pads have no inclination with respect to the piloting hole axis but the nominal backtaper if any provided. However, the true/or effective contact area will depend on the actual accuracy of the tool and guide bushing manufacture, as well as on the accuracy of their positioning within the machine tool assembly.

The functional requirement for a guide bushing is to provide a nominal clearance of about 7μm which will increase as the bushing wears out. Thus, the hole is bound to start oversize and, as the experience has shown, it will shrink as the tool progresses to close on the nominal value or, in some rare cases, even go undersize. So far, there has been no study on the significance of this change in terms of changing burnishing conditions.

The effective contact area, the distribution and the maximum values of contact stresses σ_{max1} and σ_{max2} (Fig.3.2) involved in burnishing depend on the following design parameters:

- Radius of the support pads R_n ($2R_n = D_n$ where D_n is the diameter of the tool head),
- Diameter of the piloting hole D_k,
- Central angle enclosed by the support pads ν,
- Width of the support pad b.

A number of different quantities can be used to estimate the accuracy of the support pad mating with the piloting hole. Here, a complex measure α_k is introduced as shown in Fig.3.2

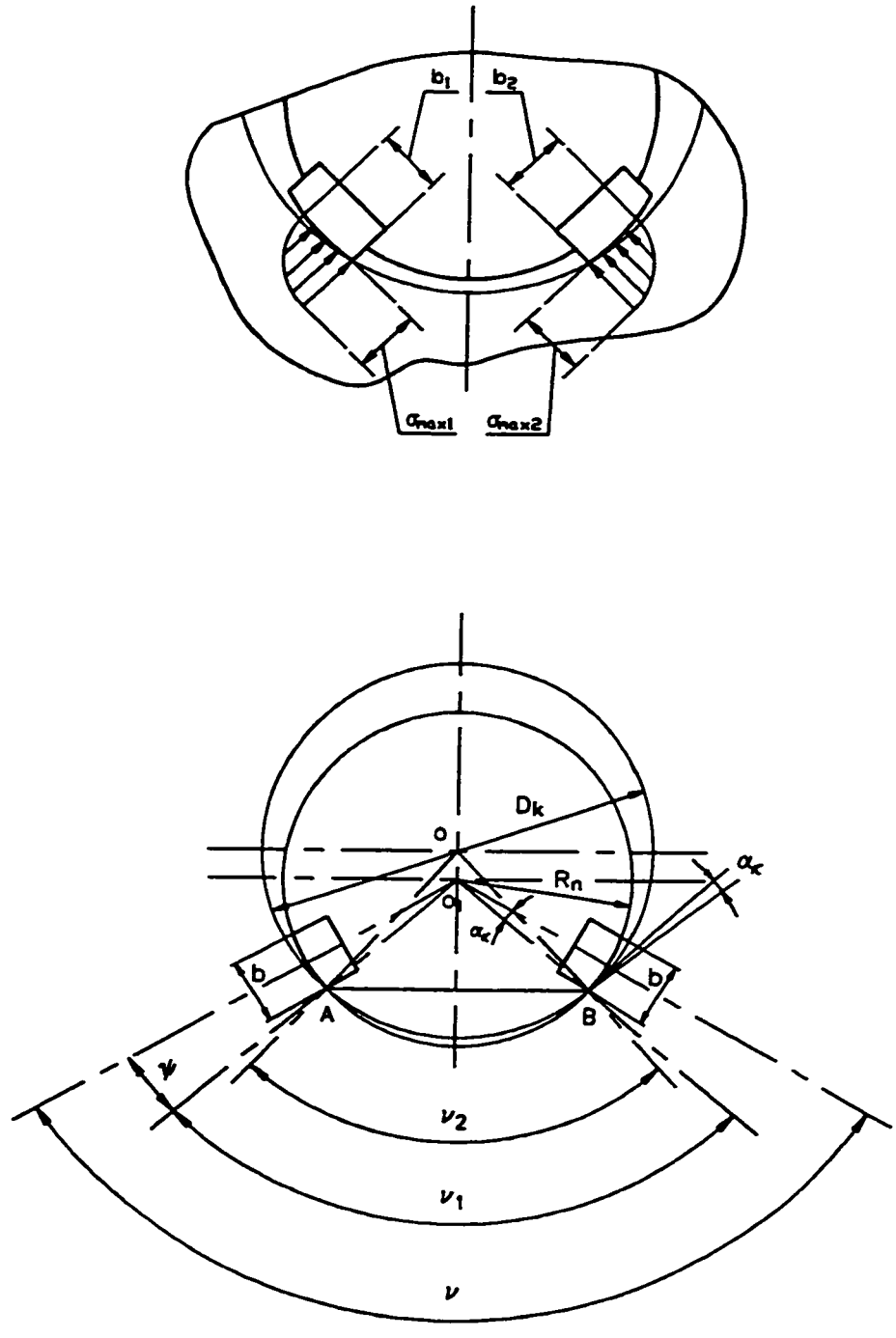

Fig.3.2. SP Tool Mating with Piloting Hole (Transverse Section Plane)

and will be referred to as the contact angle in the transverse plane. It follows from the same figure that α_k can be calculated as

$$\alpha_k = 0.5(\nu_1 - \nu_2) \tag{3.1}$$

where ν_1 is the central angle enclosed by the cornering points of contact with respect to the tool axis, and ν_2 is the central angle enclosed by the cornering points of contact with respect to the piloting hole axis (see Fig.3.2).

It follows from the same figure that the angle ν_1 can be found as

$$\nu_1 = \nu - 2\psi \tag{3.2}$$

where

$$\psi = \arcsin\left(\frac{b}{2R_n}\right) \tag{3.3}$$

and, by continuing to refer to Fig.3.2, the angle ν_2 can be found using the fact that the chord AB is common to two intersecting circles; thus, the length AB can be obtained from the triangle AO_1B as follows

$$\overline{AB} = 2R_n \sin\left(\frac{\nu}{2} - \psi\right) \tag{3.4}$$

while, from the triangle AOB, the same length can be expressed as

$$\overline{AB} = D_k \sin\frac{\nu_2}{2} \tag{3.5}$$

Now, combining Equations (3.3) - (3.5) yields

$$\nu_2 = 2 \arcsin\left(\frac{2R_n}{D_k}\sin\left(\frac{\nu}{2} - \arcsin\frac{b}{2R_n}\right)\right) \tag{3.6}$$

and, finally, the contact angle in the transverse plane can be calculated as

$$\alpha_k = 0.5\left(\nu - 2\arcsin\frac{b}{2R_n} - 2\arcsin\left(\frac{2R_n}{D_k}\sin\left(\frac{\nu}{2} - \arcsin\frac{b}{2R_n}\right)\right)\right) \tag{3.7}$$

The influence of each of the design parameters in Eq.3.7. on the accuracy of the tool mating with the piloting hole in the transverse plane can be estimated by the relative variation $\Delta\alpha_k$ under the relative variation of each of the parameters $\Delta\nu$, Δb, and $\Delta(2R_n/D_k)$. These are defined as follows:

$$\Delta\alpha_{k_i} = \left|\frac{\alpha_{k_i} - \alpha_{k_1}}{\alpha_{k_1}}\right| 100\%$$

$$\Delta v_k = \left| \frac{v_k - v_1}{v_1} \right| 100\%$$

$$\Delta b_j = \left| \frac{b_j - b_1}{b_1} \right| 100\%$$

$$\Delta \left(\frac{2R_n}{D_k} \right)_l = \left| \frac{\left(\frac{2R_n}{D_k} \right)_l - \left(\frac{2R_n}{D_k} \right)_1}{\left(\frac{2R_n}{D_k} \right)_1} \right| 100\% \qquad (3.8)$$

Here, α_{kl}, v_k, b_j, $(2R_n/D_k)_l$ are the current values of the complex measure α_k and the design parameters; α_{kl}, v_l, b_l, $(2R_n/D_k)_l$ are their initial values corresponding to the lower limits of the design parameters.

The influence of each of the design parameters on the contact angle α_k is shown in Fig.3.3.

- The most pronounced effect on the accuracy of the tool mating with the piloting hole, in the transverse plane, is that of the ratio of the tool and the piloting hole diameter. The effect is aggravated by the large angular span between the support pads which has been used in practice to ensure the tool stability and for technological reasons. The pad width which, in turn, could be varied shows comparably less influence. It may be concluded that hole oversizing relates to a significant change in the effective contact area involved in burnishing. Therefore, a process designer should pay main attention to all factors which may contribute to hole oversizing.

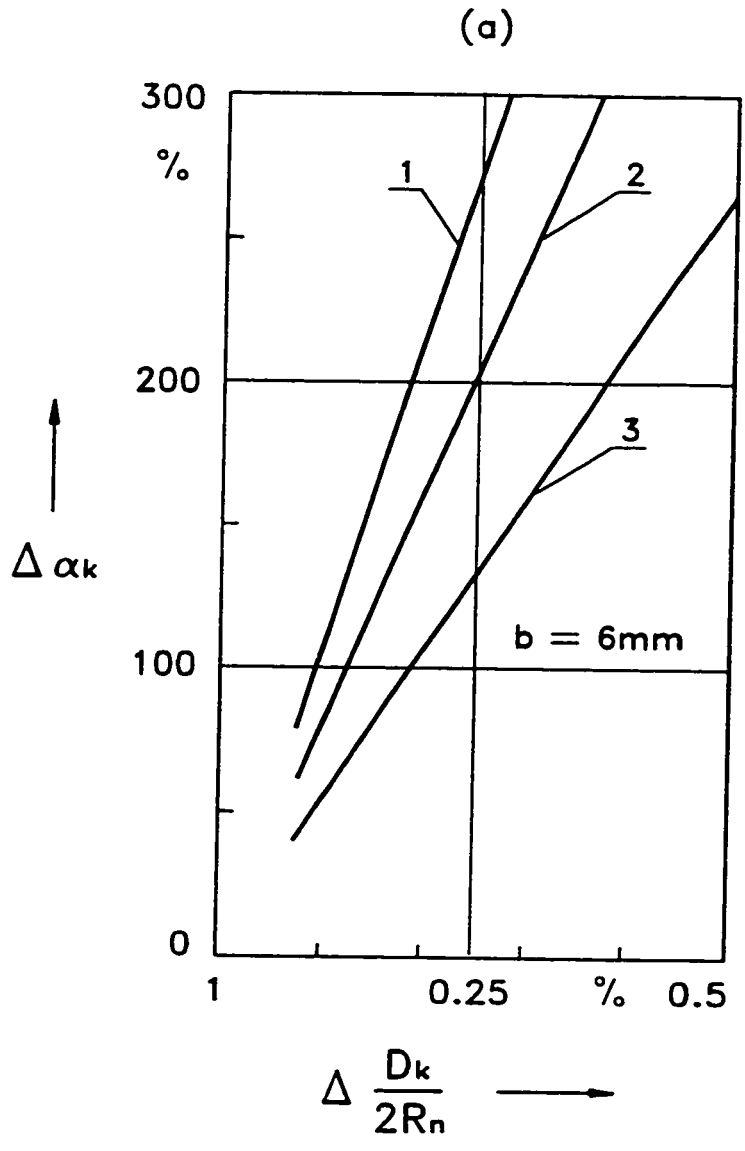

Fig.3.3.(a) The Effect of Hole Oversizing on SP Tool Mating with Piloting Hole

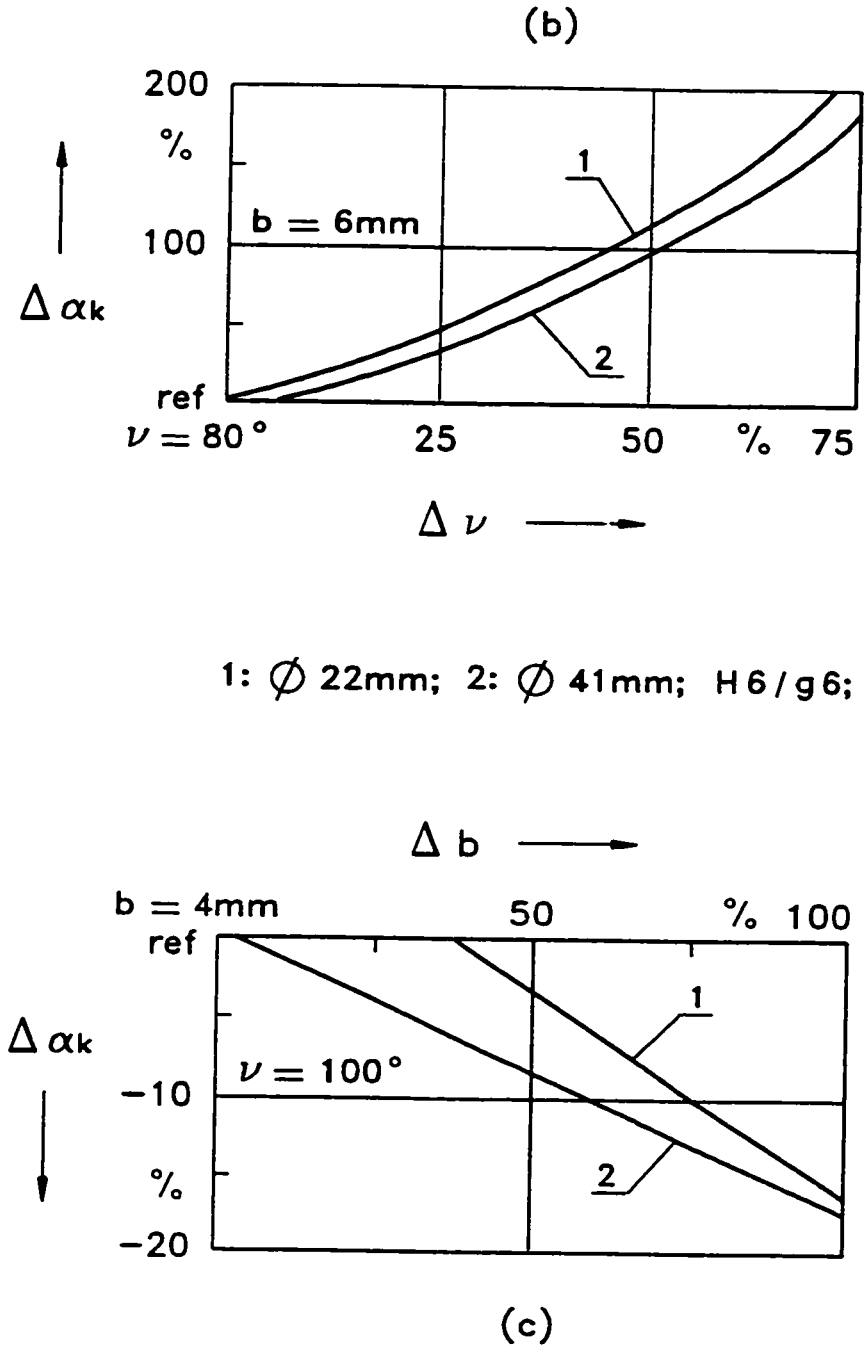

Fig.3.3. The Effect of (b) Support Pads' Angular Span, and (c) Support Pads' Width on SP Tool Mating with Piloting Hole

3.2.3. Axial Section Plane

As already discussed in Sec.3.2.2, the accuracy of the tool mating with the piloting hole in the axial section plane defines the effective dimension of the contact area in the axial direction. The ideal or "as designed" geometry assumes that the tool axis coincides with the piloting hole axis, and that the mating surface of the support pads has no other inclination but a backtaper if any provided. This arrangement would lead to the machining of a perfect hole. However, practice is bound to introduce restrictions affecting the tool inclination with respect to the piloting hole. Here, an attempt is made

- to identify all the causes that may contribute to the effective tool inclination, and
- to provide the first estimate of each effect for the sake of their comparison.

The main factors affecting the tool inclination may be identified as follows:

- The cutting forces acting on the tool tip are not balanced in the axial section plane, thus causing the boring bar to bend and the tool head to tilt about the simple supports provided by the pads.
- If the tool rotates, the weight of the boring bar adds a centrifugal force effect upon the boring bar initial curvature.
- The tolerances on the two mating shoulders of the tool-boring bar connection allow for some freedom. The shoulders have to be machined with clearance fits in order for the tool head to be easily detachable.
- Misalignment along the machine tool setup.

Thus, the total contribution to the change of the tool nominal inclination with respect to the piloting hole axis can be represented as follows:

$$\theta_{\Sigma} = \theta_1 + \theta_2 + \theta_3 + \theta_4 \tag{3.9}$$

where θ_1, θ_2, θ_3, θ_4 correspond, respectively, to the identified effects as listed above.

Hence, the effective tool mating angle in the axial cross-section can be represented by

$$\theta_{eff} = \theta_{\Sigma} + \theta_G \tag{3.10}$$

where θ_G designates the support pad inclination as ground. This includes the nominal backtaper, if any specified by the drawing, plus grinding error. The grinding error, in turn, includes the location and the kinematic errors. The first one is caused by the mounting error of the tool head on a mandrel. The second one encompasses (1) the inaccuracy of the grinding machine table motion, and (2) the grinding wheel runout.

3.2.3.1. Tool Support Conditions When Tool Subjected to Drilling Forces

This part focuses on the first of the above listed factors affecting the tool inclination with respect to the piloting hole axis: cutting forces. The analysis is conducted using the example of a single-edge, disposable BTA drill, 25.4mm in diameter by American Heller Corporation. For the tool shown in Fig.1.4, the drill pads feature a backtaper of only 2.5 μm over a 10mm-length. Since it is reasonable to count with the burnished depth of 15-20μm [30], this means virtually no taper at all, and the pads should be leaning against the hole over their full length. However, as the practice and a number of research works have shown, as far as the intensity of the contact is concerned, only the pads' front-end part of about 2mm in length rides on the wall. This holds particularly true for the leading pad as revealed by the wear marks. The following part offers an explanation to support the conclusion.

Fig.3.4 shows two sections of the tool inside the workpiece. The upper section corresponds to the plane that contains the cutting edge; the lower section shows the tool and the workpiece rotated by 90 degrees with respect to the first position. Though the real central angle enclosed by pads exceeds 90 degrees, this is good enough for the first approximation. When subject to the resultant cutting force, the tool will seek a support over the most outstanding point on the pads' envelope, this being the front-end of the leading pad. Thus, it can be seen, from the upper section in Fig.3.4, that the cutting component F_C, together with the opposing reaction force R_{N1} makes a couple of the arm h_1 imposing a bending moment on the boring bar. This causes the boring bar to bend taking the rear part of the leading pad farther away from the wall. The increase in the leading pad effective inclination angle can be estimated using the following model of the boring bar setup.

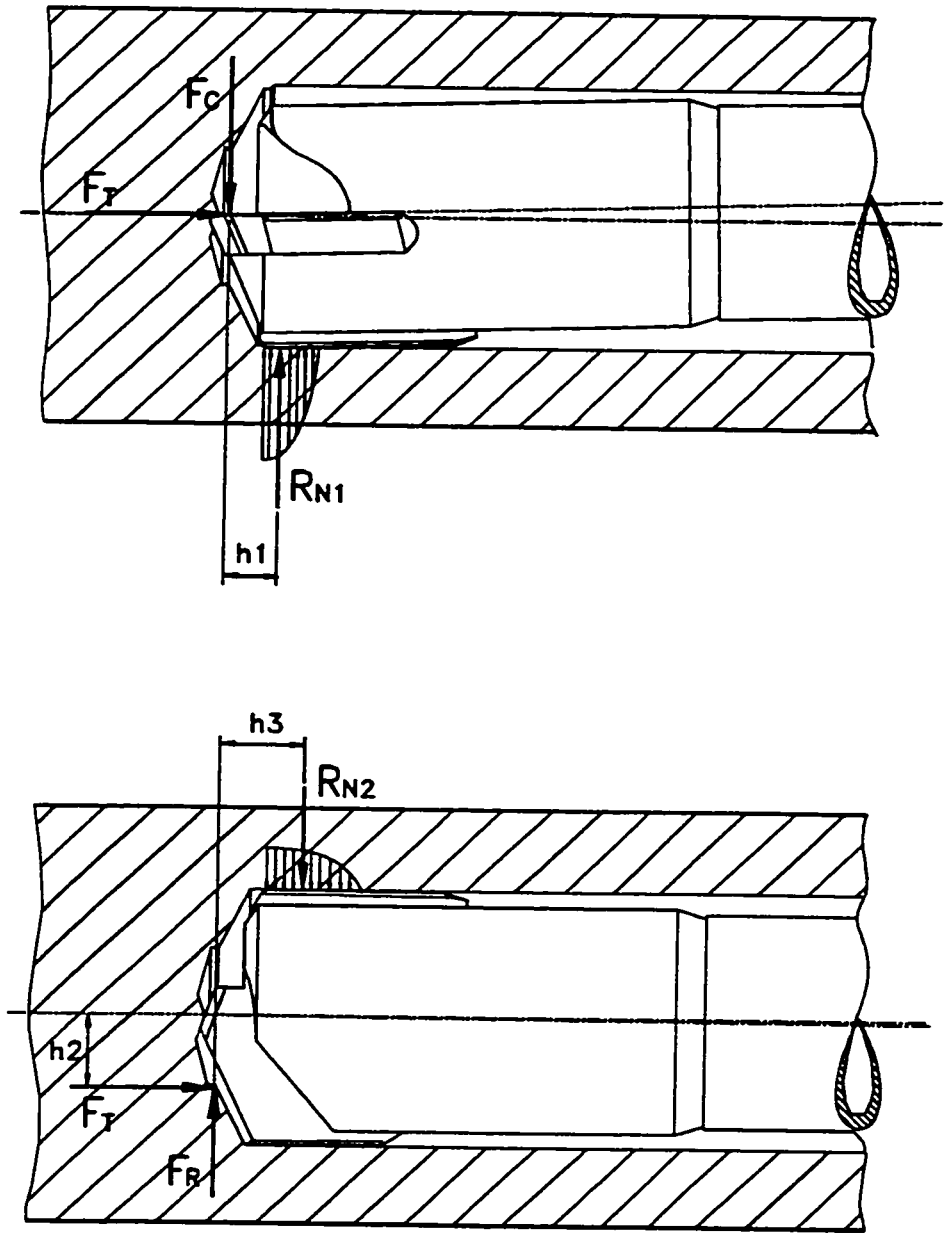

Fig.3.4. SP Tool Support Conditions (Axial Section Plane)

Fig.3.5 shows the static model of a boring bar of the length *l*. This model applies to the relatively short boring bars which can be used without a Lanchester damper providing an additional support. The boring bar appears as a propped beam with an overhang. The built-in right end corresponds to the clamping by means of a collet (point C), while the simple support is used to model the tool tip contact (point A). The beam is once statically indeterminate. The simplest way to estimate the elastic curve inclination at point A is to use the first moment-area theorem which states that

$$\theta_{A\text{-}C} = \int_{A}^{C} \frac{M_f}{EI}\, dx \tag{3.11}$$

where $\theta_{A\text{-}C}$ is the angle between the tangents drawn to the points A and C of the elastic curve; and the right side represents the area in M_f/EI diagram between these points [35].

Since the theory calls for the use of the bending moment diagram, first, the redundant reaction being the restraining moment at C has to determined. One way would be to replace the propped beam for a simply supported beam with the restraining moment M_C acting at C. The restraining moment has to compensate for the angular deflection at C (θ_C) produced by the couple acting at A (-Ph) in order for the elastic curve to come out of C horizontal. The condition has been comprised by Fig.3.5 and the following equation

$$\frac{Phl}{6EI} = \frac{M_C l}{3EI} \tag{3.12}$$

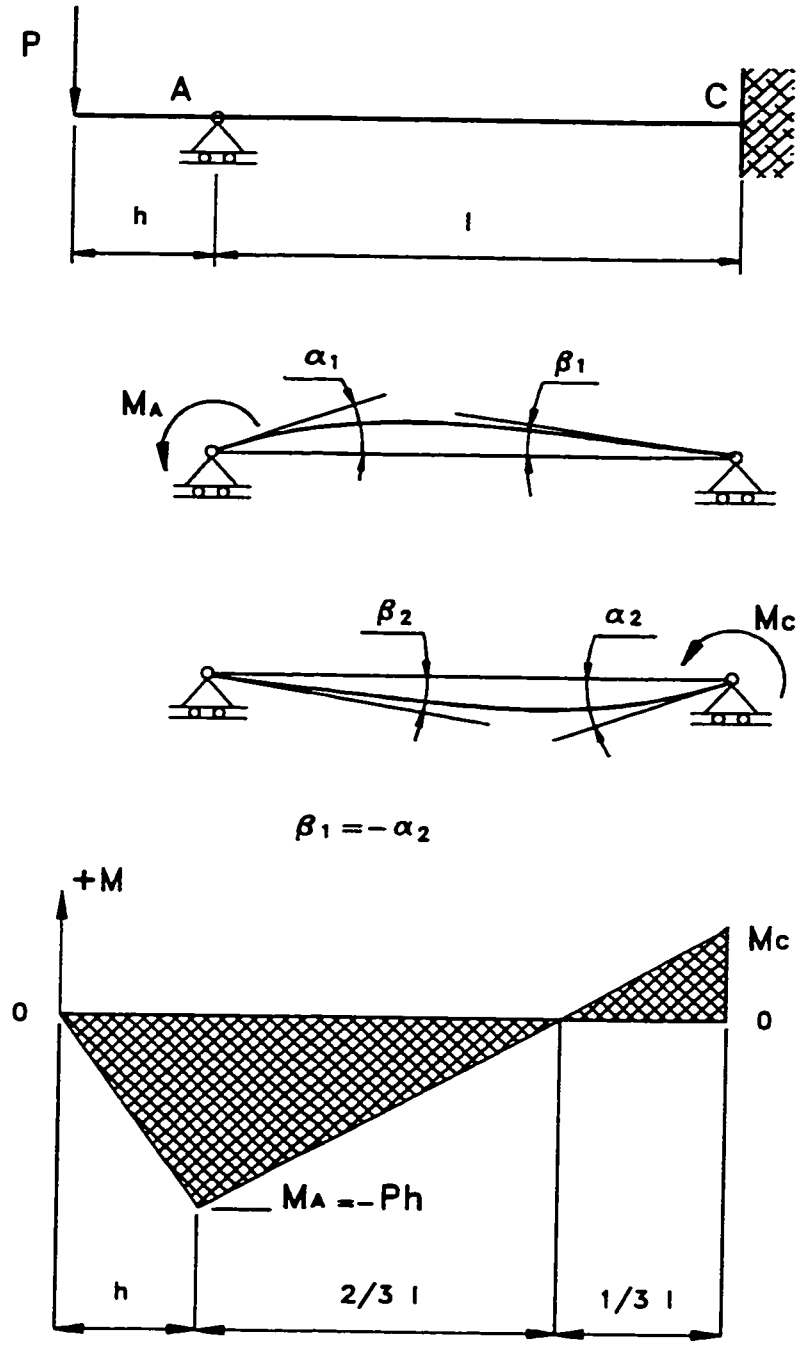

Fig.3.5. Boring Bar as a Propped Beam

from which the restraining moment value can be obtained as

$$M_C = \frac{Ph}{2} \tag{3.13}$$

Since the tangent to the elastic curve at C is horizontal, the slope at A can be directly obtained by means of the Eq.3.11 and the moment diagram shown in Fig.3.5. The areas above the 0-0 line count positive and the areas below it count negative. This gives the following tool inclination estimate

$$\theta_A = \frac{M_A l}{4EI} \tag{3.14}$$

However, longer boring bars are likely to be additionally supported by a Lanchester damper; thus requiring the model to include a mid-support at B (Fig.3.6). At B, the boring bar is held by a phenolic bushing tightened just as much as to allow for the feed movement while still producing enough friction to transfer the rotation from the boring bar to the damper's mass. It is reasonable to assume that no radial displacement will occur at this point.

Now, the system has become twice statically indeterminate. The well-known three-moment theory (by Clapeyron) can be applied to the two spans, AB and BC, to obtain

$$-Phl + 2M_B l + M_C(l - l_1) = 0 \tag{3.15}$$

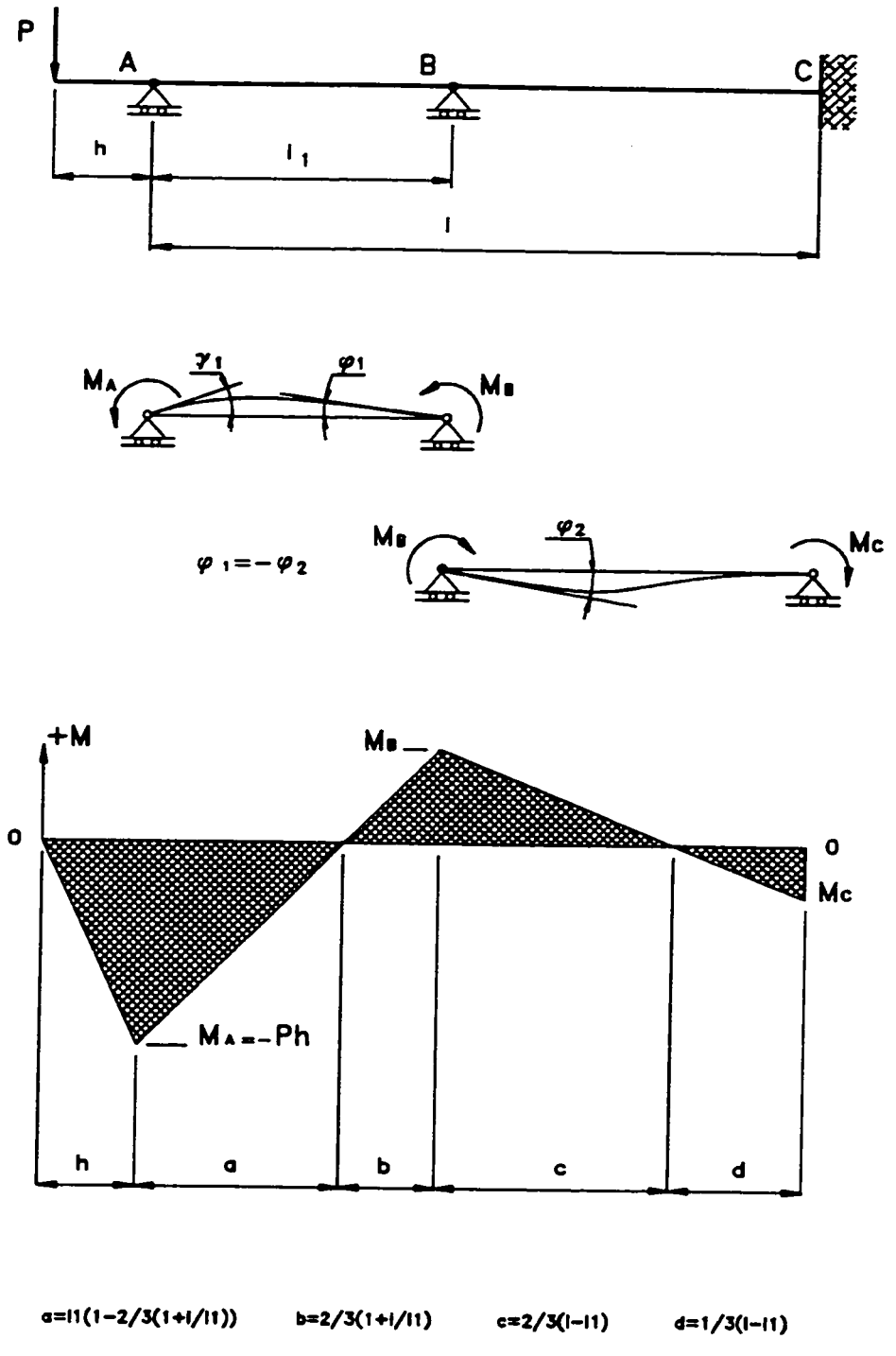

Fig.3.6. Boring Bar as a Propped Beam with an Intermediate Support

The second equation is the same as Eq.3.12 comprising the condition for the elastic curve to be horizontal at C, but now applied to the span BC as follows

$$\frac{M_C(l-l_1)}{3EI} + \frac{M_B(l-l_1)}{6EI} = 0 \qquad (3.16)$$

The Eq`s 3.15 and 3.16 can be solved for the two redundant moments to obtain

$$M_C = M_A \frac{l_1}{3l+l_1} \qquad (3.17)$$

$$M_B = M_A \frac{-2l_1}{3l+l_1} \qquad (3.18)$$

Again, the slope at A can be determined by applying the area-moment theorem (Eq.3.11) to the bending moment diagram shown in Fig.3.6. The tool inclination formula reduces, after some algebraic transformations, to the following form

$$\theta_A = \frac{M_A}{EI} \frac{l_1 l}{l_1+3l} \qquad (3.19)$$

There still remains the problem of providing the input force values in order to get a quantitative estimate of θ_A. Here, for a drill of 25.4-mm diameter, the thrust force was measured to be 2.6 kN (Chap.4), and the other two components were calculated keeping the

ratio between the forces 4:2:1 (F_C :F_T :F_R) as given by Griffiths [13]. The application point of the resultant force has been assumed to conform to the force distribution as proposed by Astakhov & Osman [1]; which resulted in $h_1 = 4$ mm, and $h_2 = 6.2$ mm. The other conditions were set as follows: workpiece material: hot-rolled steel 1045; feed rate: 0.145 mm/rev; speed: 1200_rpm. The tool inclination values have been calculated in μm/10mm by Eq.3.14 and Eq.3.19 (l_1/l =0.5) for different boring bar lengths and the results are shown in Tab.3.1.

Tab.3.1. Tool Inclination in the Plane of the Leading Pad (in μm/10mm)

B.BarLength [m]	1.0	1.5	2.0	2.5	3.0	4.0	5.0
θ_1 (Eq.3.14)	26	39	52	64	-	-	-
θ_1 (Eq.3.19)	-	-	29	37	44	59	74

One should not be deceived by the small values; they appear quite significant when compared with the burnishing step height and the nominal backtaper of the support pads. Moreover, this provides only for the initial deflection that will, in turn, bring the thrust force and the centrifugal force into effect. The inclination may be considerably higher if the model accounted for these effects, as well. However, that is beyond the scope of this work.

The lower part of Fig.3.4 shows the force arrangement in the plane of the trailing support pad. Here, unlike its projection in the other plane, the thrust force appears shifted with respect to the tool axis thus imposing a bending moment on the shank. The radial force makes the tool seek a support at the front-end of the trailing pad. The reaction, together with the radial force, makes a couple opposing the moment caused by the thrust. However, since both the thrust value and the thrust lever arm assume considerably higher values then the radial force

and its arm respectively, the thrust effect prevails. This causes the boring bar to bend closing on the rear part of the trailing pad. As the contact length increases, the reaction force application point moves farther back thus increasing the couple arm h_3. Eventually, the tool takes the position at which the opposing effects have reached an equilibrium. Tab.3.2 gives the estimates of the inclination in μm/10mm as calculated by Eq.3.14 and Eq.3.19 (l_1/l =0.5).

Tab.3.2. Tool Inclination in the Plane of the Trailing Pad (in μm/10mm)

B.BarLength [m]	1.0	1.5	2.0	2.5	3.0	4.0	5.0
θ_1 (Eq.3.14)	14	22	29	36	-	-	-
θ_1 (Eq.3.19)	-	-	16	21	25	33	41

That the contact between the trailing pad and the wall will extend, becomes even more obvious if the two inclinations are considered together. Namely, the first tilt about the leading pad will bring the rear part of the trailing pad even closer to the wall, because of the wall's curvature, thus reducing the effective clearance to close upon. This backs up the conclusion by Sakuma [30] and others, that the rear part of the trailing pad has the final touch on the surface. Finally, it may be concluded that

- The tool is subjected to the forces which impose bending moments on the boring bar thus affecting the tool alignment. The out-of-balance effect of moments *initiates* a considerable change in the effective contact area by influencing the tool mating with the piloting hole in the axial direction. The presented model of the tool head support fully complies with the common report of short, more pronounced wear marks at the leading pad, and less pronounced but extended wear marks at the trailing pad [5,25].

The measurements of the burnishing torque, done by Fuss [9], have revealed that the torque experiences a considerable change of 20-30% over those parts where the hole diameter changes (Fig.3.7.b). Based on this, the author even proposed the following equation to account for the variation

$$M_R = M_{RO} + K\frac{dD}{dl}$$

This observation directly relates oversizing to the burnishing conditions, thus supporting the result obtained in Sec.3.2.2. Moreover, this indirectly expands the significance of oversizing to the axial plane, since the change in hole diameter involves a corresponding change in the effective tool mating in the axial direction as shown in Fig.3.7.a. Thus, the conclusion of Sec.3.2.2 can be expanded to include

- An alteration in hole oversizing affects the tool mating with the piloting hole in the axial cross-section through the change of the effective mating angle.

The introduced concept of the tool seeking a balance in the axial cross-section may offer a starting point for the explanation of the burnished surface waviness reported by Sakuma [30] as well as by Weber [39]. They have offered no explanation regarding the observed macro-waviness i.e. almost-periodical exchange of more-flattened and less-flattened zones on the burnished surface. The explanation may include an excessive build-up in front of the pad chamfer causing the tool to incline more and shorten the boring bar curvature, and the build-up abrupt removal causing the tool to slide forward in a jerky manner. This would, of course, have to be related to the variations of the thrust force.

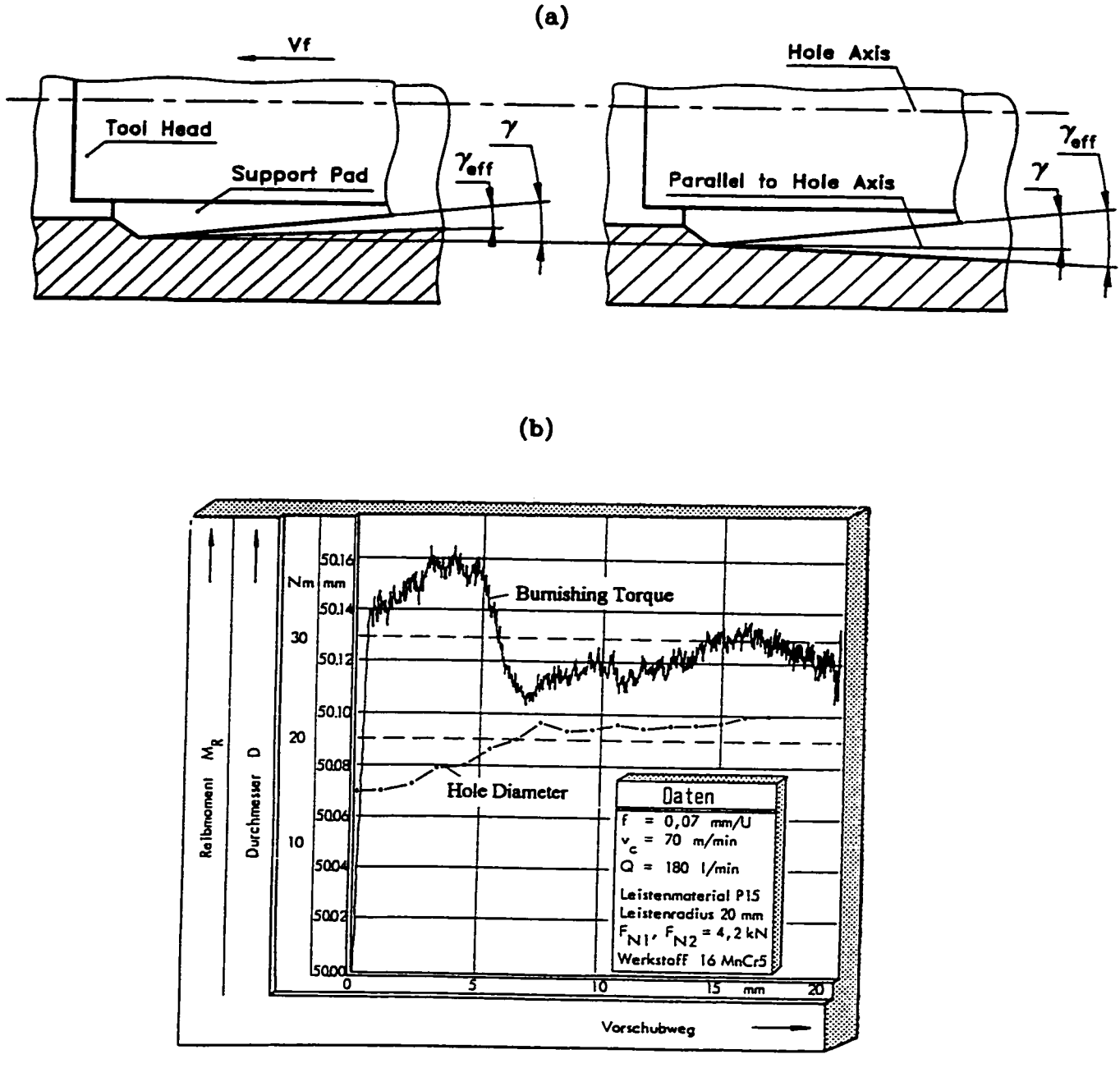

Fig.3.7. The Effect of Hole Diameter Alteration on

(a) Support Pads' Effective Backtaper and (b) Burnishing Torque [9]

3.2.3.2. Contribution of Technological Inaccuracies in Tool Head Mounting

As already mentioned in Sec.1.4, a BTA drill is centered with respect to the boring bar by means of two shoulders at a certain distance from each other. The mating surfaces are machined so as to provide clearance fits in order for the tool head to be easily detachable. The relative inclination of the tool head axis for the worst combination of mating shoulders' dimensions can easily be calculated referring to Fig.3.8 as follows

$$\theta_3 = \arctan \frac{\delta_1 + \delta_2}{l} \tag{3.20}$$

$$\begin{aligned} \delta_1 &= \frac{D_{1max} - d_{1min}}{2} \\ \delta_2 &= \frac{D_{2max} - d_{2min}}{2} \end{aligned} \tag{3.21}$$

from which the result follows as

$$\theta_3 = \arctan \frac{(D_{1max} + D_{2max}) - (d_{1min} + d_{2min})}{2l} \tag{3.22}$$

where D_{1max} , d_{1min} and D_{2max} , d_{2min} are the maximum and the minimum diameters of the mating shoulders of the tool head and the boring bar respectively, as specified by the designer's tolerances. The inclination has been calculated for a range of tool diameters and the common tolerance in commercial drills H7/g6 and results are shown in Tab.3.3.

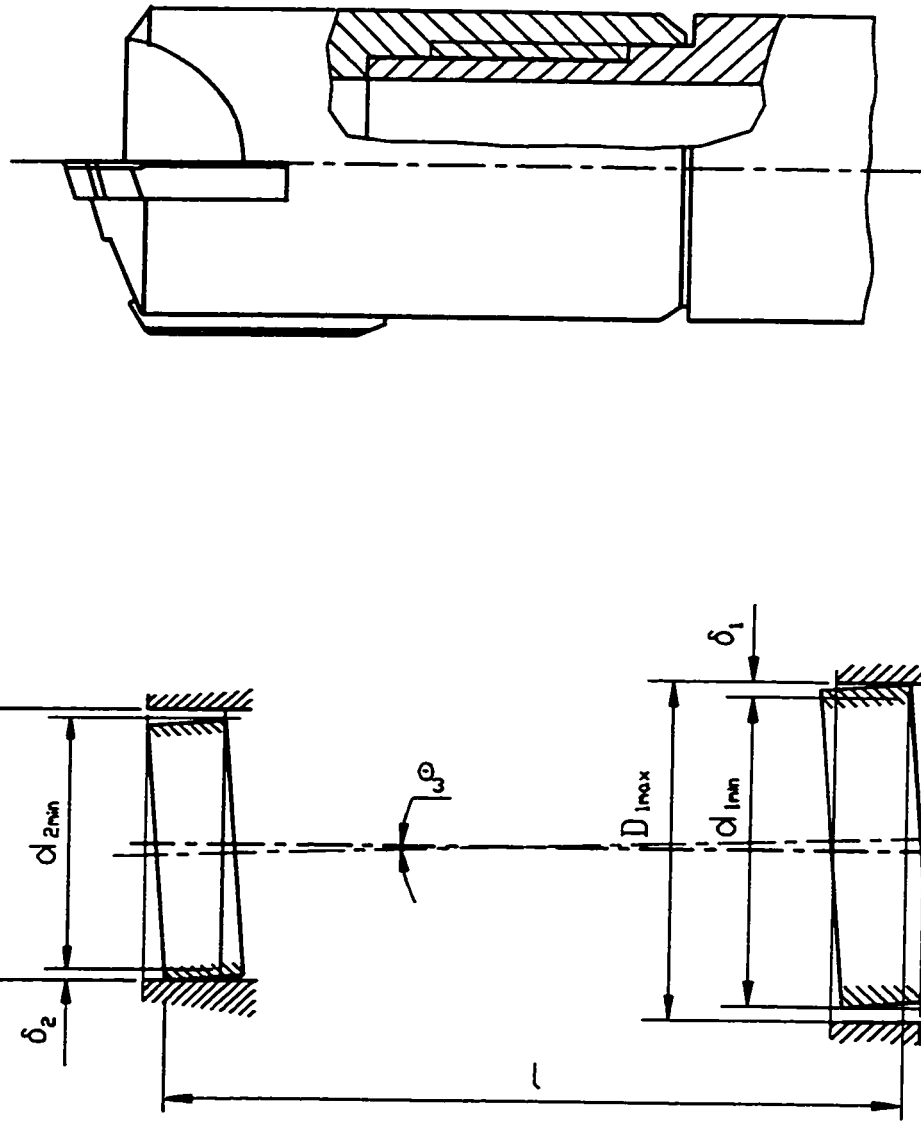

Fig.3.8. Tool Head/Boring Bar Connection

Tab.3.3. Tool Inclination as a Result of Manufacturing Tolerances

Tool Diam. [mm]	Diameters of Mating Shoulders [mm]					Inclination µm/10mm
	D_{1max}	D_{2max}	D_{1min}	D_{2min}	l	
from 20.00 to 21.90	16.518	14.518	16.483	14.483	25	14
from 21.90 to 24.90	19.021	16.018	18.980	15.983	25	15.2
from 24.90 to 26.90	20.021	17.018	19.980	16.983	25	15.2
from 26.90 to 29.90	22.021	19.021	21.980	18.980	25	16.4
from 30.00 to 31.90	24.021	21.021	23.980	20.980	25	16.4
from 31.90 to 33.90	26.021	23.021	25.980	22.980	25	16.4
from 33.90 to 36.90	27.021	24.021	26.980	23.980	40	10.3
from 36.90 to 39.90	30.021	27.021	29.980	26.980	40	10.3
from 39.90 to 43.90	33.025	30.021	32.975	29.980	40	11.4

It is worth noting that the probability of the four dimensions assuming the worst combination of their extreme values is negligibly small. Therefore, it is reasonable to assume an inclination of approximately 3-4µm/10mm which leads to the following conclusion:

- The analysis of technological inaccuracies in the tool head mounting has revealed their negligible effect on the tool head effective inclination. The tool head appears as a solid extension to the boring bar as previously expected.

3.2.3.3. Alignment

As a rule, all manufacturers of tooling for deep hole machining refer to the alignment as being "critical". Alignment accuracy must be held throughout the setup including the tool drive spindle, the driver, the boring bar, the guide bushing, the workpiece reception plate and the chuck. The line is to include the Lanchester damper and fixturing if any present. The usual requirement for the total alignment is to be less than 15-100μm/m starting from the spindle, the tougher requirement applying to the machine shops doing high precision machining. To attain this alignment, the machine bed ways should be of one-piece construction or ground in sets, whether they be round, flat or V-shaped. The ways must not be curved or twisted, and they must be leveled as accurately as possible. The accuracy of the spindle is to be determined relative to the ways to assure the spindle axis is parallel with feed travel. The rigidity of the pressure head assembly must allow no bushing support deflection. The boring bar must be straight and ground uniformly in size. All components should show true-on-axis at normal running temperatures and should be checked periodically.

So far, there has been no systematic study of the overall effect of misalignment on tool wear and tool performance, except for the study on its effect on runout [29]. As far as materials written by authors from practice are concerned, they attribute the whole variety of undesirable effects to misalignment but mostly as experience-based guessing. The complaints include the cutting edge flaking or chipping, the leading pad wear, poor surface finish, straightness and roundness. Interesting enough, the literature reports that misalignment related problems may and may not be accompanied by excessive vibration [2]. Unfortunately, the original idea of

the author to investigate this has been abandoned for the reason of high cost involved.

Here, it will only be pointed out that any two elements along a deep hole machine setup may feature two basically different misalignments: (1) parallel offset of their axes, and (2) angular misalignment. The former assumes a constant value along the setup while the latter increases with length. Thus, the angular misalignment encountered in clamping elements is the most undesirable case. If present, this kind of misalignment is most likely to adversely affect tool performance especially for longer strokes. To compensate for this effect the author proposes that a simple spherical joint be integrated in the tool drive spindle assembly as schematically shown in Fig.3.9.a.

As this means an effective change to the boundary conditions on the boring bar, it is only logical to check the buckling stability of the proposed setup. Here, to be fully correct, a strict criterion will be established to account not only for the compressive thrust but also for the drilling torque, since previous research has offered no proof of the drilling torque being negligible. The model of the boring bar setup is shown in Fig.3.9.b. The spherical joint at A corresponds to the tool tip support, and the spherical joint at B represents the proposed modification to the tool drive spindle assembly. Let the boring bar have the length L, the bending rigidity EI and the torsional rigidity GI_o. The initially straight boring bar is subjected to the thrust F_T and the torque T. Any small deflection of the boring bar may, under certain circumstances, give rise to the boring bar buckling. If this occurs, the boring bar seeks a new equilibrium position which, in general, will be described by a space (3D) deflection curve. The

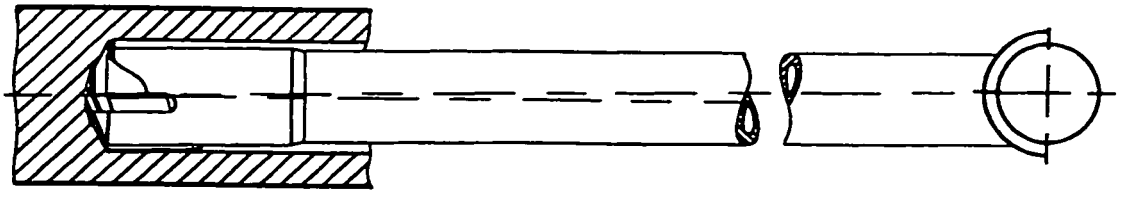

(a)

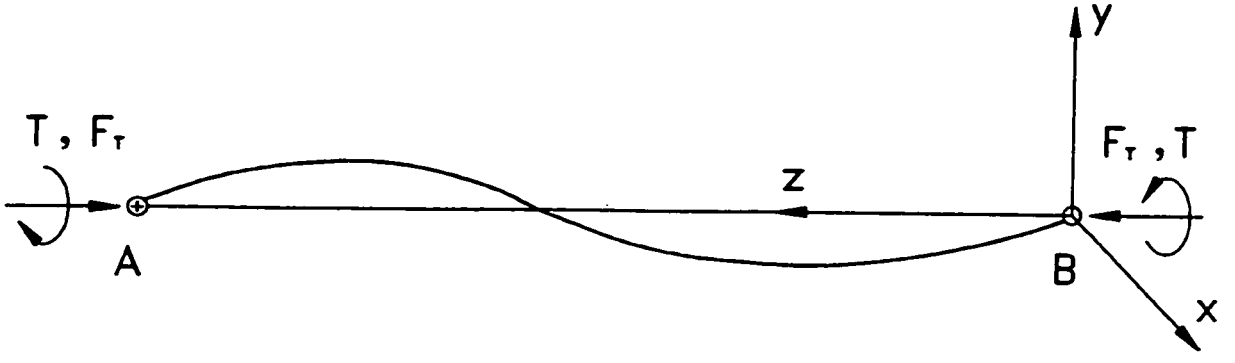

(b)

Fig.3.9. Proposed Modification to The Boring Bar Setup

theory of elastic stability [3] gives two vector equations for the new equilibrium as follows

$$\frac{d\underline{F}}{ds} = 0$$
$$\frac{d\underline{M}}{ds} = \underline{t} \times \underline{F} \qquad (3.23\text{-}3.24)$$

where $\underline{F}$ is the stress vector and $\underline{M}$ is the moment of all external forces in an arbitrary cross-section of the elastic rod (boring bar). The vector $\underline{t}$ is tangential to the deflection curve in the same cross-section and equal

$$\underline{t} = \frac{d\underline{r}}{ds} \qquad (3.27)$$

where $\underline{r}$ describes the center line of the deformed elastic rod in the $(\underline{i},\underline{j},\underline{k})$ coordinate system, and ds is an infinitesimally small element of the deflection curve. It follows from Eq.3.23 that $\underline{F}$=const. and, since for $s = L$: $\underline{F} = -F_T\,\underline{k}$, it may be concluded that

$$\underline{F} = -F_T\,\underline{k} \qquad (3.25)$$

By substituting Eq.3.25 into Eq.3.24 and integrating, M can be obtained as follows

$$\underline{M} = -\int(\underline{t} \times \underline{F})\,ds \qquad (3.26)$$

$$\underline{M} = -\int(\frac{d\underline{r}}{ds} \times \underline{F})\,ds = -\underline{r} \times \underline{F} + const. \qquad (3.28)$$

It can be easily seen that, since for $\underline{r}=0$: $\underline{M}=T\underline{k}$, the Eq.3.28 becomes

$$\underline{M} = T\underline{k} - \underline{r} \times \underline{F} \tag{3.29}$$

Eq.3.29 gives the moment of the external forces for an arbitrary cross-section of the elastic rod. The moment of the internal forces can be obtained by the generalized theory of Euler-Bernoully as follows:

$$\underline{T} = EI\underline{t} \times \frac{d\underline{t}}{ds} + GI_o\Omega_z\underline{t} \tag{3.30}$$

where Ω_z designates the rod torsion.

By equating the expressions 3.30 and 3.29, one obtains a nonlinear vector equation for a 3D equilibrium of the rod in Fig.3.9.b as follows

$$EI\underline{t} \times \frac{d\underline{t}}{ds} + GI_o\Omega_z\underline{t} = T\underline{k} - \underline{r} \times \underline{F} \tag{3.31}$$

All vectors in Eq.3.31 can be expressed in terms of the center line componential deflections u,v and w in x,y and z direction, respectively, to give the following equation:

$$EI\begin{bmatrix} \underline{i} & \underline{j} & \underline{k} \\ u' & v' & w' \\ u'' & v'' & w'' \end{bmatrix} + GI_o \frac{\begin{vmatrix} u' & v' & 1+w' \\ u'' & v'' & w'' \\ u''' & v''' & w''' \end{vmatrix}}{(u'')^2 + (v'')^2 + (w'')^2} [u'\underline{i}+v'\underline{j}+(1+w')\underline{k}] = T\underline{k} - \begin{bmatrix} \underline{i} & \underline{j} & \underline{k} \\ u & v & s+w \\ 0 & 0 & -F_T \end{bmatrix}$$

(3.32)

After expanding Eq.3.32 and neglecting small values of higher order such as uv, uw, u`v`, etc., one obtains

$$\begin{aligned} -EIv'' + GI_o\Omega_z u' &= F_T v \\ EIu'' + GI_o\Omega_z v' &= -F_T u \\ GI_o\Omega_z(1 + w') &= T \end{aligned} \qquad (3.33\text{-}3.35)$$

Since Ω_z w` is also small Eq.3.35 reduces to

$$GI_o\Omega_z = T \qquad (3.36)$$

After substituting this result into Eq`s 3.33 and 3.34, the system reduces to the following Eq`s

$$\begin{aligned} EIv'' &= Tu' - F_T v \\ EIu'' &= -Tv' - F_T u \end{aligned} \qquad (3.37\text{-}3.38)$$

and the corresponding boundary conditions

$$\begin{aligned} u(0) &= u(L) = 0 \\ v(0) &= v(L) = 0 \end{aligned} \qquad (3.39)$$

After introducing the constants m and n as given by

$$m = \frac{T}{EI}; \qquad n^2 = \frac{F_T}{EI} \qquad (3.40)$$

the system can be rewritten as follows:

$$\begin{aligned} u'' + mv' + n^2 u &= 0 \\ v'' - mu' + n^2 v &= 0 \end{aligned} \qquad (3.41\text{-}3.42)$$

The solution to the system can be assumed in the following form:

$$\begin{aligned} u &= A\sin r_1 s + B\cos r_1 s + C\sin r_2 s + D\cos r_2 s \\ v &= -A\cos r_1 s + B\sin r_1 s - C\cos r_2 s + D\sin r_2 s \end{aligned} \qquad (3.43\text{-}3.44)$$

where r_1, r_2, A, B, C and D are constants. Substituting 3.43 and 3.44 into 3.41 and 3.42 one obtains the condition to be met by r_1 and r_2:

$$r^2 + mr - n^2 = 0 \qquad (3.45)$$

Thus, if $m \neq 0$, r_1 and r_2 assume the following values

$$r_{1/2} = -\frac{m}{2} \pm \sqrt{\frac{m^2}{4} + n^2} \qquad (3.46\text{-}3.47)$$

Substituting the boundary conditions 3.39 for $s = 0$ into Eq`s 3.43 and 3.44 gives

$$\begin{aligned} B + D &= 0 \\ A + C &= 0 \end{aligned} \qquad (3.48\text{-}3.49)$$

This, together with the boundary conditions 3.39 for s =L, will give further

$$\begin{aligned} A(\sin r_1 L - \sin r_2 L) + B(\cos r_1 L - \cos r_2 L) &= 0 \\ -A(\cos r_1 L - \cos r_2 L) + B(\sin r_1 L - \sin r_2 L) &= 0 \end{aligned} \qquad (3.50\text{-}3.51)$$

A nontrivial solution to the system 3.49-3.50 exists only if the following condition is satisfied

$$\begin{aligned} (\sin r_1 L - \sin r_2 L)^2 + (\cos r_1 L - \cos r_2 L)^2 &= 0 \\ \cos((r_1 - r_2)L) &= 1 \end{aligned} \qquad (3.52)$$

The first non-zero value to satisfy Eq.3.51 would be

$$(r_1 - r_2)L = 2\pi \qquad (3.53)$$

It follows from Eq's 3.46-3.47 that

$$r_1 - r_2 = 2\sqrt{\frac{m^2}{4} + n^2} \qquad (3.54)$$

$$\frac{\pi^2}{L^2} = \frac{m^2}{4} + n^2 \qquad (3.55)$$

Finally, substituting 3.40 into 3.55, one obtains the critical load to make the buckling possible

$$\frac{\pi^2}{L^2} = \frac{1}{4}\left(\frac{T_{cr}}{EI}\right)^2 + \frac{F_{Tcr}}{EI} \tag{3.56}$$

$$F_{Tcr} = EI\left(\frac{\pi^2}{L^2} - \frac{1}{4}\left(\frac{T_{cr}}{EI}\right)^2\right) \tag{3.57}$$

Now, it can be seen that for the usually encountered boring bar rigidities and drilling torques, the torque effect on the setup buckling stability does not exceed 1% and can be readily neglected. Thus, the setup buckling stability after the proposed modification can be estimated with high accuracy by using only the first member in Eq.3.57.

However, it should be mentioned that the real rigidity of the setup will always be higher because of the additional supporting provided by the stuffing box and possibly a Lanchester damper. Moreover, in the view of the discussion presented in Sec.3.2.3, the whole analysis has a very limited significance since the boring bar always deflects even if it is initially straight. Therefore, it can be concluded that the new design offers the advantage of having insurance against the worst case of misalignment at a reasonable cost of rigidity reduction. While the feasibility of the design in drilling applications will become more obvious in Chapter 5, at this point, the design can be claimed advantageous in SP boring and SP reaming applications.

Fig.3.10 shows a possible design of the tool drive spindle assembly incorporating a spherical joint and a damper as an option. The design has proved successful in a particular application by German Bekker Co.[6].

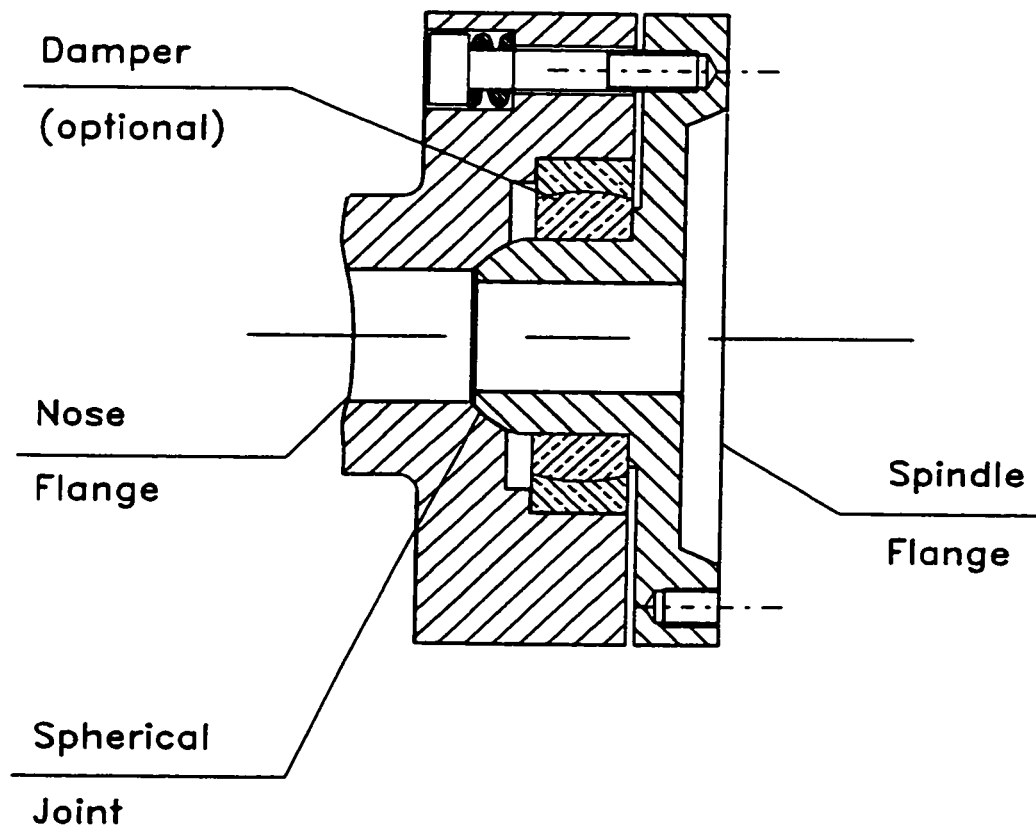

Fig.3.10. A Spindle Assembly Incorporating a Spherical Joint [6]

3.2.4. Tool Inclination in Different Working Methods

So far, this work has shown, that the inherent feature of the conventional SP tool design is to bring about the effective tool inclination as soon as the drilling forces are applied. The problem of maintaining a near-perfect alignment of a deep hole drilling setup has also been emphasized with a reference to reports from people in deep hole machining practice. As an answer to the question raised by some works on SP burnishing, the previous sections have established the fact that the effective tool inclination of a SP tool with respect to the piloting hole affects burnishing. As the analysis has revealed, the reason for this, is that a very small tool inclination appears significant when considered in the small area at the front-end of the support pads where burnishing occurs.

Here, it is only logical to look for another small area in the machining zone where the tool inclination may appear significant. As the literature review has shown (p.31), the one that stands out would be the flanks. This is because, over just a few tents of a millimeter right below the cutting edge, the flanks of a cutting element are subjected to the wear which is often considered the main factor limiting the tool life. Therefore, it is reasonable to bring the focus forward to include the effect of the tool inclination on the tool flanks' interference with the bottom of the hole. Fig.3.11 shows the tool inclination effect on the effective tool flank geometry in (a) workpiece rotating and (b) tool rotating method.

Fig.3.11 is to point out a fact which is self-evident but it has never been acknowledged explicitly. A SP tool will assume the effective cutting geometry as designed only if the tool axis perfectly coincides with the hole axis. Furthermore, the tool will perform virtually the

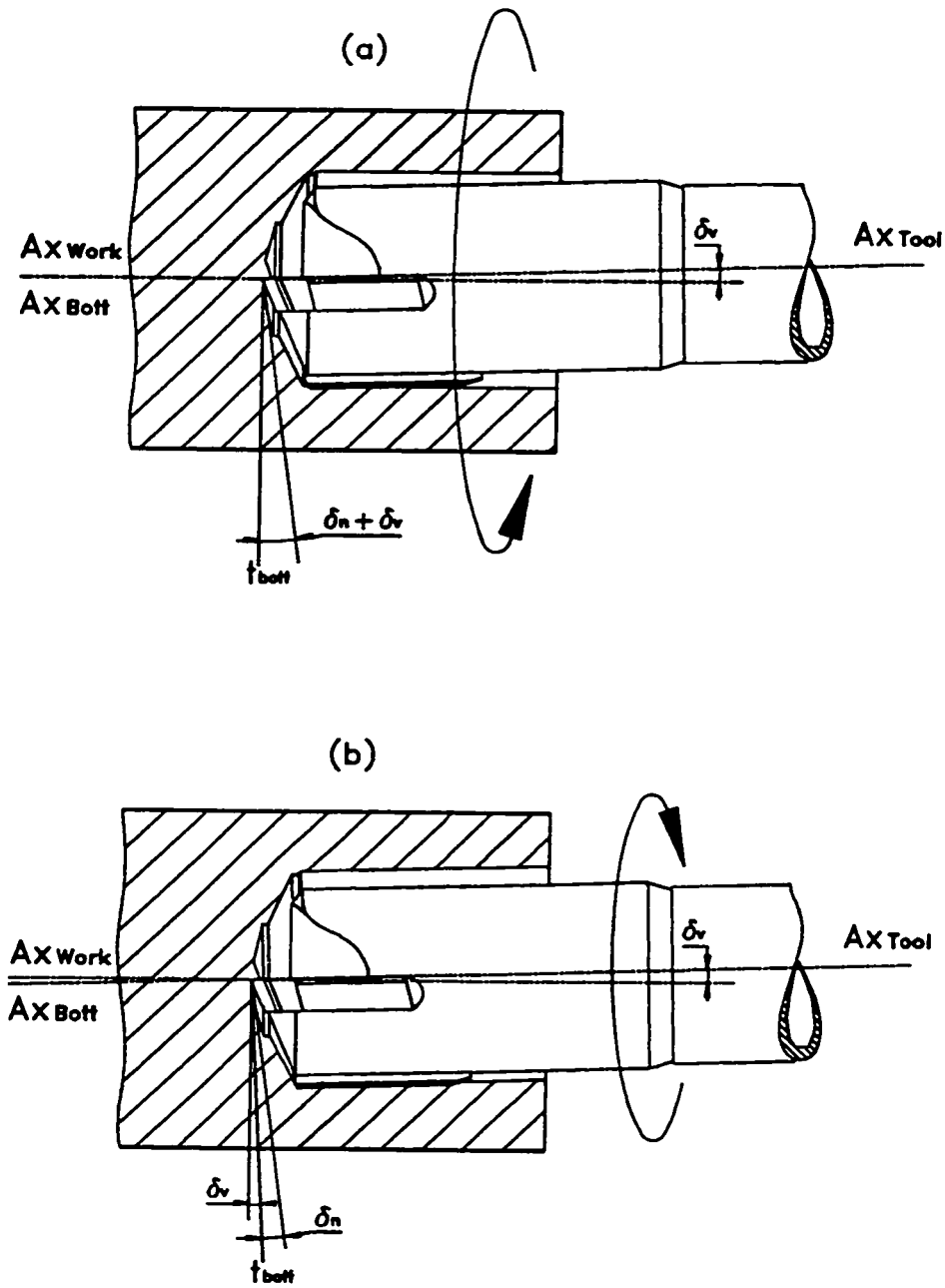

Fig.3.11. Tool Inclination in (a) Workpiece Rotating and (b) Tool Rotating Method

same in different kinematic schemes only as long as the tool and the workpiece share the same axis. This is the ideal case where no matter which of the two components rotates, the relative motion will result in the generation of the identical bottom of the hole. The bottom assumes the same shape and the same relative position with respect to the tool. However, as soon as the tool inclination occurs, various kinematic schemes introduce an effective difference in the cutting process. If the workpiece rotates, the inclined cutting edge will continue to cut a hole around the workpiece axis. The projection of a 3D tool inclination on the plane of the cutting element will result in a slight change in the bottom opening. The other projection in the perpendicular plane will result in the change of the effective flank angle since the bottom does not follow the tool inclination (Fig.3.11.a). In the tool rotating method, the tool will assume a new direction and will restore the bottom of the hole around its own axis thus keeping the cutting geometry unchanged (Fig.3.11.b) but in a runout hole. In a case of counter-rotating components, the change will be in between the two illustrated and will depend on the ratio of the speeds on the tool and the workpiece. One should only be aware of the difference between a steady inclination and one with the axis following the tool rotation. The former occurs in various cases of misalignment and leads to runout holes. The latter is caused by the drilling forces in conjunction with the tool design as shown in Sec.3.2.3 and may possibly lead to oversized holes. Here, a general conclusion may be stated as follows:

- A SP tool appears the same in different kinematic schemes only as long as its axis perfectly coincides with the axis of the workpiece. Any tool inclination with respect to the workpiece brings about an effective difference between the working methods.

Chapter 4

Measurements

4.1. Objective

Chapter 4 is to provide as much reliable information on the dynamics of a BTA-type machine tool as it has been possible to measure with the equipment available. Three measuring setups have been used to conduct both system and signal analysis. In all cases, a Fast Fourier Transform (FFT) Unit, shown in Fig.4.1, has been used to resolve the signal energy content over a frequency range and facilitate the interpretation of the results.

4.2. System Analysis - Boring Bar Bending

Some previous work [10,28] has attributed boring bar vibrations to its resonances in bending modes as they were measured out of cutting. Bearing this in mind, the author has conducted a simple test on a boring bar mounted on the machine and without cutting. A hammer with a built-in load cell has been used to provide an impulse excitation to the structure while an accelerometer has been used to measure the response. First, an autospectrum of the input channel has been acquired to make sure the hammer is capable of providing enough input energy over the frequency range of interest. Since the response is a transient function, the autospectrum has been scaled to show the energy spectral density of the signal (ESD). When equipped with a metal tip, the hammer has provided a uniform input over a broad frequency range from 0Hz to 6kHz (see Fig.4.2). Here, a drop of less than 20dB has been tolerated following the common recommendation for resonance measurements [26]. The whole

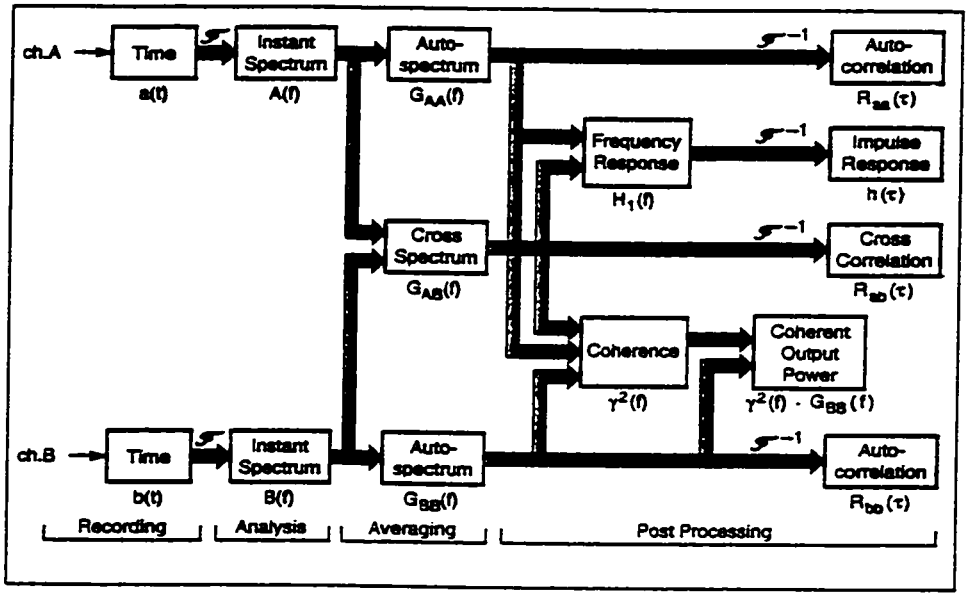

Fig.4.1. A Block Diagram of a Dual-Channel FFT Spectrum Analyzer

measurement chain including both transducers with allied preamplifiers and the FFT analyzer has been calibrated by hammering a known mass (1.25 kg). By checking on the reciprocal value of the frequency response function (FRF), the chain has been calibrated for the correct ratio to ensure the accurate FRF measurements. The result is shown in Fig.4.2.

Once, the setup has been calibrated the tool head is hammered in transverse direction at about 100mm from the guide bushing face. The accelerometer has been mounted on the boring bar between the stuffing box and the Lanchester damper so as to avoid the node points of as many modes as possible. An isolated mounting stud has been used to prevent the ground loops since the machine has been grounded for safety reasons. Here presented result corresponds to a 2.1m-long boring bar for a 25.4mm-diameter tool.

The validity of the measurement has been checked by calculating the coherence function. The measurement has shown that the boring bar assembly features high damping. The bar has been so "soft" that the author could hardly hammer it without a double hit. The conclusion is backed up by the heavily rounded peaks in Fig.4.3 as well as with the large circles in the Niquist diagram in Fig.4.4. To conclude how this relates to the dynamics of the setup under real operating conditions, it is necessary to carry out a signal analysis first.

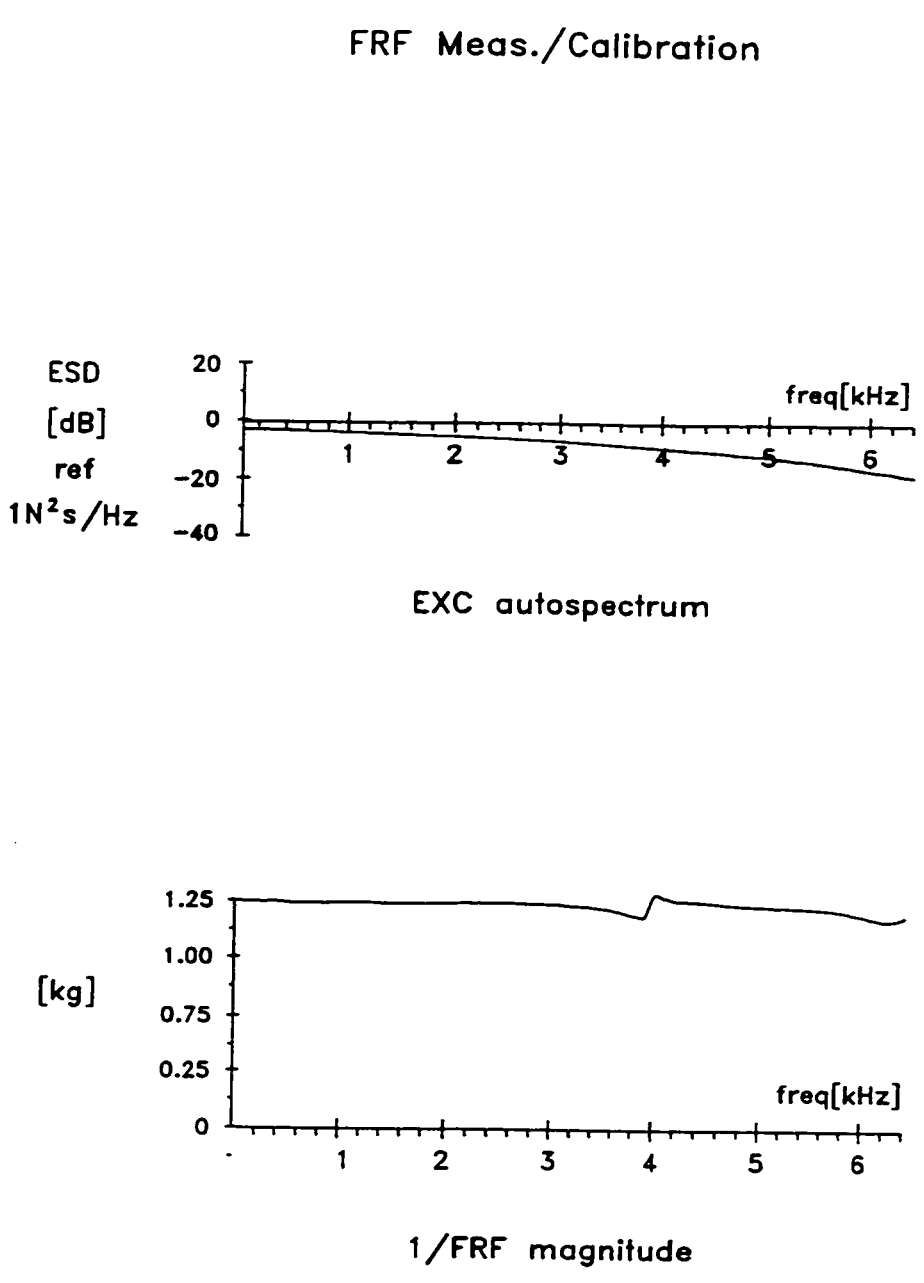

Fig.4.2. Calibration for FRF Measurements

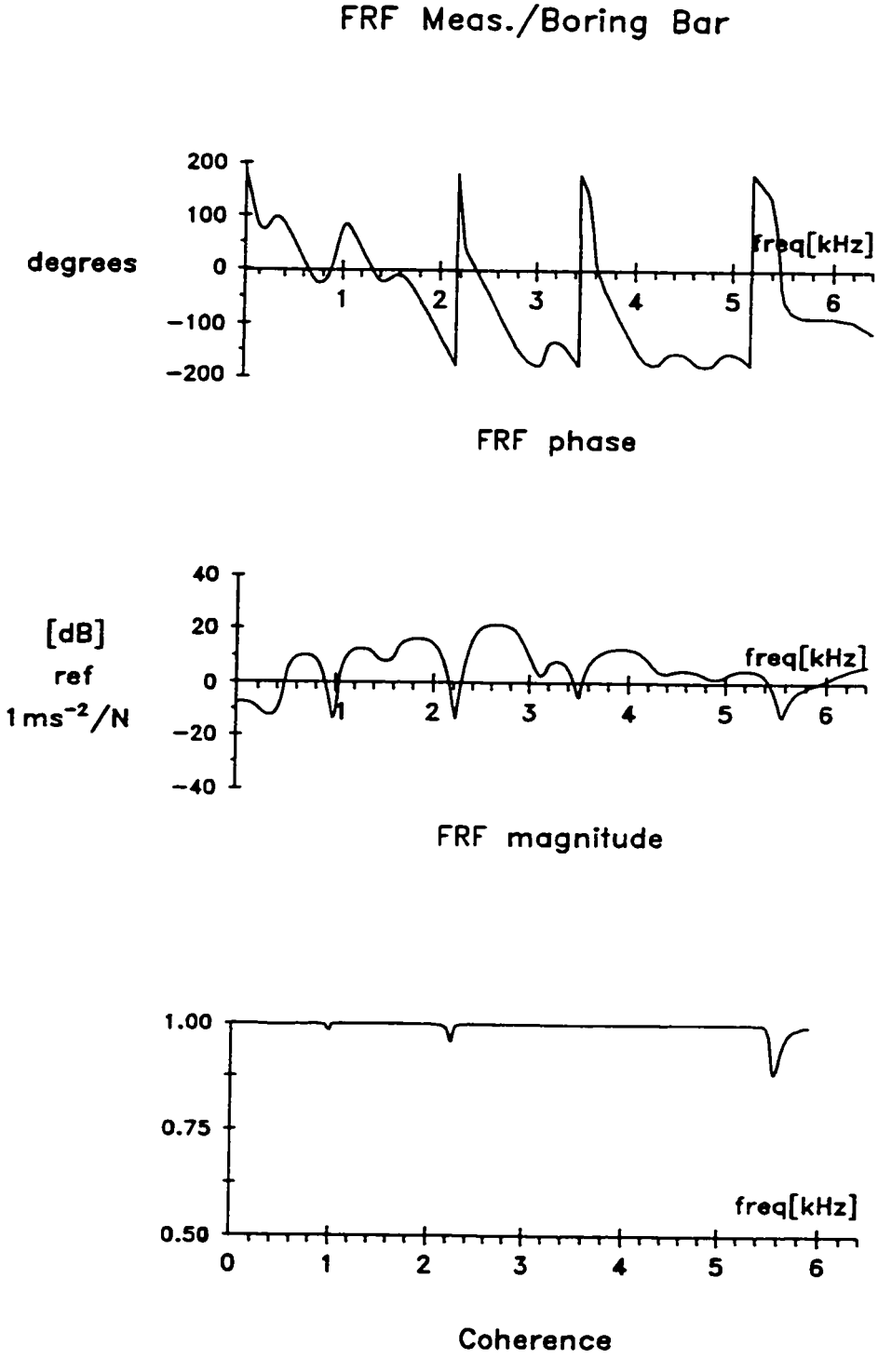

Fig.4.3. FRF of a Boring Bar in Bending Modes
(Non-Operating Conditions)

FRF Meas./Niquist

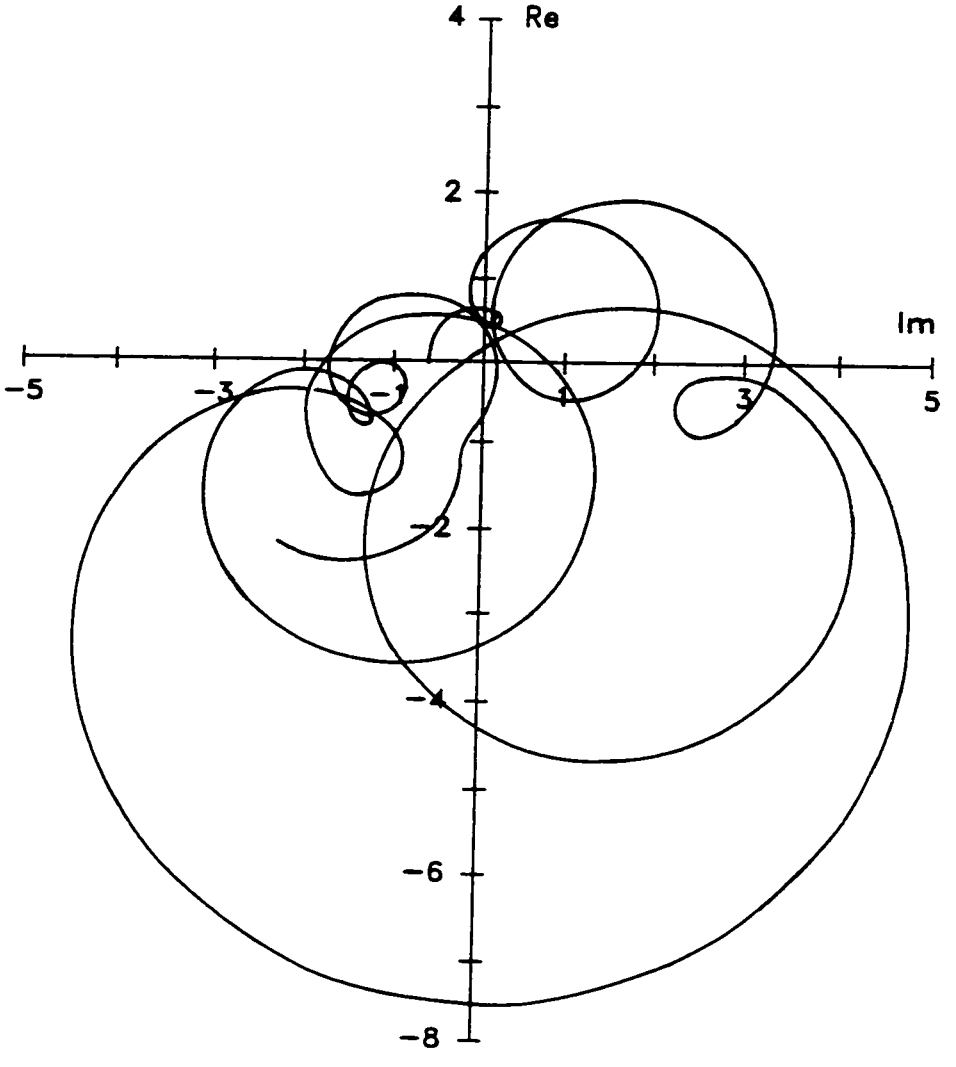

Fig.4.4. FRF of a Boring Bar in Bending (Niquist Plot)

4.3. Signal Analysis - Boring Bar Bending

Provided it has been properly conducted, a signal analysis offers the advantage of a 100%-authentic results since the measurements are carried out under real operating conditions. It is only reasonable that the dynamic system of a machine tool assumes its final properties after the operating forces are applied to take up the clearances in the assembly, introduce friction, establish the interaction with the cutting process' dynamics, etc. Thus, a simple signal analysis would be the logical choice to start an investigation into the dynamics of a machine tool as complex as a deep hole drilling machine.

In the view of the discussion presented in Chapters 2&3, the output has been chosen to cover (1) the lateral deflection of the boring bar, and (2) the thrust and the drilling torque. The former has been acquired by a non-contact, eddy current-based proximity probe by Kaman Measuring Systems (KD-2350). The latter have been measured by a piezo-electric, two-channel load washer by Kistler Instruments (Mo.9065) integrated into a robust dynamometer designed at Concordia University following Kistler's recommendations. The details of both measuring setups and their calibration can be found in the Appendix.

The following pages will simply present a number of spectra acquired under various conditions clearly stated in or below the figures. The spectra will be arranged in pairs so as to facilitate the final analysis as much as possible. The conclusions will be provided together with a particular reference to each and every of the spectra.

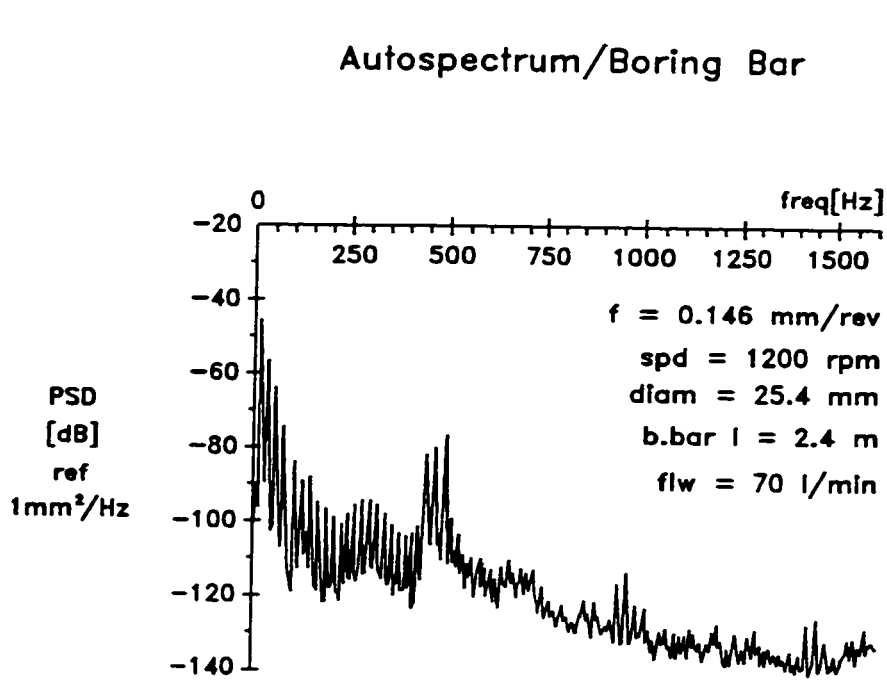

(a) vibration signature (PSD format)

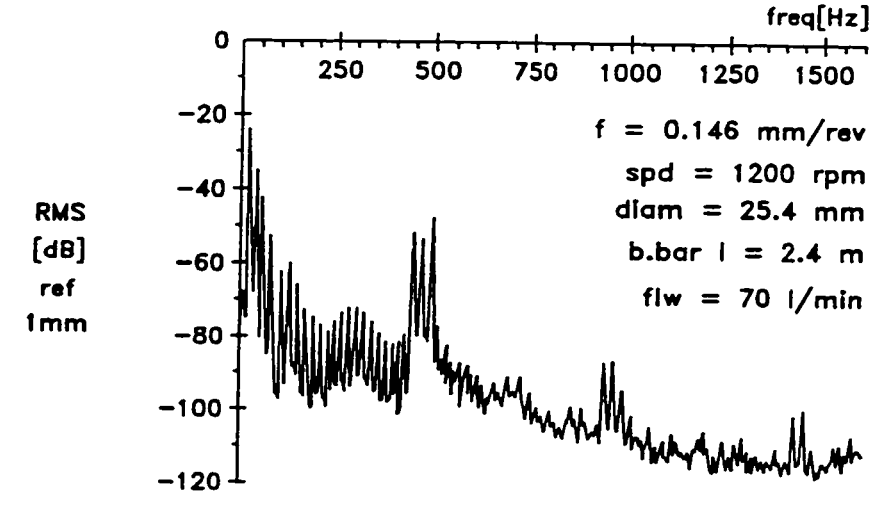

(b) vibration signature (RMS format)

Fig.4.5. Autospectra (PSD vs. RMS Format)

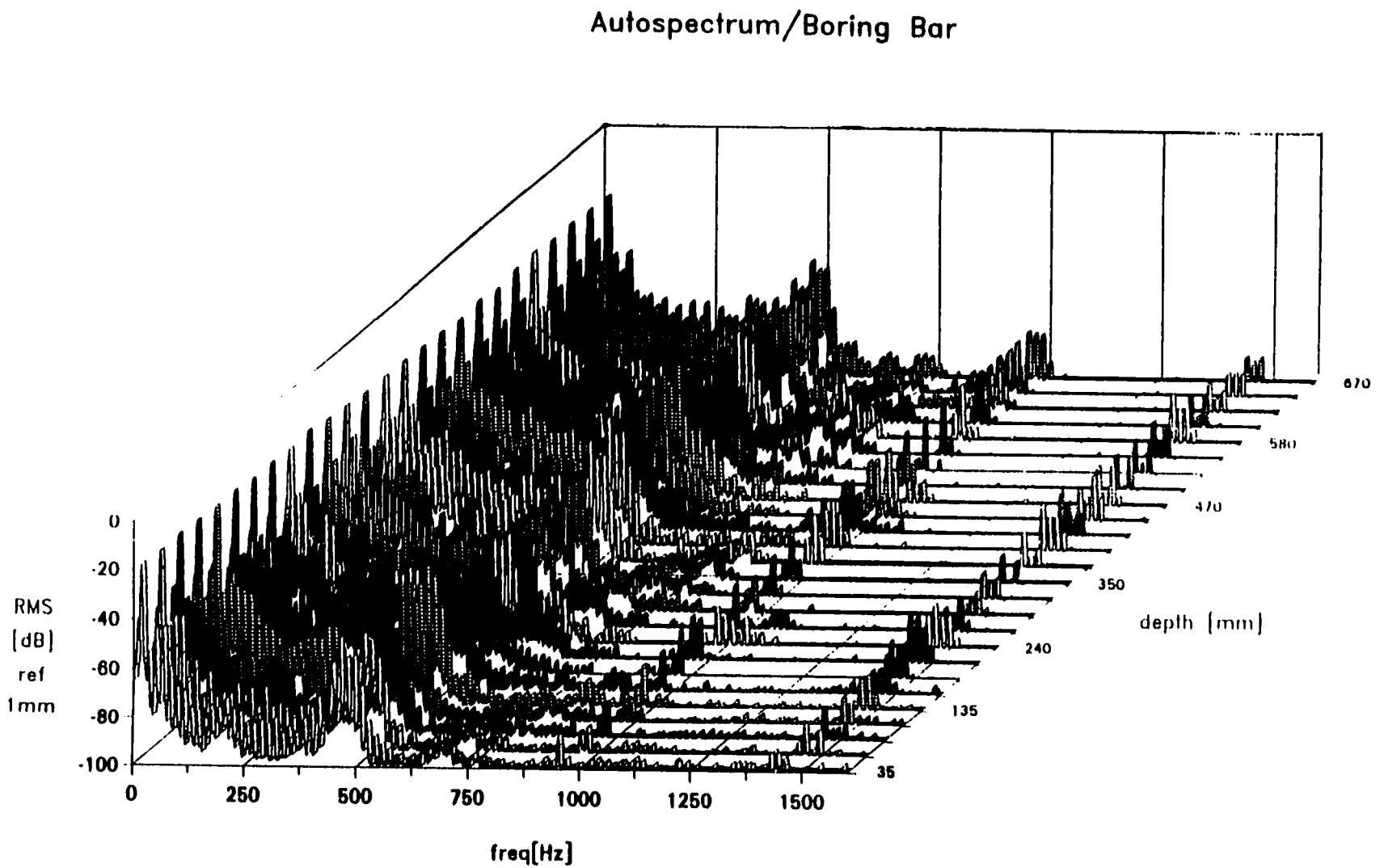

Fig.4.6. Autospectra/Waterfall Diagram

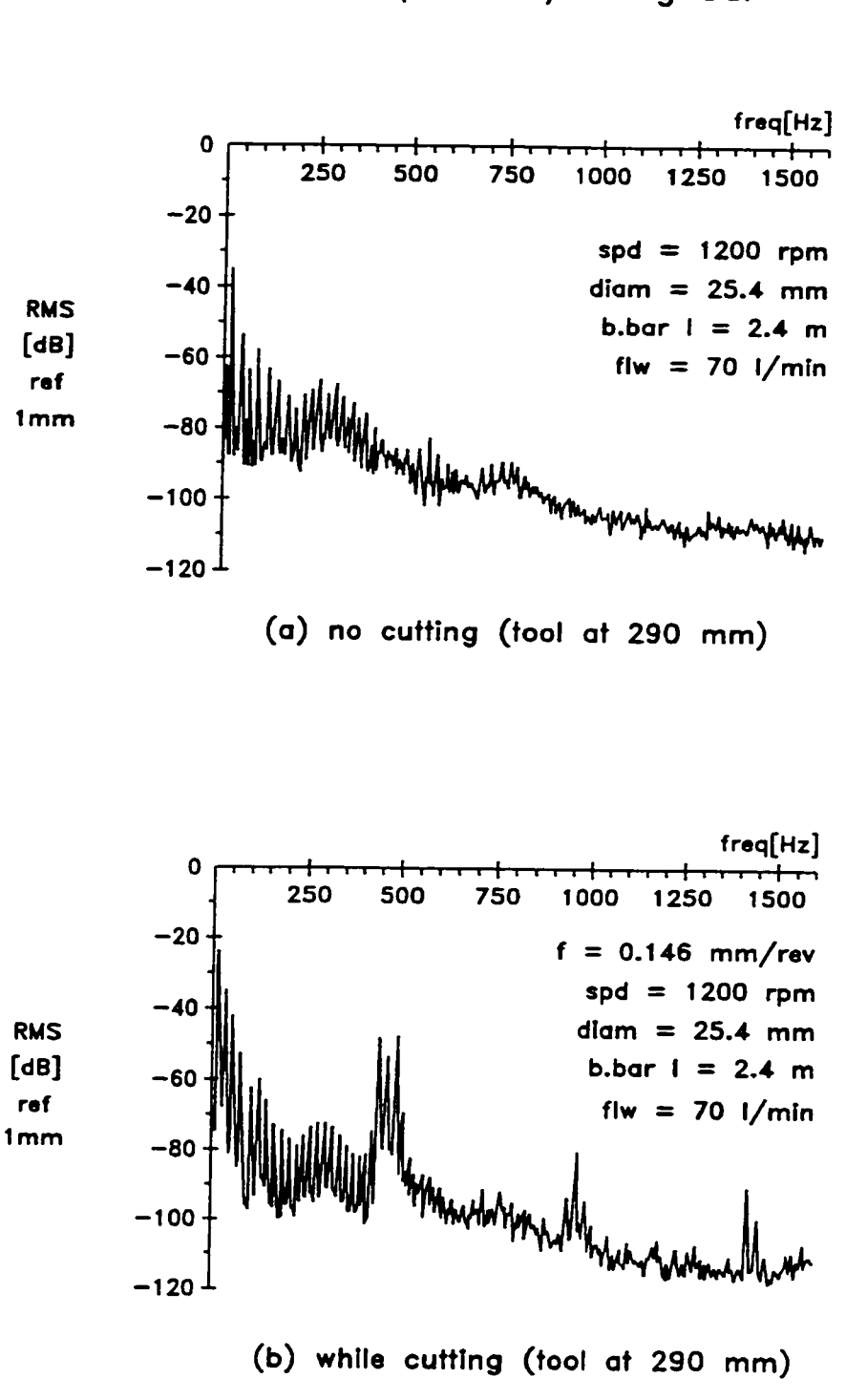

Fig.4.7. Autospectra (Cutting Signature)

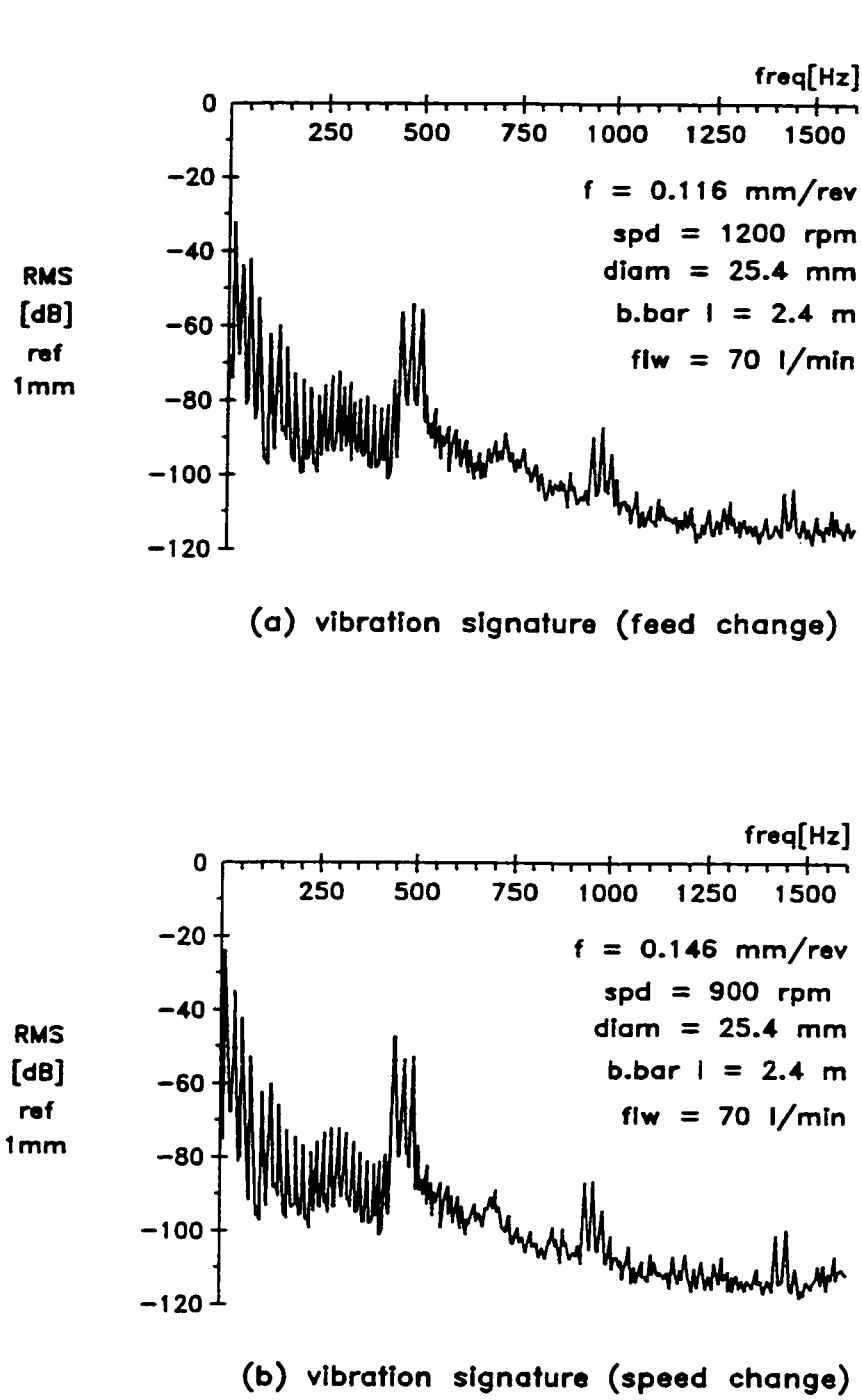

Fig.4.8. Autospectra (Feed vs. Speed)

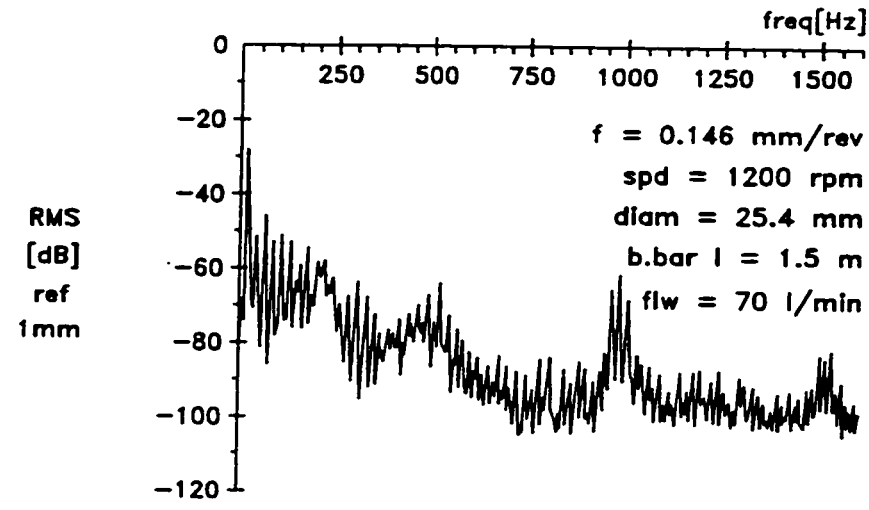

(a) vibration signature (short b.bar)

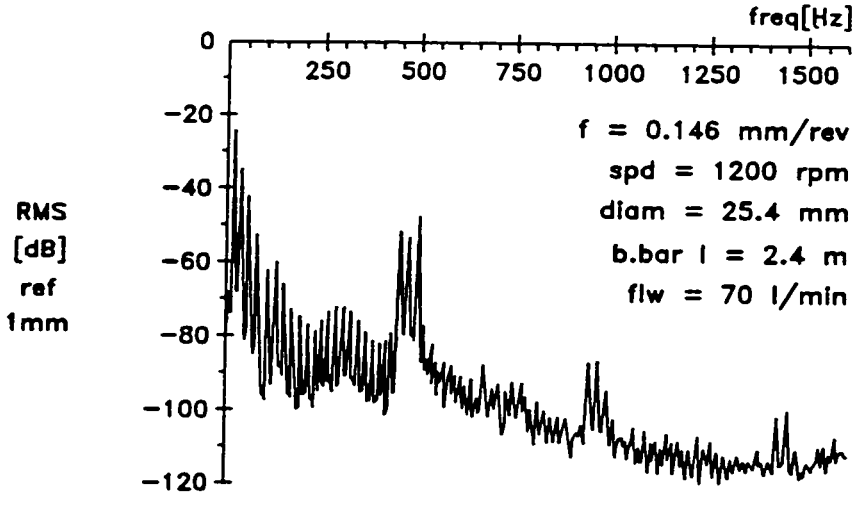

(b) vibration signature (long b.bar)

Fig.4.9. Autospectra (Short vs. Long B.B)

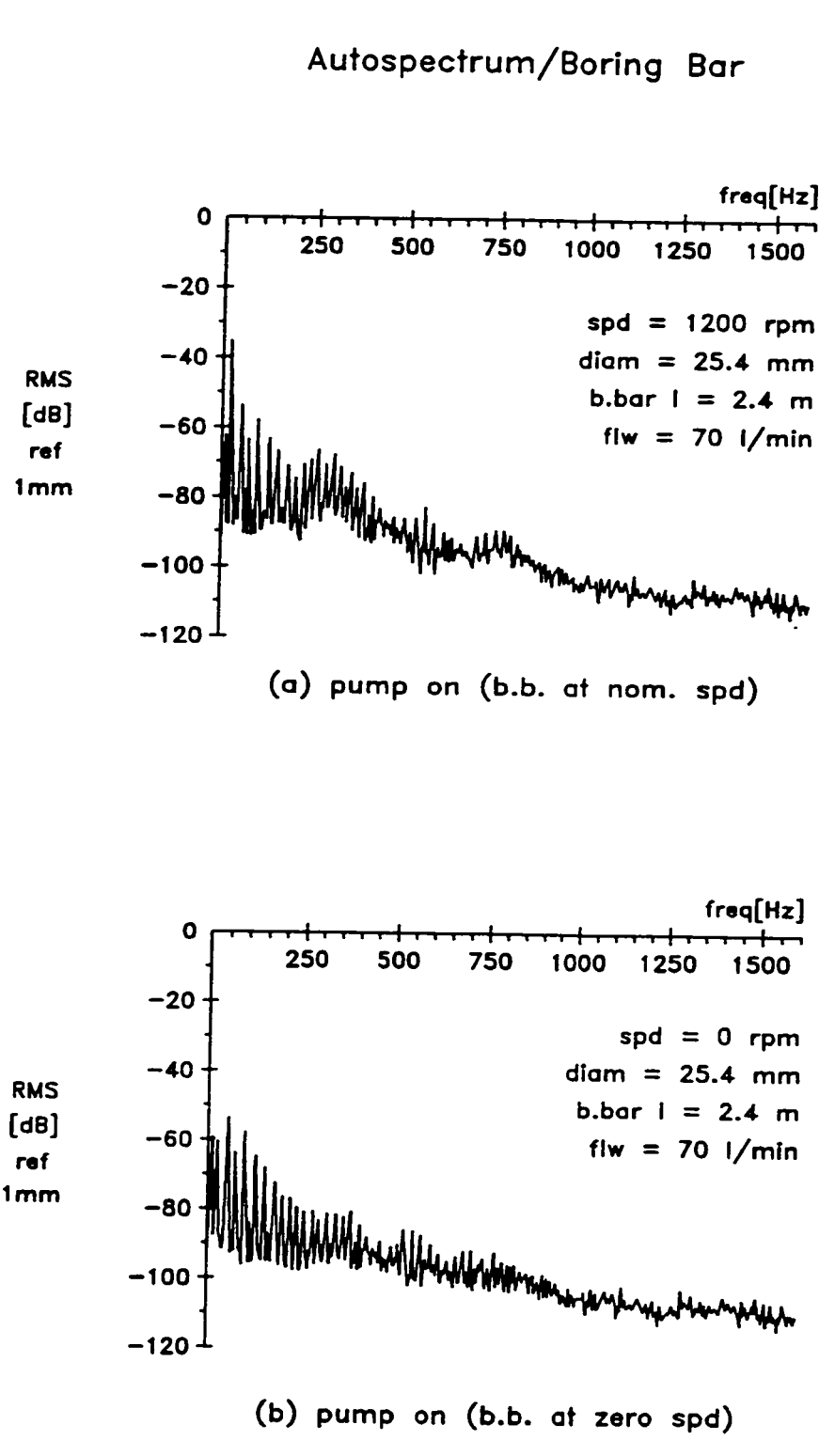

Fig.4.10. Autospectra (Pressurized Flow)

Autospectrum/Boring Bar

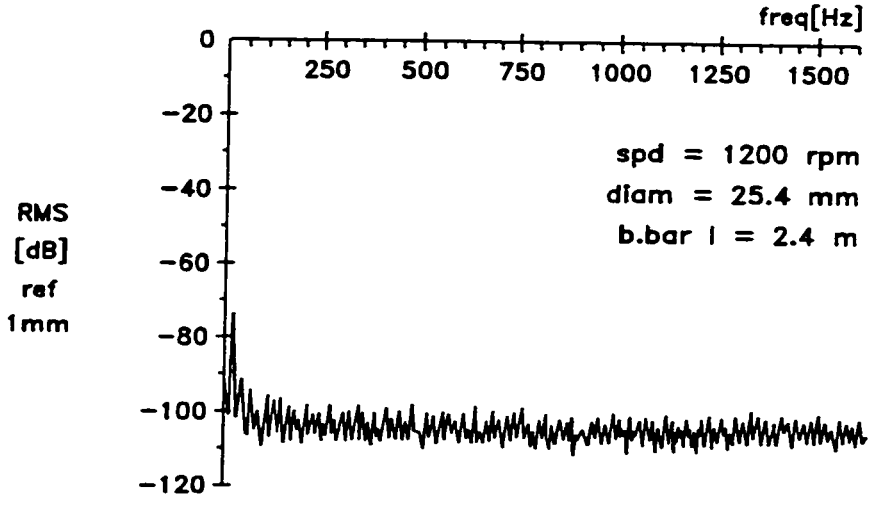

(c) pump off

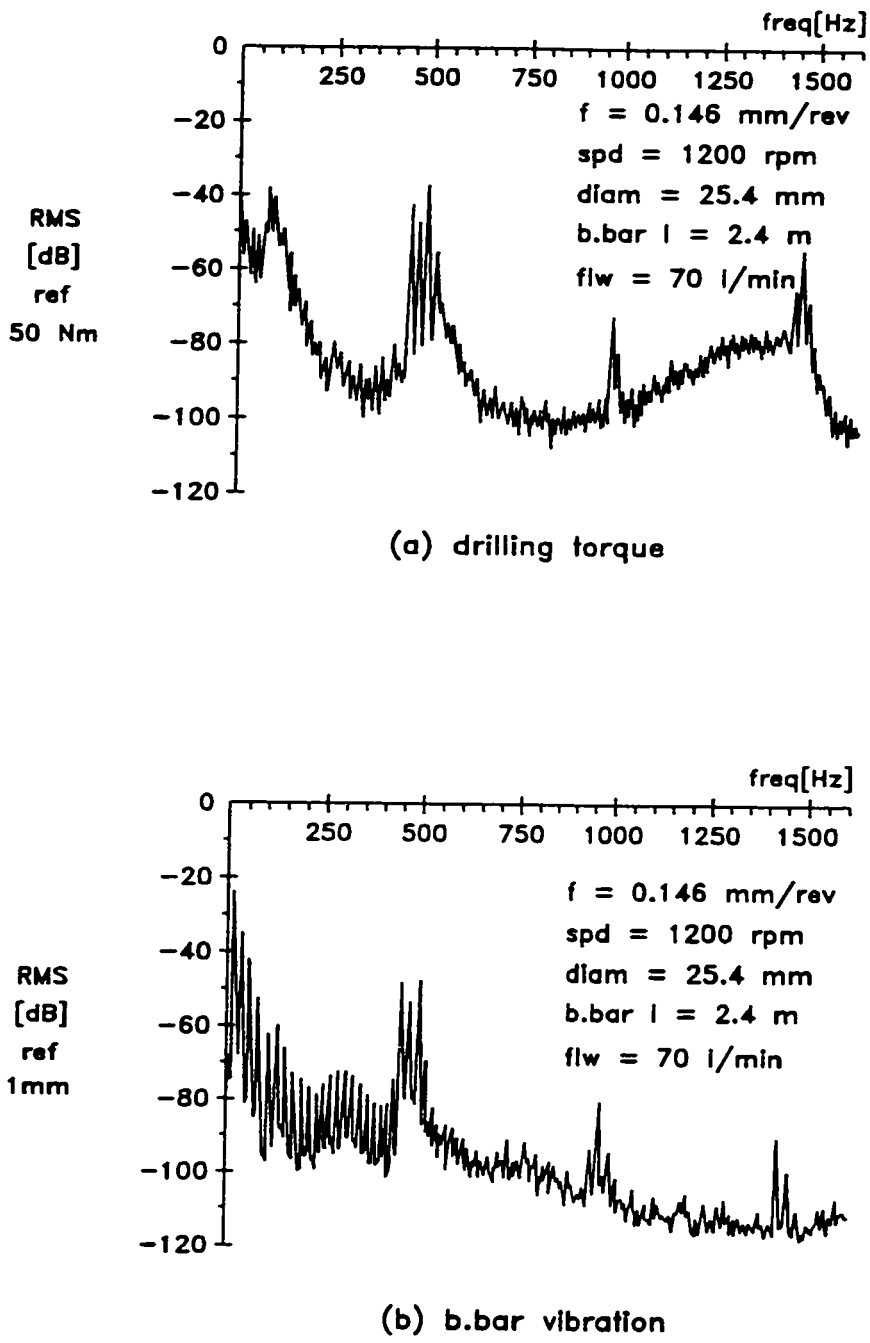

Fig.4.11. Autospectra (Torque vs. B.B. Lateral Motion)

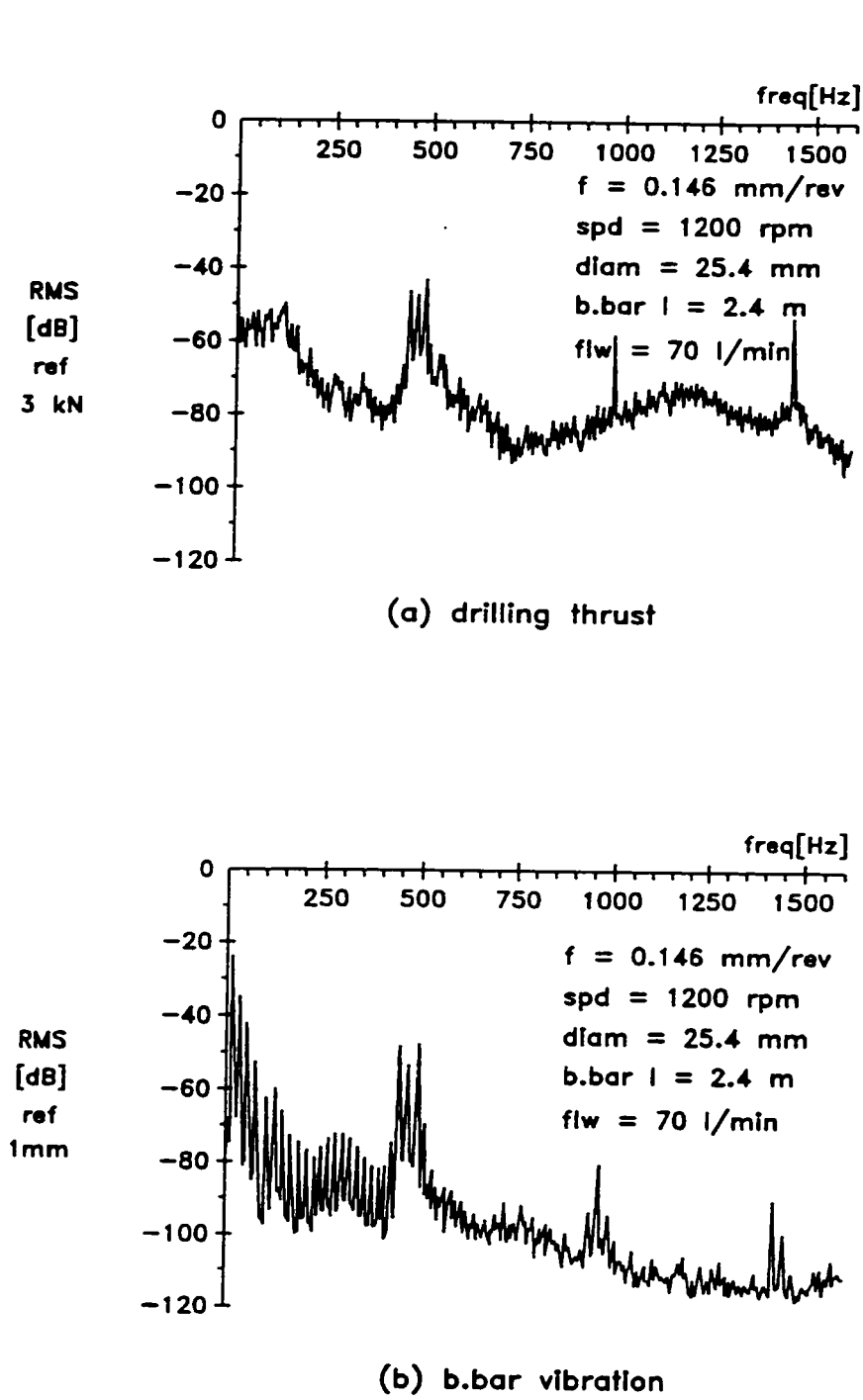

Fig.4.12. Autospectra (Thrust vs B.B. Lateral Motion)

4.4. Conclusions Based on Measurement Results

Signal analysis presented in Sec.4.3 has revealed a typical lateral vibration signature of the boring bar as it appears under real operating conditions i.e. while drilling.

(1) Fig.4.5 shows two autospectra of boring bar lateral vibrations which have been acquired simultaneously but scaled using two different measures i.e. the power spectral density (PSD) and the root mean square value of the signal (RMS). The record reveals the discrete form of the spectra thus confirming that the signal is stationary deterministic as one would expect from a mechanical system featuring rotating components. The figure shows that, for the analysis bandwidth sufficiently narrow to separate all individual components, the use of RMS format is fully justified. The only reason for using the PSD format as a more complex measure normalizing the "power" with respect to the analysis bandwidth could be that, for random signals, the RMS value for each frequency is zero since an infinite number of frequencies are present and the total power is finite. Thus, the result denies the conclusion of some previous work [4], which has recommended the use of the PSD measure as applicable to the continuous spectra of random signals.

(2) Fig.4.6 shows a (3D) waterfall diagram of autospectra calculated for a sequence of records sampled as the tool progressed down the hole. The vibration signature appears steady against a logarithmic scale which is usually applied when studying resonant phenomena. It can be easily seen that the basic dynamic features of the system hold unchanged throughout the operation. The result denies the influence of the increasing overhang of the boring bar on system's resonances as suggested by some authors [10,30]. It is reasonable to assume that the

change in quality encountered depthwise can be related only to the changes over particular parts of the spectra as these appear against a linear scale.

(3) The parts of spectra that reflect the cutting process contribution have been identified by simple comparison of spectra acquired out of cutting and while cutting (Fig.4.7). The "a" spectrum corresponds to a tool rotating in the pressurized flow of cutting oil after being retracted by 2mm from the bottom of the hole. The "b" spectrum has been previously acquired with the drill cutting at the same depth. The rise in the peak at 20Hz (1200 RPM) shows that the application of the drilling forces causes the additional bending of the boring bar. Furthermore, the peak appears the highest in the spectrum which altogether substantiates the conclusions made in Chapter 3.

The cutting action also gives rise to three well distinguished peaks at about 500Hz for the given setup. Their second and third harmonics are visible, as well. Since the peaks are close to each other this in effect indicates a new modulated vibration known as "beating". It is worth mentioning that the same phenomenon has been recognized in numerous experimental works on cutting process dynamics but, so far, there has been no explanation to it.

(4) System analysis presented in Sec.4.2, Fig's 4.3 & 4.4, has revealed a heavy damping on the bending modes of a boring bar under non-operating conditions. Signal analysis in sec.4.3 has shown that the related vibration signature acquired while cutting features sharp peaks in its autospectrum. Thus, the boring bar resonances in bending, as they appear in an open setup, cannot be responsible for a sharp peak in the tooi vibration signature. There could be two possible explanations to this: either (1) the dynamic properties of the boring bar setup

significantly change when the bar is subjected to the real operating conditions, or (2) the peaks in the spectrum of the boring bar lateral vibrations reflect its resonance in torsional modes and the energy transfer to bending. The last explanation fully complies with the result of some previous work [33,34].

(5) Fig.4.8 illustrates an attempt to induce a change in the spectrum of the boring bar lateral vibration by moderate change in speed and feed. Neither of the two seems to be affecting the form of the spectrum or the basic dynamic properties of the system. Speed appears to have virtually no influence on the spectrum, at least not for the two particular values considered (900 rpm and 1200 rpm) and the given setup. Feed per revolution directly relates to the magnitude of the peak corresponding to the boring bar rotation as well as to that of the peaks originating from cutting.

(6) Fig.4.9 shows the difference between the spectra of a short boring bar and a less rigid, longer boring bar. The spectra are the same in form. As one would expect, the spectrum of the short boring bar features peaks at higher frequencies. The spectrum shows not only an offset for the peaks originating from the cutting process but, interesting enough, the broadband vibration at frequencies below has been extended to cover the increased span. The broadband vibration also assumes the same order of magnitude as the vibration from cutting.

(7) Fig.4.10 finally reveals the origin of the broadband vibration following the boring bar rotation up to the first peaks coming from the cutting process. The spectra point towards the pump and the pressurized, turbulent flow of the cutting oil as the cause. They further show that the vibration reflects a steady input from the pump together with a dynamic effect of the

boring bar rotation on the flow. Since it covers a broad range of frequencies with a more-or-less steady amplitude, this vibration appears significant in terms of its energy contribution to the total signal. The small peak left in the spectrum "c", sampled with the retracted tool and the pump off, reflects the initial curvature of the boring bar rotated in the setup. Very small value at the peak is a proof of near-perfect alignment of the setup.

(8) Fig's 4.11 & 4.12 show the striking similarity between the spectra of the drilling torque, and the drilling thrust, versus the spectrum of the boring bar lateral vibration. The spectra sampled from the dynamometer reflect all the peaks as well as the broadband content of the spectrum sampled from the proximity probe. The only difference is the broadband background at higher frequencies in the torque and thrust spectra. At this point, no explanation could be offered regarding this phenomenon. Nevertheless, as far as the major energy content and amplitudes are concerned, the measurement is a proof of the boring bar lateral vibration affecting the drilling forces and vice versa.

Chapter 5

Conclusions

5.1. Summary

This work has been set out to pinpoint and explain what appears to be the major shortcoming of the conventional self-piloting (SP) tool design. The work has been motivated by reports on inconsistent tool performance in seemingly identical applications. These reports have been common in both academic research and the deep hole machining practice.

The study has focused on burnishing, a process known for featuring high sensitivity to minor changes in its input. The work has addressed the question raised by some past research on SP burnishing which has found it difficult to reproduce results obtained with another tool or another machine tool. Special attention has been paid to the so far inexplicable pattern of the support pads' wear.

What has served as a starting point is the fact that the accuracy of a SP tool mating with the piloting hole determines the effective contact area involved in burnishing thus affecting the output quality. Bearing in mind the small burnishing step height and high quality requirements, the author has emphasized that the mating geometry is to be considered with a close look in terms of micrometers. The analysis of the tool head mounting for the worst case of technological inaccuracies has shown that the tool head appears as a solid extension to the boring bar. Therefore, the author has taken a new approach considering the tool head geometry and the force system together with the boring bar setup arrangement. In this way, for the first time, the tool balance considerations have been extended beyond the transverse

plane to include the tool effective inclination in 3D. The analysis has resulted in a comprehensive model of the tool head support in the machining zone. The model explains the support pads' wear pattern as it has been known for years. It also explains the inherent difficulty to alter the pattern by changing the pads' backtaper which has been acknowledged by past research.

The study has included a comprehensive analysis of the influence of various tool design parameters on the effective geometry involved in burnishing. The significance of changing various parameters at the tool design stage has been estimated and compared with the contribution of in-process encountered effects which are beyond the tool designer's control. The comparison has favored in-process encountered effects, especially hole oversizing, thus very much limiting the tool designer's influence. The major reason for this is that the engineer designs only the tool head but, in process, the head is integral with a long boring bar and the piloting function of the support pads does not reach back away from the cutting point. The boring bar, in turn, connects to a number of elements and heavily depends on their true alignment. Here, the difficulty to maintain a near-perfect alignment of the setup has been acknowledged with a reference to reports from experts in the deep hole machining practice. Since the tool support model has shown that the inherent feature of the design is to bend the boring bar even if it is initially straight, the usual check out on the boring bar buckling stability has lost much of its first significance. In that context, the author has proposed that a spherical joint be integrated in the tool drive spindle assembly. This would compensate for the worst case of angular misalignment in clamping elements which is likely to adversely affect the tool performance.

The study has also pointed out a fact that is almost self-evident but it has never been acknowledged explicitly. A SP tool appears virtually the same in different kinematic schemes only as long as the axis of the tool perfectly coincides with that of the workpiece. As soon as an inclination of the tool with respect to the workpiece occurs, the working methods introduce an effective difference in the process.

Finally, a signal analysis under real operating conditions has been carried out with a scope on the boring bar lateral movements and the drilling forces. A Fast Fourier Transform (FFT) unit has been used to facilitate the interpretation of the results in frequency domain. The signal has been shown to be stationary deterministic and the use of the RMS measure to scale the spectra has been justified. The parts of the spectra reflecting the cutting process signature have been identified. It has been shown that the boring bar rotation dominates the spectra of its lateral movements proving in-process encountered boring bar bending. The spectra show a broadband energy contribution of the pressurized, turbulent flow of the cutting oil. This finding can be significant since the input occurs beyond the stuffing box as the last conceivable boring bar support. The major finding is that the spectra of the drilling torque and thrust reflect the spectra of the boring bar lateral movements. This confirms the influence of the boring bar lateral movements, and its inclination as dominant, on the drilling forces and vice versa. These are only the experimental results which stand out since they substantiate the theoretical findings of the work. The full list of measurement results can be found in Sec.4.4.

As far as the industrial application is concerned, this work will hopefully make the SP tool designers aware of the constraints they are facing when trying to ensure high SP tool performance at the tool design stage. Moreover, for industrial research, the author would like to put into perspective a new design of SP tools which may overcome the inherent drawbacks of the conventional design (Fig.5.1).

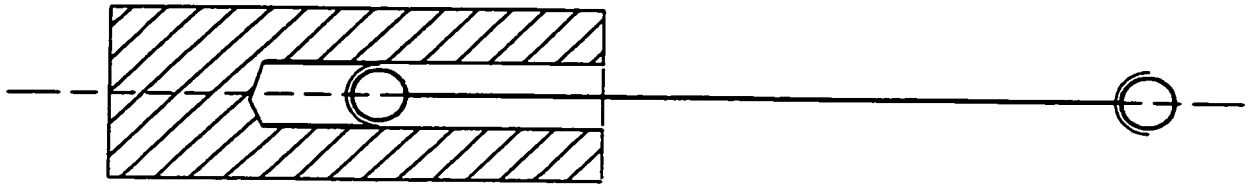

Fig.5.1. A Scheme of a SP Setup with Compensation for Boring Bar Inclination

5.2. Recommendations for Future Work

The main goal behind this work has been to actually start a new line of research in the area of deep hole machining which will hopefully have practical implications. The study has introduced a new approach considering the tool head as the integral part of the boring bar setup thus expanding the traditional research scope to include a look at the tool in 3D. The study has surfaced out the unfavorable fact that the boring bar is capable of transmitting all kinds of disturbances encountered along the setup to the cutting tip. The work does not claim to have documented the finding thoroughly, however it does claim to have made the first step into the new direction.

The logical next step would be to reach beyond the first-approximation analysis to document the interaction between the boring bar and the cutting tip. In that context, a thorough investigation into the effect of different cases of misalignment would probably come first. Re-designing the elements along the boring bar setup to compensate for their misalignment might be a practical outcome. The application of the proposed approach to a study of the tool entrance conditions would be a logical follow up. This would hopefully lead to the first practical guidelines regarding wear tolerances in the guide bushing.

Eventually, in the long term, the final application of the new approach would be in the development of a SP tool design which uses the full width of the support pads for burnishing. In addition to that, the design should allow the tool designer to assume the full control over the pressures involved in burnishing by realizing the effective contact length at the tool design stage.

References

1. Astakhov, V., and Osman, M.O.M., 1996, An Analytical Evaluation of the Cutting Forces in Self-Piloting Drilling Using the Model of Shear Zone with Parallel Boundaries, Part 2:Application, Int. J. Mach. Tools Manufact., 36(12), pp.1335-1345.
2. ASTME Ed., 1967, Gundrilling, Trepanning and Deep Hole Machining, Dearborn, MI.
3. Atanackovic, T, 1987, Theory of Elastic Rod Stability, University of Novi Sad, YU (in Serbian).
4. Chandrashekhar, S., 1984, An Analytical and Experimental Stochastic modeling of the Resultant Force System in BTA Deep Hole Machining and Its Influence on the Dynamics of the Machine Tool Workpiece System, PhD Thesis, Concordia University, Montreal.
5. Corney, T. and Griffiths, B. J., 1976, A Study of the Cutting and Burnishing Operation During Deep Hole Drilling and Its Relation to Drill Wear, Int. J. Prod. Res., 14(1).
6. Druxeis, R., 1977, Deep Drilling - Reduction of Radial Loads on Deep Hole Machine Tools, VDI Nachrichten, 31(6), pp. 19, (in German).
7. Doi, S., Kitano, M., and Yagishita, H., 1973, Torsional Vibration of Workpiece, ASME Design Engineering Technical Conference, Cincinnati, Ohio, Sep.
8. Fink, P. G., 1977, Optimum Cutting Speed and Feed Rate in Deep Hole Drilling, Proc. 2nd Int. Conf. on Deep Hole Drilling and Boring, Brunel University, Uxbridge, UK.
9. Fuss, H., 1986, On Parameters Affecting Quality of BTA Drilled Holes, Tiefbohren, 4/1986, University of Dortmund, (in German).

10. Gessesse, Y. B., 1990, Stability of BTA Deep Hole Machining Process, MASc Thesis, Concordia University, Montreal.

11. Greuner, B., 1970, Investigation of Cutting Edge- and Pad Forces in Single-Lip Carbide Deep Hole Tools, PhD Dissertation, Technical University of Hannover, (in German).

12. Grieve, R. J. And Griffiths, B. J., 1984, The Economics of Multi-Cutting and Deformation Region Tools, Int. J. Prod. Res., 22(5), pp. 724-745.

13. Griffiths, B. J., 1973, The Machining Action During Deep Hole Boring and the resultant Hole Form and Force System, Proc. 2nd Int. Conf. on Production Research, Copenhagen, Denmark.

14. Griffiths, B. J., 1975, Deep Hole Drilling Processes and Surface Integrity, Proc. 2nd Int. Conf. on Deep Hole Drilling and Boring, Brunel University, Uxbridge, UK.

15. Griffiths, B. J., 1977, Guidelines for Planning a Deep Hole Drilling Operation, Proc. 2nd Int. Conf. on Deep Hole Drilling and Boring, Brunel University, Uxbridge, UK.

16. Griffiths, B. J., 1977, Axial Hole Run-Out During Deep Drilling, Proc. 2nd Int. Conf. on Deep Hole Drilling and Boring, Brunel University, Uxbridge, UK.

17. Griffiths, B. J., 1982, An Investigation into the Role of the Burnishing Pads in the Deep Hole Drilling Process, PhD Dissertation, Brunel University, Uxbridge, UK.

18. Jin-Hua, C, and Li-Wei, L., 1995, A Study of the Tool Eigenproperties of a BTA Deep Hole Drill - Theory and Experiments, Int. J. Mach. Tools Manufact., 35(1), pp. 29-49.

19. Katsuki, A., Sakuma, K, and Onikura, H., 1987, Axial Hole Deviation in Deep Drilling - the Influence of the Shape of the Cutting Edge, 20(6), pp.50-56.

20. Lukic, Lj., 1987, Contribution to Investigation of Factors Affecting Quality in BTA Deep Hole Machining, Masinstvo, 36(11), pp. 1061-1066, (in Serbian).

21. Osman, M.O.M., Latinovic, V. N. and Greuner, B.,1981, On the Performance of Cutting Fluids for B.T.A. Deep Hole Machining, Int. J. Prod. Res., 19(5), pp. 491-503.

22. Pfleghar, F., 1974, Cutting Edge- and Pad Forces in Gundrills, Werkzeugmaschine International, 6, pp. 51-57, (in German).

23. Pfleghar, F., 1977, Guidelines for Deep Hole Tool Design, WT Zeitschrift fuer Industrielle Fertigung, 67, pp. 211-218, (in German).

24. Rao Ramakrishna, P. K. and Shunmugam, M. S., 1987, Accuracy and Surface Finish in BTA Drilling, Int. J. Prod. Res., 25(1), pp. 31-44.

25. Rao Ramakrishna, P. K. and Shunmugam, M. S., 1988, Wear Studies in Boring Trepanning Association Drilling, Wear, 124, pp. 33-43.

26. Randall, R. B., 1987, Frequency Analysis, K. Larsen & Son, Glostrup, Denmark.

27. Sakuma, K., Taguchi, K. and Kinjo, S., 1978, The Effect of Tool materials on the Cutting Performance, Bull. JSME, 21(153), pp. 532-539.

28. Sakuma, K., Taguchi, K. and Katsuki, A., 1980, Behavior of Tool and Its Effects on Profile of Machined Hole, Bull. Jap. Soc. Prec.Eng., 14(3), pp. 143-148.

29. Sakuma, K., Taguchi, K. and Katsuki, A., 1981, Self-Guiding Action of Deep Hole Drilling Tools, Annals of CIRP, 30/1, pp. 811-815.

30. Sakuma, K., Taguchi, K. and Katsuki, A., 1980, The Burnishing Action of Guide Pads and Their Influence on Hole Accuracies, Bull. JSME, 23(185), pp. 16-23.

31. Shunmugam, M. S., 1986, On Assessment of Geometric Errors, Int. J. Prod. Res., 24(2), pp. 413-425.

32. Stockert, R. and Weber, U., 1978, Layout of Single-lip Deep Hole Tools with Two Cutting Edges, VDI Berichte 120, 22, Nov., pp. 1057-1061.

33 Stockert, R., 1978, Contribution to Optimal Layout of Deep Hole Tools, PhD Dissertation, University of Dortmund, (in German).

34. Streicher, P. 1971, Study of Vibrations in Slender Gundrills, VDI-Berichte, 166, pp. 147-150, (in German).

35. Timoshenko, S, and MacCullough, G., 1977, Elements of Strength of Materials, D. Van Nostrand Co., Toronto.

36. Troicky, N. D., 1971, Deep Hole Drilling, Машиностроение Ленинград, (in Russian).

37. Weber, U., 1977, Distribution of Load and Balance of Energie in Deep Hole Boring, Proc.2nd Int. Conf. on Deep Hole Drilling and Boring, Brunel University, Uxbridge, UK.

38. Weber, U., 1977, Cutting Force Measurements in Deep Hole Drilling, VDI Berichte, 301, p.27-35, (in German).

39. Weber, U., 1978, Contribution to Deep Hole Process Measurements, PhD Dissertation, University of Dortmund, (in German).

Appendix

In the experimental part of this work, a Kaman Ins. Displacement Measuring System (Mo. KD-2310) has been used to perform non-contact measurements of the boring bar lateral movement. The system includes a proximity probe (sensor), a coaxial cable and signal conditioning electronics. The electronics package provides for the zero, gain and linearity adjustments. The system uses the principle of impedance variation caused by eddy currents induced in a conductive metal target. The coupling between a coil in the sensor and the target depends on their relative displacement (gap). The system is designed to provide an output voltage proportional to the gap. The parallelism between the sensor face and the target is not critical as long as the angle they make does not exceed 15 degrees. The system has a measuring range of 0-80 mils, a recommended offset of 15 mils, and provides a voltage output of 0-0.8 V and a sensitivity of 10 mV/mil.

The calibration procedure comprises the following steps:

Step 1: Set the FINE LINEARITY control to mid range. With the target at full scale displacement (plus offset), adjust COARSE LINEARITY control to the desired full scale output voltage. Step 2: With the target at "zero" displacement (the recommended offset from the face of the sensor), adjust ZERO control until the output is zero volts. Step 3: Move the sensor away from the target by the displacement equal to one-half of the chosen full range; adjust the GAIN control to obtain half-scale output voltage. Step 4: Move the sensor away from the target to the chosen full scale displacement point, read the output and note the difference between the actual reading and the desired reading. Using the COARSE LINEARITY control, adjust the output to the desired setting and then continue past the desired setting by an amount equal to the noted difference. Step 5: Repeat steps 2 through 4 until the calibration is attained.

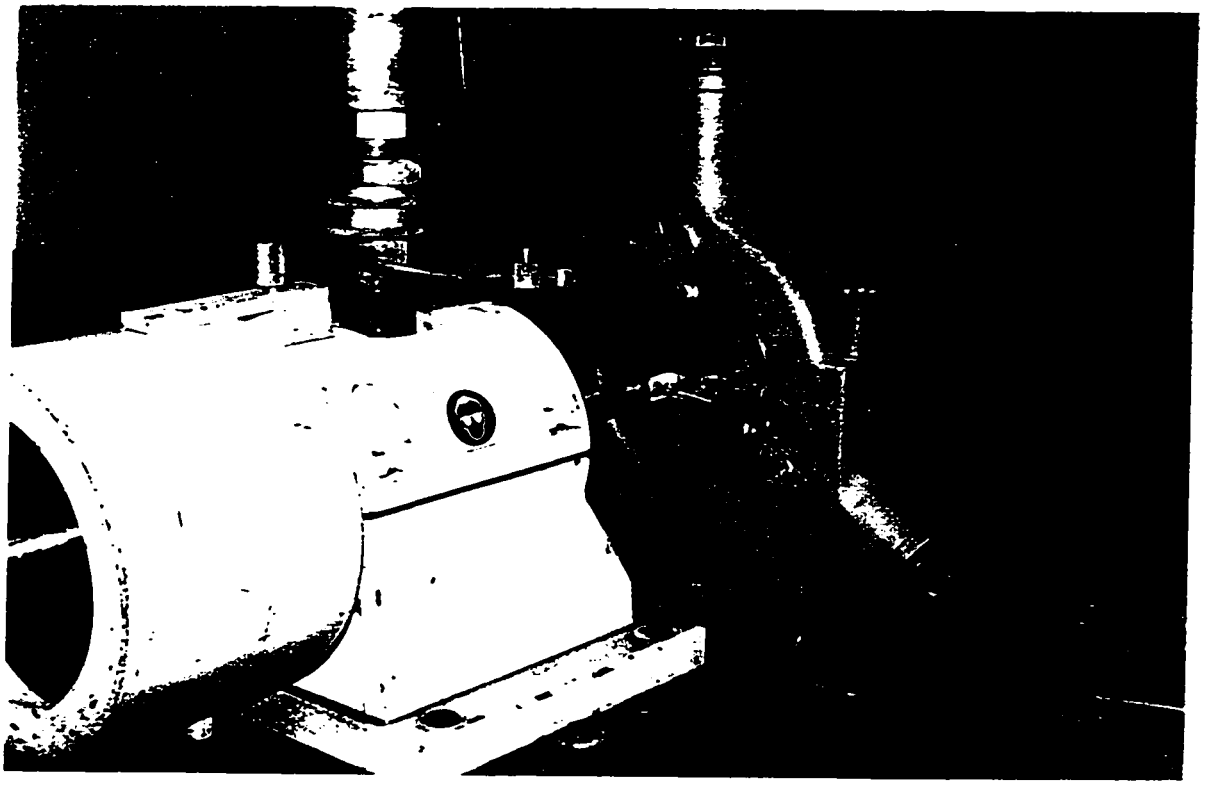

Fig.A.1. Proximity Probe Mounting

To measure the thrust and the torque while drilling, a 2-component piezo-electric load washer by Kistler (Mo. 9065) has been used. The transducer incorporates two disks, each with a ring of quartz cristals precisely oriented in the corresponding direction (circumferential or axial). The load washer has been integrated into a dynamometer (Fig.A.2) to be held in the chuck. The washer has been preloaded by two flanges and 10 bolts in order to attain its elastic pretension since the torque has to be transmitted by friction. Tab.A.1. gives the technical details of the transducer.

Tab.A.1. Load Washer 9065 by Kistler - Technical Data

Range	F_z	kN	±20	1)
	M_z	Nm	±200	1)
Overload		%	20	
Max. normal force	F_z	kN	144	
Max. shear		kN	±12	1)
Max. moment	M_x, M_y	Nm	±200	1)
Threshold	F_z	N	≈0,02	
	M_z	Ncm	≈ 0 , 0 2	
Sensitivity	F_z	pC/N	−1,8	
	M_z	pC/Ncm	−1,6	
Linearity		%FSO	≦±1,0	
Hysteresis		%FSO	≦1,0	
Crosstalk	$F_z \rightarrow M_z$	Ncm/N	≦±0,02	
	$M_z \rightarrow F_z$	N/Ncm	≦±0,01	
	F_x, $F_y \rightarrow F_z$	%	≦±2,0	
	F_x, $F_y \rightarrow M_z$	Ncm/N	≈±0,1	
Rigidity	x, y direction	kN/µm	≈1,3	
	z direction	kN/µm	≈6,5	
	torsion z axis	Nm/mrad	≈500	
Natural frequency		kHz	≈40	
Operating temperature range		°C	−196...150	
Temperature coefficient of the sensitivity		°C⁻¹	$-2 \cdot 10^{-4}$	
Temperature error	F_z	N/°C	÷30	
	M_z	Ncm/°C	−5	
Capacitance		pF	350	
Insulation resistance		Ω	$>10^{13}$	
Shock and vibration		*g*	<2000	
Weight		g	≈150	

1) Standard mounting with 120 kN prestress

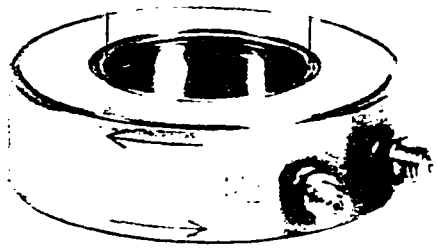

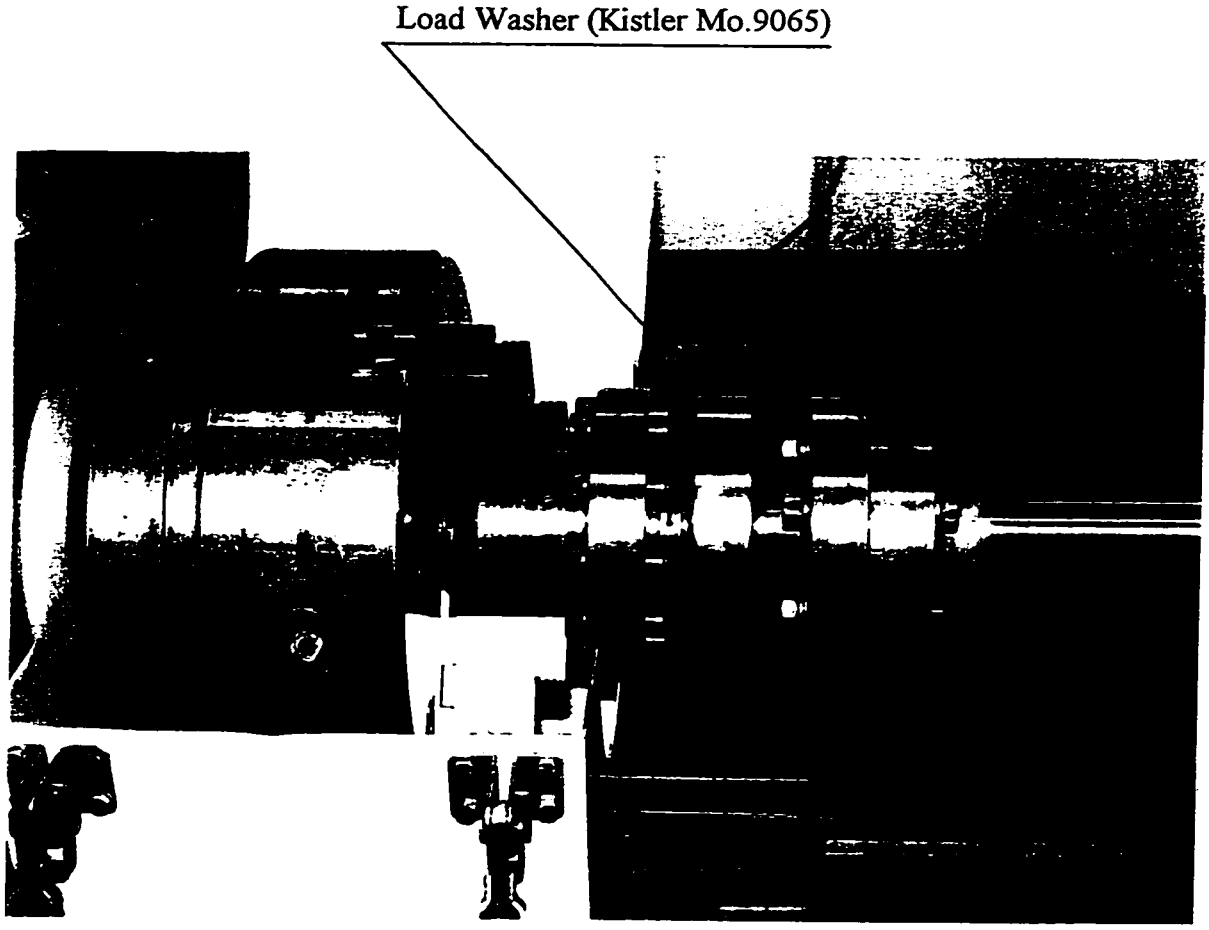

Fig.A.2. Dynamometer Incorporating a 2-Component Load Washer

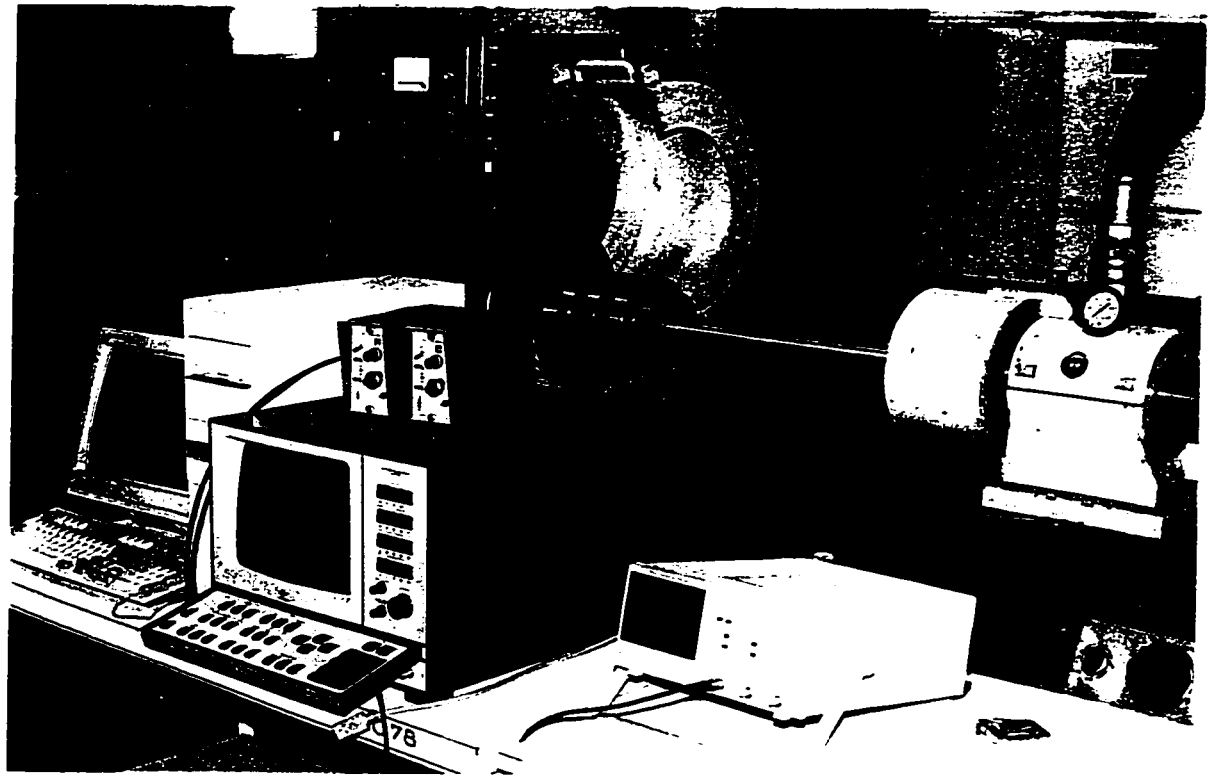

Fig.A.3. Measurement Setup Built around an FFT Unit B&K 2032

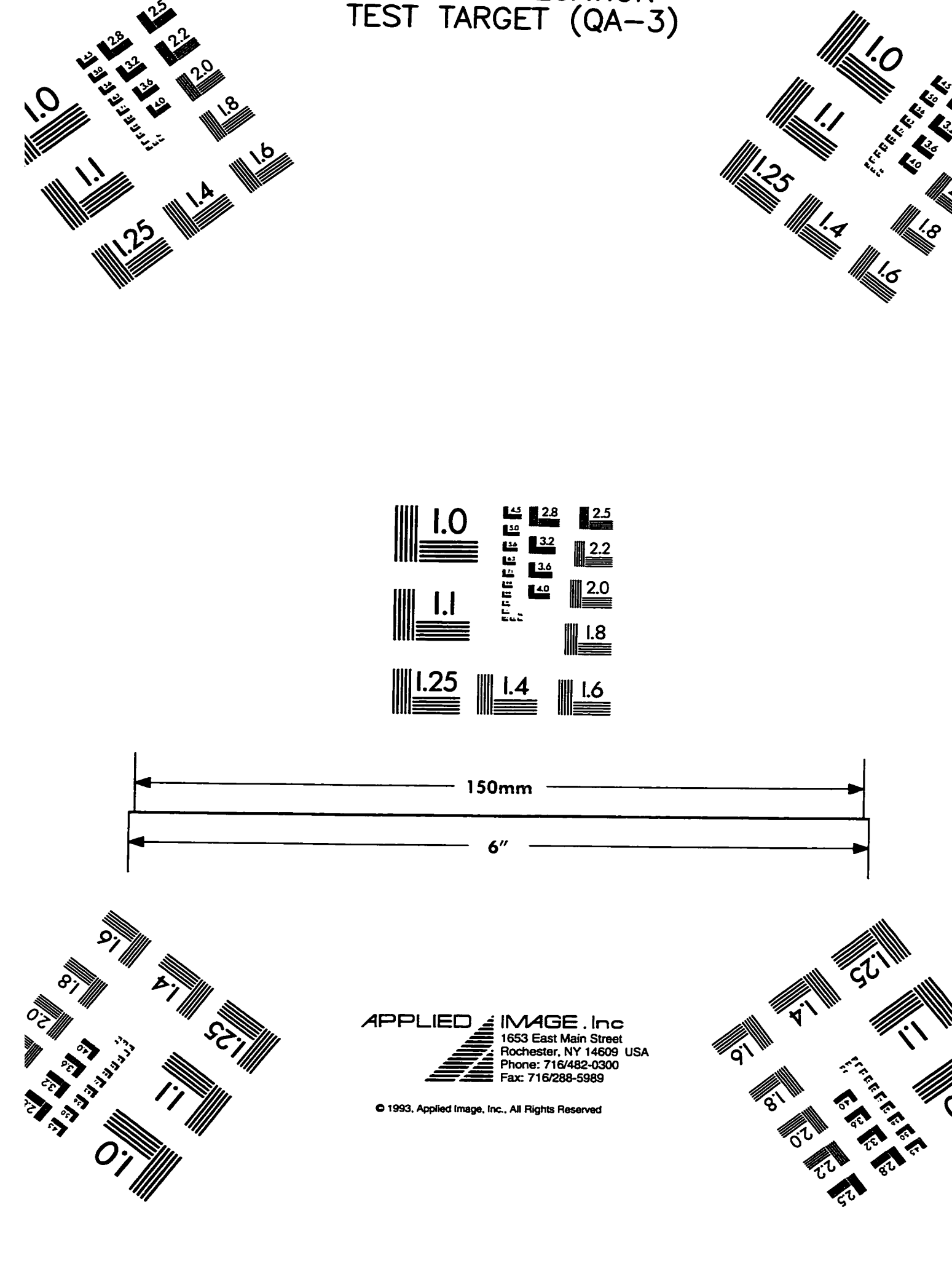
TEST TARGET (QA-3)
1.0
1.1
1.25
1.4
1.6
1.8
2.0
2.2
2.5
2.8
3.2
3.6
4.0
150mm
6"
APPLIED IMAGE, Inc
1653 East Main Street
Rochester, NY 14609 USA
Phone: 716/482-0300
Fax: 716/288-5989
© 1993, Applied Image, Inc., All Rights Reserved